

CHARACTERIZATION OF SOYBEAN SEED YIELD USING OPTIMIZED PHENOTYPING

by

BRENT SCOTT CHRISTENSON

B.A., Saint John's University, 2011

A THESIS

submitted in partial fulfillment of the requirements for the degree

MASTER OF SCIENCE

Department of Agronomy  
College of Agriculture

KANSAS STATE UNIVERSITY  
Manhattan, Kansas

2013

Approved by:

Major Professor  
William T. Schapaugh Jr.

# **Copyright**

BRENT SCOTT CHRISTENSON

2013

## **Abstract**

Crops research moving forward faces many challenges to improve crop performance. In breeding programs, phenotyping has time and economic constraints requiring new phenotyping techniques to be developed to improve selection efficiency and increase germplasm entering the pipeline. The objectives of these studies were to examine the changes in spectral reflectance with soybean breeding from 1923 to 2010, evaluate band regions most significantly contributing to yield estimation, evaluate spectral reflectance data for yield estimation modeling across environments and growth stages and to evaluate the usefulness of spectral data as an optimized phenotyping technique in breeding programs. Twenty maturity group III (MGIII) and twenty maturity group IV (MGIV) soybeans, arranged in a randomized complete block design, were grown in Manhattan, KS in 2011 and 2012. Spectral reflectance data were collected over the growing season in a total of six irrigated and water-stressed environments. Partial least squares and multiple linear regression were used for spectral variable selection and yield estimation model building. Significant differences were found between genotypes for yield and spectral reflectance data, with the visible (VI) having greater differences between genotypes than the near-infrared (NIR). This study found significant correlations with year of release (YOR) in the VI and NIR portions of the spectra, with newer released cultivars tending to have lower reflectance in the VI and high reflectance in the NIR. Spectral reflectance data accounted for a large portion of variability for seed yield between genotypes using the red edge and NIR portions of the spectra. Irrigated environments tended to explain a larger portion of seed yield variability than water-stressed environments. Growth stages most useful for yield estimation was highly dependent upon the environment as well as maturity group. This study found that spectral reflectance data is a good candidate for exploration into optimized phenotyping techniques and with further research and validation datasets, may be a suitable indirect selection technique for breeding programs.

# Table of Contents

List of Figures .....	vi
List of Tables .....	vii
Chapter 1 - Precision Phenotyping Using Canopy Reflectance Measurements in Field Crops	
Research: A Review .....	1
Introduction.....	1
Plant Biophysical and Biochemical Properties .....	2
Canopy reflectance Properties .....	3
Water Status .....	4
Leaf Biochemical Properties.....	5
Yield Estimation .....	8
Canopy Temperature for Yield .....	10
Reflectance indices for Yield.....	11
Yield estimation using hyper spectral data .....	14
Conclusion .....	16
References .....	16
Chapter 2 - Characterizing Changes in Soybean Spectral Response Curves with Breeding	
Advancements.....	27
Abstract.....	27
Introduction.....	28
Materials and Methods.....	31
Experimental and Field Design.....	31
Phenotypic Traits .....	31
Canopy Reflectance Measurements .....	32
Data Pretreatment.....	33
Statistical Analyses .....	33
Results and Discussion .....	34
Genotypic Performance for Yield and Reflectance Data.....	34
Correlation of Spectral Reflectance Data to Year of Release.....	36

Conclusions.....	39
References.....	40
Chapter 3 - Characterizing Soybean Seed Yield Using Optimized Phenotyping with Canopy	
Reflectance .....	57
Abstract.....	57
Introduction.....	58
Materials and Methods.....	63
Experimental and Field Design.....	63
Phenotypic Traits .....	64
Data Analysis .....	64
Analysis of Variance.....	64
Partial Least Squares (PLS) .....	65
Outlier Identification and Data Synthesis.....	65
Pre-treatment Before Modeling .....	66
Predictor Variable Selection .....	66
Multiple Linear Regression.....	67
Results and Discussion .....	67
Genotypic Performance in MGIII and MGIV Yield and Spectra.....	67
Waveband Region Selection.....	69
Correlation Between Parameters.....	75
Growth Stage Selection.....	76
Yield Estimation Model Development .....	79
Yield Estimation Model Validation .....	80
Conclusions.....	82
References.....	83

## List of Figures

Figure 2.A. Relationship between year of release and two-year yield means for MGIII and MGIV experiments. Least square line with equation and coefficient of determination ( $R^2$ ) represented at the top of the figure.....	53
Figure 2.B. Mean spectral response curves of MGIII genotypes (without ‘Illini’). Wavebands are 10nm intervals and reflectance is the percentage of a white reference panel. ....	54
Figure 2.C. Mean spectral response curves of MGIV genotypes. Wavebands are 10nm intervals and reflectance is the percentage of a white reference panel. ....	55
Figure 2.D. Correlation coefficient (r) values between wavelength (nm) and year of release for MGIII and MGIV two-year mean reflectance values. An r value $\geq \pm 0.37$ is significant at the $Pr \leq 0.05$ level, and an r value $\geq \pm 0.56$ is significant at the $Pr \leq 0.01$ . ....	56
Figure 3.A. Variable importance in projection plots displaying results from partial least squares regression (PLS) analyses. (A) Maturity group III (MGIII) 2011–2012 two-year means, (B) MGIII 2011 A-I means, (C) MGIII 2011 A-D means, (D) MGIII 2012 B-I means, (E) MGIII 2012 B-D means, (F) MGIII 2012 C-I 1 means, (G) MGIII 2012 C-I 2 means, (H) maturity group IV (MGIV) 2011–2012 two-year means, (I) MGIV 2011 A-I means, (J) MGIV 2011 A-D means, (K) MGIV 2012 B-I means, (L) MGIV 2012 B-D means, (M) MGIV 2012 C-I 1 means. ....	113
Figure 3.B. Relationships between observed and predicted seed yield for maturity group III (MGIII) and maturity group IV (MGIV) two-year waveband means with selected growth stage .....	114

## List of Tables

Table 2.1. Cultivars used for spectral data evaluation with year of release and two-year yield averages.....	48
Table 2.2. Analysis of variance for seed yield of MGIII and IV experiments. ....	49
Table 2.3 Band regions with genotypic differences from analysis of variance (N=20), for MGIII and MGIV experiments.....	50
Table 3.1. Mean seed yield by environments and range in yield across genotypes within environments.....	92
Table 3.2. Maturity group III (MGIII) and maturity group IV (MGIV) analysis of variance F-values for seed yield, maturity (Mat), and spectral wavelengths used for yield estimation models. ....	93
Table 3.3. Maturity group III (MGIII) and maturity group IV (MGIV) analysis of variance F-values for 2011 and 2012 experiments, and wavelengths used for yield estimation models. ....	94
Table 3.4. Maturity group III (MGIII) Pearson’s correlation coefficients and p-values for two-year averages of seed yield, maturity, and wavebands used for yield estimation models. MGIII on upper right; maturity group IV (MGIV) on lower left.....	96
Table 3.5. Results of the maturity group III (MGIII) stepwise regression models by growth stage within environments, coefficient of determination (R <sup>2</sup> ), root means square error (rMSE), percentage rMSE of dependent means (% rMSE of mean), and waveband(s) in final model. ....	97
Table 3.6. Results of the maturity group IV (MGIV) stepwise regression models by growth stage with experiment, coefficient of determination (R <sup>2</sup> ), root means square error (rMSE), percentage rMSE of dependent mean (% rMSE of mean), and wavebands in final model (wavebands). ....	98
Table 3.7. Results of stepwise regression yield estimation models for maturity group III (MGIII) and maturity group IV (MGIV) selected datasets. ....	99

Table 3.8. Yield estimation model validation results for maturity group III (MGIII) and maturity group IV (MGIV) growth stages and season totals (ST) for optimized yield estimation models. I indicates an irrigated environment; D indicates a water-stressed environment... 99



# Chapter 1 - Precision Phenotyping Using Canopy Reflectance Measurements in Field Crops Research: A Review

## Introduction

One of the challenges of plant breeders moving forward is to create genotypes that produce more with fewer inputs and on fewer acres. Over the last decade, advancements in genotyping techniques have reached new heights, whereas phenotyping techniques have stayed stagnant (Furbank and Tester, 2011). As crops research moves forward, characterization and screening of large populations as well as more efficiently selecting superior genotypes for quantitative traits such as yield is necessary. The phenotyping constraints make this exploration and selection process difficult due to the time and economic investment as well as the destructive nature and single time point of such techniques (Reynolds et al., 1999). To increase efficiency in crop research and development and utilize the genotypic resources available, precise and effective phenotyping techniques need to be developed (Montes et al., 2007; Furbank, 2009).

These challenges and constraints have led to studies focused on precision phenotyping techniques using canopy reflectance and canopy temperature measurements that are both precise and high-throughput allowing for more genetic material to be screened in less amount of time (Reynolds et al., 2007). These techniques look to accurately characterize morphological and physiological traits that can be used as an indirect selection method and improve yield (Richards et al., 2001; 2002). Precision phenotyping techniques can also give researchers a repeatable, accurate, nondestructive method of characterizing plant functions throughout the growing season (Hatfield et al., 2008).

Precision phenotyping is based on the reflectance and absorption characteristics of vegetation and the spectral response recorded by remote sensors (Holland et al., 2006). Remote

24 sensors have been utilized in close proximity with the plant, mounted on tractors for high-  
25 throughput measurements, or mounted on satellites, such as LandSat. These spectral responses  
26 can then be used to calculate vegetation indices or in the case of full spectra techniques, used  
27 independently in model building. Most of the indices, such as the widely used NDVI, are  
28 functions of ratios or proportions between wavelengths that correlate to specific plant  
29 biophysical or biochemical properties such as leaf composition, biomass production, or  
30 pigmentation (Osborne et al., 2002).

31 In a research setting, the accurate prediction of quantitative traits such as yield can be  
32 used as an important tool for identifying superior lines or used as a screening tool in many trait  
33 mining studies, without the need for high input costs such as harvesting (Ma et al., 2001; Montes  
34 et al., 2007). This can lead to larger breeding programs that utilize more plots and material in the  
35 pipeline. To accurately estimate yield, an understanding of the biophysical/biochemical  
36 components influencing the spectra to understand what the sensor is sensing as well as  
37 conclusions made based upon the spectral response curves. These biophysical/biochemical  
38 components, such as canopy and leaf structure and pigment status may not allow the plant to  
39 fully reach its genetic yield potential (Clevers, 1997), and many researchers have suggested that  
40 yield gains seen in field crops can be attributed to more efficient photosynthetic parameters  
41 (Waddington et al., 1986; Caldirini et al., 1995; Sayre et al., 1997; Reynolds et al., 1999).

#### 42 ***Plant Biophysical and Biochemical Properties***

43 Leaf reflectance and emittance of solar radiation is the basis for canopy reflectance and  
44 canopy temperature research (Inman et al., 2007). The amount of reflectance observed is a  
45 product of the leaf tissues, cellular structure, and the air-cell wall-protoplast-chloroplast  
46 interaction (Kumar and Silva, 1973). Chlorophyll a and b as well as anthocyanins and

47 carotenoids preferentially reflect and absorb wavelengths, which can then be used to estimate the  
48 concentration and status of these pigments (Hatfield et al., 2008). The wavelengths that correlate  
49 well with certain plant functions or parameters can then be used to model plant phenotypes  
50 (Thomas and Oerther, 1972; Filella et al., 1995). Emitted and reflected wavelengths can be used  
51 in the same fashion to correspond to canopy temperature using infrared thermometers (Gausman  
52 et al., 1969; Blackmer et al., 1994).

### 53 *Canopy reflectance Properties*

54 Canopy structure has a tremendous influence on the electromagnetic spectral response  
55 obtained by remote sensors. Because researchers are collecting solar radiation reflecting from the  
56 leaf surface, canopy biochemical and biophysical properties play a large role in what light and in  
57 what capacity the light is in, that the sensors are detecting (Asner et al., 1998). As the canopy  
58 structure changes, light may be reflected or diffused from different portions of the leaf and the  
59 canopy, causing a magnitude of variation from sample-to-sample (Asner et al., 1998). Also, soil  
60 background may confound these scans, creating unwanted variability in the sample. However,  
61 researchers can also take advantage of these variations and model these differences (Richie et al.,  
62 2010). By modeling the canopy structure, researchers can make inferences about the health of the  
63 plant and desired attributes such as photosynthetic capabilities (Thomas and Gausman 1977;  
64 Wessman, 1990).

65 Early research was focused on finding new wavelengths and spectral regions that  
66 correlated to plant function. Tucker (1978) proposed 5 primary and 2 transition regions of the  
67 visible and near infrared spectrum to characterize plant functions. 400-500nm (blue region)  
68 correlates to chlorophyll and carotenoid concentrations, 500-620 (green region) correlates to a  
69 reduction in chlorophyll absorption, which is why plants appear green, 620-700nm (red) which

70 correlates to an upswing in chlorophyll absorption (creation of the red edge), 700-740, which is a  
71 transition stage from red absorption to near infrared radiation (NIR) reflection, resulting in a  
72 sharp spike in reflection percentages in the spectral response, and from 750-1100 nm. The last  
73 region, NIR, is a high reflection region and also contains possible water absorption regions.  
74 Signal to noise ratio in remote sensing research is always a concern and sensing reflectance of  
75 plant canopies increases this ratio (Weber et al., 2012). Equations that have been proposed try to  
76 take into account background aspect such as soil and dead biomass with some success, but  
77 researchers have yet to fully account for all in-field variables when capturing reflectance data  
78 from full plant canopies (Daughtry et al., 2000; Hatfield et al., 2008).

#### 79 *Water Status*

80 Evaluating water status using any technique has its basis in the fundamentals of water  
81 status and movement in the plant, such as total water content, water potential of the roots and  
82 cells, and transpiration and photosynthetic rates (Percy et al., 1989). Water stress research using  
83 remote sensing techniques has been used for many years, starting with Tanner (1963) studying  
84 plant temperature variations from air temperature (Hatfield et al., 2008). This early research led  
85 to characterizing water stress through leaf and canopy temperature and water absorption bands  
86 within the EMS. This research has even been used to create irrigation schedules (Bausch and  
87 Duke, 1996) to reduce excess water use and characterize superior water use efficient plants in  
88 breeding programs.

89 Researchers have been able to characterize plant water status and stress through the  
90 preferential absorption of water and more specifically the hydroxyl ions within the  
91 electromagnetic spectrum (Peñuelas et al., 1993; 1997; Gao, 1996; Serrano et al., 2000). The  
92 NIR (730-1300) and middle infrared (1300-2500 nm) has been shown to correlate well with

93 water status/content of plants and the wavelengths 970, 1240, 1400, and 2700 nm have been  
94 proposed as water absorption bands indicative of water status (Tucker, 1980; Peñuelas et al.,  
95 1993; Gao, 1996; Zarco-Tejada et al., 2001; Gutierrez et al., 2010).

96 Peñuelas et al. 1993 developed the water index (WI) defined as  $R_{970}/R_{900}$ , to predict water  
97 stress and was found to strongly correlate with the relative water content of the plants and. The  
98 normalized difference water index, proposed by Gao (1996) defined as  $(R_{860}-R_{1240})/(R_{860}+R_{1240})$   
99 has been used to evaluate water stress in corn and soybeans (Anderson et al., 2004) with  
100 favorable results. Babar et al., 2006a proposed normalizing the WI, using the wavelengths 970,  
101 900, and 850nm, developed by Peñuelas et al., 1993 found it to be useful for screening wheat  
102 genotypes for water stress and water use efficiency (Gutierrez et al., 2010). Prasad et al., 2007a,  
103 b also normalized the WI, using the wavelengths 970, 920, and 880nm to screen winter wheat  
104 lines under dry-land conditions (Gutierrez et al., 2010). These authors propose that the  
105 normalization of the WI provides added genotypic variation explanation. However, Gutierrez et.,  
106 al 2010 found that only the normalized water index using wavelengths 970 and 880 nm proposed  
107 by Prasad et al., 2007 a, b was the only index sufficient for predicting water stress within field  
108 experiments.

### 109 ***Leaf Biochemical Properties***

110 Leaf biochemistry is a major portion of the physiological function of plant leaves and  
111 serves as the building block for energy production. Many of the physiological parameters that  
112 show genotypic variation pertain to biochemical parameters, with most of the components being  
113 pigment concentration and status (Reynolds et al., 2009). The photosynthetic capacity and  
114 efficiency of a plant is a function of the chlorophyll and other pigment content of the plant.

115 Chlorophyll status can then estimate biomass production and photosynthetic capacity (Curran et  
116 al., 1990; Filella et al., 1995). Also, due to chlorophyll content being directly influenced by  
117 nitrogen status, chlorophyll status estimation can directly relate to nitrogen status (Filella et al.,  
118 1995; Moran et al., 2000). Chlorophyll content is also related to plant stress and senescence,  
119 suggesting chlorophyll can be used to characterize genotypes for stress (Hendry et al., 1987;  
120 Merzlyak and Gitelson, 1995; Peñuelas and Filella, 1998; Merzlyak et al., 1999; Carter and  
121 Knapp, 2001). Remote sensing leaf pigments can serve as a non-destructive, repeatable way to  
122 characterize plant functions and relate this to overall plant health (Hatfield and Prueger, 2010).

123         With new advancements in the understanding of leaf structure and remote sensing  
124 interaction, many modern studies have developed indices expressing the relationship between  
125 leaf biochemical properties and spectral responses obtained. Peñuelas et al., 1995 and Gitelson  
126 and Merzlyak, 1994 have expressed various chlorophyll and chlorophyll:carotenoid ratios using  
127 specially derived indices, Gamon et al., 1992, 1997 have characterized photosynthetic  
128 performance based on spectral responses. The ratio  $(R_{531}-R_{570})/(R_{531}+R_{570})$ , where  $R_{570}$  is the  
129 reflectance at 570nm and  $R_{531}$  is the reflectance at 531 nm, has been widely used to characterize  
130 leaf pigment status (Gamon et al., 1992; Peñuelas et al., 1995). Chappelle et al., 1992 found that  
131 wavebands 650, 675, and 700 nm could be used to predict chlorophyll and beta carotene in  
132 soybean leaves. Also, alternative wavelengths have been used based on correlation to specific  
133 physiological functions (Gamon et al., 1992; Inoue et al., 2006; Garbulsky et al., 2008). Being  
134 able to model genotypic responses that incorporate these functions have potential to exploit  
135 important traits in breeding programs.

136         Chlorophyll A and B are essential pigments within a plant that convert light energy into  
137 chemical energy through the process of photosynthesis. From chlorophyll, researchers can

138 directly determine photosynthetic potential and primary productivity of the plant (Curran et al.,  
139 1990; Filella, 1995). Chlorophyll A and B absorb solar radiation at specific wavelengths to  
140 covert this energy into chemical energy. Based on the wavelengths that are either absorbed or  
141 reflected by these pigments, scientists are able to assess overall health and efficiency of the plant.  
142 Chlorophylls have a high absorbance in the red (600-730 nm) and blue (400-500nm) regions of  
143 the spectrum. Chlorophyll b preferentially absorbs light in the 460 and 650 nm regions,  
144 chlorophyll a absorbs in the 580, 630, and 670 nm regions of the spectrum, and 415 nm is a  
145 preferential absorption of both (Chappelle et al., 1992). Blue regions of the spectrum also  
146 correlate to carotenoid preferential absorption, and therefore are not commonly used in  
147 chlorophyll concentration and status estimates (Sims and Gamon, 2002). The green and red  
148 region of the spectrum around the 550nm and 700nm regions are primarily used due to high  
149 chlorophyll concentrations needed to saturate these wavelengths (Sims and Gamon, 2002). Many  
150 researchers such as Thomas and Gausman, 1977; Buschman and Nagel, 1993; Datt, 1998, 1999;  
151 Gitelson and Merzlyak 1996; 1997; Gitelson et al., 1996b; and Schepers et al., 1996, have  
152 characterized the chlorophyll wavelength absorption into chlorophyll concentration models  
153 utilizing mainly the red. Sims & Gamon, (2002), correlated the 700nm region of the spectrum to  
154 chlorophyll concentration, which is used by many researchers as a base line for new chlorophyll  
155 indices. Gitelson and Merzlyak 1994 used  $(R_{780}/R_{700})$  and  $(R_{750}-R_{705}/R_{750}+R_{705})$ , where  $R_{780}$  is  
156 the reflectance at 780nm,  $R_{700}$  is the reflectance at 700nm,  $R_{750}$  is the reflectance at 750nm and  
157  $R_{705}$  is the reflectance at 705nm, to estimate chlorophyll content with great success. Other  
158 researchers have also used the 550nm and 700 nm regions of the spectrum (Aoki et al., 1986;  
159 Gitelson and Merzlyak, 1997; Datt, 1998; Gamon and Surfus, 1999; Carter and Knapp, 2001;  
160 Richardson et al., 2002; Sims and Gamon, 2002). Chlorophyll content has many variables, and

161 Gitelson et al. 2002 suggest that broadband reflectance is necessary for broad scale adaptation of  
162 chlorophyll estimation across species and ecosystems.

163 Anthocyanins and carotenoids are important pigments of the plant biochemical process as  
164 well. Few researchers have delved into anthocyanin and carotenoid research due to numerous  
165 variables such as other pigment absorption and leaf cell structure problems. Gamon and Surfus  
166 (1999), developed a model and indices for anthocyanin concentration estimation based on a red  
167 to green ratio,  $R_{600}-R_{700}/R_{500}-R_{600}$ , and the green channel on LandSat has been explored by Vina  
168 and Gitelson et al., 2011, to estimate anthocyanin status with success, but has yet to be  
169 replicated. Hatfield et al., 2008 hypothesized that 2 band indices are confounded by variables  
170 such as other pigment absorption and leaf scattering of light. Gitelson et al., 2001, Gitelson et al.,  
171 2003a, and Gitelson et al., 2006, found 3-band indices in the (waveband regions) ineffective in  
172 developing reliable models to estimate carotenoid and anthocyanin concentrations, suggesting  
173 full spectrum hyperspectral data collection may be necessary for reliable model estimations.

174 Many authors have studied chlorophyll and other pigment models with varying success,  
175 but the consensus seems to be, full spectra indices or statistical models are necessary to fully  
176 capture the relationship between leaf pigments and reflectance spectra. However, models  
177 utilizing regions know to correlate well with plant function can be used to characterize many  
178 traits that are of importance to crop researchers. These models may also be able to be used for  
179 screening of specific traits that may not be necessarily captured by visual phenotyping  
180 techniques.

### 181 *Yield Estimation*

182 With the new challenges of feeding an ever-growing population with fewer resources, it  
183 is necessary for crops researchers to streamline the breeding approach and develop techniques



184 that allow for more genetic material to be screened within a program in a shorter amount of time.  
185 Due to high genetic variability and extensive genotype x environment interactions associated  
186 with yield, precise phenotyping is essential for future development. Most of the field based  
187 research that is conducted on yield estimation models using canopy reflectance and canopy  
188 temperature measurements are focused on 2 or 3 band indices, which can be highly variable and  
189 inconsistent (Babar et al., 2006 a,b). Some of these indices have been useful in estimating yield  
190 through other plant characteristics such as chlorosis (Adams et al., 1999), green cover (Dusek et  
191 al., 1985; Daughtry et al., 2000), chlorophyll (Datt, 1999; Daughtry et al., 2000), and  
192 photosynthetically active tissue (Wiegand et al., 1991). These indices, like pigment status have  
193 had varying degrees of success, but none have fully captured the underlying physiological and  
194 environmental factors leading to phenotypic yield. New studies that focus on utilizing full  
195 spectrum instruments and models have been published in recent years in wheat (Hansen et al.,  
196 | 2002; Hansen and Schjoering, 2003; Pimstein et al., 2007; 2011), corn (Hong et al., 2001; Weber  
197 | et al., 2012), rice (Lin et al., 2012), cotton (Zhao et al., 2006) and soybean (Kaul et al., 2005) in  
198 optimal and drought environments. Incorporating these new models into high efficiency  
199 platforms has also been characterized and explored (Montes et al., 2007; Walter et al., 2012;  
200 White et al., 2012). Other researchers have also related canopy temperature, which is emitted  
201 thermal radiation to yield (Reynolds et al., 1994; Fischer et al., 1998). Combining reflectance  
202 models with canopy temperature can integrate many physiological parameters that lead to robust  
203 yield prediction models that account for a large portion of the variability among genotypes  
204 (White et al., 2012). Leaf and canopy reflectance data can give insight into many physiological  
205 parameters such as photosynthetic capacity, aboveground biomass, and water status that have  
206 highly correlated association with yield (Royo et al., 2003; Weber et al., 2012). Many of these

207 studies have focused on wheat and are seen to correlate more effectively with optimal  
208 environments due to yield potential being fully met (Aparicio et al., 2000; Royo et al., 2003;  
209 Gutierrez et al., 2010).

### 210 *Canopy Temperature for Yield*

211 Canopy temperature (CT) measurements are a fast and accurate way to study stomatal  
212 conductance and leaf transpiration (Jones et al., 2009). Canopy temperature measurements are  
213 based on using thermal infrared (IR) radiation which relates to evaporation or transpiration from  
214 a plant leaf. When a plant stops transpiration and closes the stomata, the temperature of the leaf  
215 and ultimately canopy increases. This is due to the assumption that transpired water evaporated  
216 from the leaf surface and cools the leaf below ambient air temperatures (Jackson, 1981). CT  
217 measurements can then be used to distinguish genotypes and make selection for high yielding  
218 varieties (Reynolds et al., 2009).

219 Canopy temperature and canopy temperature depression (CT - ambient air temperature)  
220 can be used for many essential plant functions. Early research focused on crop stress indicators  
221 using canopy temperature with great success (Jackson et al., 1981). Blum et al., 1989 related  
222 yield stability to canopy temperatures in wheat under drought conditions with correlations of  
223 0.64 and 0.72 between the drought susceptible index and CT. In soybean Fletcher et al., 2007  
224 and Ries et al., 2012 found that canopy temperature can be utilized to characterize slow wilting  
225 and radiation use efficiency. Research has suggested that lower CT correlate with high yielding  
226 wheat varieties in well watered and stressed environments (Reynolds et al., 1999; Babar et al.,  
227 2006b; Gutierrez et al., 2010). Research also suggests that selecting for lower CT varieties can  
228 increase yields in a breeding program in well watered and water stressed environments (Amani et  
229 al., 1996; Reynolds et al., 2009). Research conducted suggests a correlation with CT and grain

230 yield in soybean (McKinney et al., 1989), cotton (Hatfield et al., 1987), millet (Singh and  
231 Kanemasu, 1983), as well as wheat. Incorporating canopy temperature into breeding programs for  
232 high yielding varieties may be a useful indirect selection tool for plant breeders. Therefore, CT is  
233 well suited to be utilized in yield estimation models.

#### 234 ***Reflectance indices for Yield***

235 Recent research conducted suggests that reflectance wavelength equations called indices  
236 correlating to yield can be used as an indirect selection method (Araus et al., 2001). Most of the  
237 research conducted on yield prediction using canopy reflectance techniques focuses on the  
238 reflected solar radiation in the visible red (600nm-730nm) and near infrared (730nm-1100nm)  
239 regions of the electromagnetic spectrum, which was first shown to correlate to crop conditions  
240 by Bauer 1981 and Walburg et al., 1982. Researchers can then develop rapid, nondestructive,  
241 and repeatable measurements (Field et al., 1995).

242 Vegetation indices are used to maximize the relationship between certain solar radiation  
243 wavelengths and plant function, while minimizing the effect of background noise (Huete et al.  
244 2002; Hatfield and Prueger 2010). Hatfield and Prueger 2010 studied various vegetation indices  
245 in corn and soybean and concluded that multiple indices must be used to account for the  
246 variations seen between different crops and different growing conditions. Babar et al., 2006a  
247 concluded that vegetation indices using NIR reflectance were the most correlated with yield in  
248 wheat. Wiegand et al., 1991 also illustrates that yield prediction by spectral indices must be site-  
249 independent in order to create a prediction model that can be used and fully accepted in crop  
250 research.

251 Most of the indices correlate plant parameters such as pigment status to grain yield.  
252 Indices such as the simple ratio (SR), first used by Jordan 1969 and Rouse et al., 1973 described

253 by the equation ( $R_{\text{NIR}}/R_{\text{RED}}$ ), captures the ratio of NIR reflectance to reflectance in the red. SR has  
254 been shown to correlate well with biomass, LAI, fractional photosynthetically active radiation  
255 (FPAR), and ground cover, and yield in wheat and soybeans (Hatfield, 1983; Wiegand et al.,  
256 1991; Ball and Konzak, 1993; Price and Bausch 1995; Aparicio et al., 2000; Serrano et al., 2000;  
257 Ma et al., 2001; Royo et al., 2003; Hatfield and Prueger, 2010). The basis for the SR is the strong  
258 absorption of red light and the strong reflection of NIR by healthy plant vegetation, and small  
259 changes in these reflectance or absorption patterns can give researchers a lot of information  
260 about overall plant health, especially chlorophyll a and b. The normalized difference vegetation  
261 index (NDVI), derived by Deering 1978 and Tucker 1979 to estimate green biomass and  
262 intercepted PAR, defined as  $(R_{\text{NIR}}-R_{\text{RED}}/R_{\text{NIR}}+R_{\text{RED}})$ , has been used extensively to predict yield and  
263 other plant functions with many crops using hyper-spectral and satellite imagery (Wiegand et al.,  
264 1991; Peñuelas et al., 1997; Lewis et al., 1998; Aparicio et al., 2000; Ma et al., 2001; Shanahan  
265 et al., 2001; Royo et al., 2002; Royo et al., 2003; Prasad et al., 2007a;b; Marti et al., 2007). The  
266 NDVI captures plant health, with healthy plants having high absorption in the red and high  
267 reflection in the NIR. If the plant is under stress or is starting to senesce, the absorption of red  
268 light by the chlorophylls and other pigments and cellular components will decrease. Gitelson et  
269 al., 1996a proposed the GNDVI as a substitute to the high saturation point of the red region in  
270 the NDVI. Shanahan et al., 2001 have successfully predicted yields in corn under normal  
271 growing conditions in Nebraska using the GNDVI. Researchers found that normalizing the green  
272 and NIR relationship was highly correlated with grain yield, explaining 70 to 92% of yield  
273 variability at mid grain fill in corn (Shanahan et al., 2001). Ma et al., 2001 used the NDVI ( $R_{613}-$   
274  $R_{559}/R_{613}+R_{559}$ ) to predict soybean yield, and concluded a high correlation with soybean yields  
275 under irrigated conditions and explained up to 80% of the variation within yield. The

276 photochemical reflectance index (PRI), defined by the equation  $(R_{550} - R_{531}) / (R_{550} + R_{531})$   
277 captures the normalized difference between the major green wavelength reflectance of the plant  
278 canopy and leaves, which can be used to quantify radiation use efficiency (Gamon et al., 1992).  
279 Trotter et al., 2002 and Garbulsky 2011 used the PRI to assess nitrogen use efficiency and  
280 radiation use efficiency to distinguish genotypes that were superior compared to checks. These  
281 indices have been used estimate yield varying environments on many platforms.

282 Other indices focus on the biophysical parameters, such as water content and leaf area.  
283 The leaf area index (LAI), first illustrated by Tucker and Sellers, 1986 was developed to predict  
284 vegetation parameters such as green biomass and green leaf area (Babar et al. 2006b). The leaf  
285 area index captures the genotypic differences between photosynthetically active radiation (PAR)  
286 being absorbed and used by leaves with more area and being able to monitor important crop  
287 variables throughout the growing season (Clevers, 1997). Elliot and Regan 1993 and Aparicio et  
288 al., 2000 and 2002 have determined that LAI plays a large part in plant function and correlates  
289 well with yield prediction. Many water indices have been developed to relate reflectance  
290 measurements with success in the 850 and 970 nm regions with bread and durum wheat yield  
291 (Royo et al., 2003; Prasad et al., 2007b; Gutierrez et al., 2010). The water indices focus on the  
292 minor water absorption bands within the spectrum and capture relative water content based on  
293 absorption strength by water within the plant leaves. Capturing biophysical properties can  
294 capture properties that influence yield production of field crops.

295 Most of the research conducted using reflectance measurements for yield estimation  
296 focus on calculated indices. These indices are easy to calculate and give researchers a way to  
297 easily handle the large amount of data associated with such research, however, indices tend to be  
298 environment specific and outside of wheat, have a low correlation with yield (Aparicio et al.,

299 2000; Ma et al., 2001; Guitierrez-Rodrigues et al., 2004; Prasad et al., 2007a and b; Gutierrez et  
300 al., 2010). Therefore, more complex models need to be developed using more of the spectrum to  
301 capture the necessary variation within yield across different environments and crops (Osborne et  
302 al., 2002; Pimstein et al., 2007; 2011; Weber et al., 2012).

### 303 *Yield estimation using hyper spectral data*

304 Recently, studies utilizing full spectrum models focusing on several hundred bands  
305 contributing to yield estimation have been conducted. Full spectrum models are considered for  
306 yield estimation due to confounds such as biomass saturation, dense cover, high LAI, and high  
307 chlorophyll levels (Pimstein et al., 2007). High yielding varieties tend to have high  
308 biophysical/biochemical properties, making it unreliable to distinguish these genotypes using  
309 spectral indices (Baret and Guyot, 1991; Buschmann and Nagel, 1993; Aparicio et al., 2002;  
310 Pimstein et al., 2007). None of the developed indices can meet these needs, therefore, more  
311 complex characterization models based on more of the spectra must be developed (Hansen and  
312 Schjoering, 2003). Due to yield being a function of many physiological and environmental  
313 parameters that change throughout the growing season, combining many different wavebands  
314 over an entire growing season should give more precise yield estimation models (Araus et al.,  
315 2008).

316 Full spectrum multivariate data analysis with spectral reflectance data to create yield  
317 estimation models in field crops has been utilized in recent years (Hong et al., 2001; Hansen et  
318 al., 2002; Chang et al., 2003; Ferri et al., 2004; Kaul et al., 2005; Poss et al., 2006; Pimstein et  
319 al., 2007; 2011; Gutierrez et al., 2011; Weber et al., 2012; Lin et al., 2012). This is mainly due to  
320 the large datasets associated with spectral research, high multicollinearity that is associated with  
321 wavebands close to each other, and fears of over fitting models with more bands (Thenkebail et

322 al., 2002; Lin et al., 2012). To deal with these dilemmas, researchers have turned to approaches  
323 such as partial least squares (PLS), principal component analysis (PCA), and artificial neural  
324 networks (ANN) to develop hyper spectral yield estimation models. Incorporating more bands  
325 into a model may allow for more variability within certain predictors without reducing the  
326 effectiveness of the model.

327         The main approach used to deal with the challenges of hyper spectral data analysis focus  
328 on reducing the correlation between predictor variables, causing multicollinearity and  
329 normalizing the variability within predictor variables from sample to sample. Also, researchers  
330 use these new techniques to tease apart the spectral response curves into meaningful spectral  
331 waveband regions. PCA has been used by researchers to build yield prediction models that  
332 explain 70 to 90% of the yield variability in maize (Hong et al., 2001; Chang et al., 2003) and  
333 39% of the variability in yield among soybean genotypes (Hong et al., 2001). Stepwise  
334 regression explained almost 95% of the variability within maize yield using 6 bands (Osborne et  
335 al., 2002). ANN has also been used in soybean to build prediction models that explain between  
336 46 and 81% of the variability in yield and 42 to 77% in corn (Kaul et al., 2005). Hansen et al.,  
337 2002 compared three different PLS methods and concluded the N-PLS was the most consistent  
338 for yield and protein content estimation in wheat and barley, explaining up to 75% of the  
339 variation in protein content and up to 97% of the variation in yield. Similarly, under different  
340 water regimes, Weber et al., 2012 found that PLS explained a maximum of 40% of the  
341 variability within corn yield, and found that prediction models created explained more variability  
342 in water limited environments than non-water limited environments. Lin et al., 2012 used  
343 orthogonal projections to latent structure PLS in rice and could distinguish 3 cultivars with 90%  
344 accuracy but dropped to 80% when distinguishing 1 cultivar. Researchers also determined that

345 reducing the dataset to 10 nm intervals reduced the noise within the dataset. Utilizing  
346 multivariate analysis is new to precision phenotyping research but appears to have potential to  
347 create yield prediction models as well as explain other important phenotypic parameters.

### 348 ***Conclusion***

349 With the challenges needing to be met by plant breeders moving forward, new and  
350 innovative phenotyping technologies need to be developed that allows for more genetic material  
351 and advanced genotyping technologies to be utilized. Precision phenotyping using canopy  
352 reflectance data can be utilized by plant breeders to characterize a large number of genotypes in a  
353 precise and cost effective manner. Reflectance indices can be used to classify many different  
354 plant functions that are vital to characterizing field crops and screen genotypes for traits vital for  
355 plant breeders to meet the challenges. With the advancements in statistical analysis, hyper  
356 spectral data can be used to create models that can quantify quantitative traits such as yield and  
357 allow plant breeders to screen more genotypes in more environments. Moving forward, more  
358 research needs to be conducted in order for yield prediction models to be fully implemented into  
359 breeding programs, but reflectance data can be utilized to characterize large genotype  
360 experiments.

### 361 **References**

362 Adams, M.L., Philpot, W.D., and Norvell, W.A. 1999. Yellowness index: an application of  
363 spectral 2nd derivatives to estimate chlorosis of leaves in stressed vegetation. *International*  
364 *Journal of Remote Sensing*. 20:3663–3675.

365  
366 Amani, I., Fischer, R.A., and Reynolds, M.P. 1996. Canopy temperature depression association  
367 with yield of irrigated wheat cultivars in a hot climate. *J. Agron. Crop Sci*. 176:119-129.

368  
369 Anderson, M.C., C.M.U. Neale, F. Li, J.M. Norman, W.P. Kustas, H. Jayanthi, and J. Chavez.  
370 2004. Upscaling ground observations of vegetation water content, canopy height, and leaf area  
371 index during SMEX02 using aircraft and Landsat imagery. *Remote Sens of Env*. 92: 447-464.



- 372  
 373 Aoki, M., Yabuki, K., Totsuka, T., and Nishida, M. 1986. Remote sensing of chlorophyll content  
 374 of leaf: I. Effective spectral reflection characteristics of leaf for evaluation of chlorophyll content  
 375 in leaves of dicotyledons. *Environmental Control in Biology*. 24: 21– 26.  
 376
- 377 Aparicio, N., Villegas, D., Araus, J., Casadesus, J., and Royo, C. 2002. Relationship between  
 378 growth traits and spectral vegetation indices in durum wheat. *Crop Science*. 42(5):1547-1555.  
 379
- 380 Aparicio, N., Villegas, D., Casadesus, J., Araus, J., and Royo, C. 2000. Spectral vegetation  
 381 indices as nondestructive tools for determining durum wheat yield. *Agronomy Journal*. 92(1):83-  
 382 91.  
 383
- 384 Araus, J.L., J. Casadesus, and J. Bort. 2001. Recent tools for the screening of physiological traits  
 385 determining yield. p. 59–77. In M.P. Reynolds, J.I. Ortiz-Monasterio, and A. McNab (ed.)  
 386 Application of physiology in wheat breeding. CIMMYT, Mexico, D.F.  
 387
- 388 Asner, G.P., Wessman, C.A., and Archer, S., 1998. Scale dependence of absorption of  
 389 photosynthetically active radiation in terrestrial ecosystems. *Ecol. Appl.* 8 (4):1003–1021.  
 390
- 391 Babar, M., Reynolds, M., Van Ginkel, M., Klatt, A., Raun, W., and Stone, M. 2006a. Spectral  
 392 reflectance indices as a potential indirect selection criteria for wheat yield under irrigation. *Crop*  
 393 *Science*. 46(2):578-588.  
 394
- 395 Babar, M., Reynolds, M., Van Ginkel, M., Klatt, A., Raun, W., and Stone, M. 2006b. Spectral  
 396 reflectance to estimate genetic variation for in-season biomass, leaf chlorophyll, and canopy  
 397 temperature in wheat. *Crop Science*. 46(3):1046-1057.  
 398
- 399 | Ball, S., and Konzak, C. 1993. Relationship between grain yield and remotely sensed data in  
 400 | wheat breeding experiments-. *Plant Breeding*. 110(4):277-282.  
 401
- 402 Baret, F., and Guyot, G. 1991. Potentials and limits of vegetation indices for LAI and APAR  
 403 assessment, *Remote Sens. Environ.* 35:161-174.  
 404
- 405 Bauer, M. E., C. S. T. Daughtry and V. C. Vanderbilt. 1981. Spectral agronomic relationships of  
 406 corn, soybean, and wheat canopies. Report SR-P1-04187. West Lafayette, IN: Laboratory for  
 407 Applications of Remote Sensing, Purdue University. pp: 17.  
 408
- 409 Bausch, W.C., and H.R. Duke. 1996. Remote sensing of plant nitrogen status in corn. *Trans.*  
 410 *ASAE*. 32:1869–1875.  
 411
- 412 Blackmer, T.M., J.S. Schepers, and G.E. Varvel. 1994. Light reflectance compared with other  
 413 nitrogen stress measurements in corn leaves. *Agron. J.* 86:934–938.  
 414
- 415 Blum, A. 1988. *Breeding for stress environments*. CRC Press, Boca Raton, FL.  
 416

- 417 Buschman, C., and Nagel, E. 1993. In vivo spectroscopy and internal optics of leaves as a basis  
418 for remote sensing of vegetation. *International Journal of Remote Sensing*. 14:711 – 722.  
419
- 420 Calderini, D.F., M.F. Dreccer, and G.A. Slafer. 1995. Genetic improvement in wheat yield and  
421 associated traits. A re-examination of previous results and the latest trends. *Plant Breeding*.  
422 114:108–112.  
423
- 424 Carter, G.A., and A.K. Knapp. 2001. Leaf optical properties in higher plants: Linking spectral  
425 characteristics to stress and chlorophyll concentration. *Am. J. Bot.* 84:677–684.  
426
- 427 Chang, J., Clay, D.E., Dalsted, K., Clay, S., O’Neill, M. 2003. Corn (*Zea Mays* L.) yield  
428 prediction using multispectral and multivariate reflectance. *Agron. J.* 95:1447-1453.  
429
- 430 Chappelle, E.W., M.S. Kim, and J.E. McMurtrey, III. 1992. Ratio analysis of reflectance spectra  
431 (RARS): An algorithm for the remote estimation of the concentrations of chlorophyll a,  
432 chlorophyll b, and carotenoids in soybean leaves. *Remote Sens. Environ.* 39:239–247.  
433
- 434 Clevers, J.G.P.W. 1997. A simplified approach for yield prediction of sugar beet based on optical  
435 remote sensing data. *Remote Sens. Environ.* 61:221–228.  
436
- 437 Curran, P.J., J.L. Dungan, and H.L. Gholz. 1990. Exploring the relationship between reflectance  
438 red edge and chlorophyll content in slash pine. *Tree Physiol.* 7:33–48.  
439
- 440 Datt, B. 1999. Remote sensing of water content in Eucalyptus leaves. *Australian Journal of*  
441 *Botany*. 47: 909 - 923.  
442
- 443 Datt, B. 1998. Remote sensing of chlorophyll a, chlorophyll b, chlorophyll a+b, and total  
444 carotenoid content in eucalyptus leaves. *Remote Sens. Environ.* 66:111–121.  
445
- 446 Daughtry, C.S.T., C.L. Walthall, M.S. Kim, E. Brown de Colstoun, and J.E. McMurtrey, III.  
447 2000. Estimating corn leaf chlorophyll content from leaf and canopy reflectance. *Remote Sens.*  
448 *Environ.* 74:229–239.  
449
- 450 Deering, D.W. 1978. Rangeland reflectance characteristics measured by aircraft and spacecraft  
451 sensors. Ph.D. diss. Texas A&M Univ., College Station.  
452
- 453 Dusek, D.A., Jackson, R.D. and Musick, J.T. 1985. Winter wheat vegetation indices calculated  
454 from combinations of seven spectral bands. *Remote Sensing of Environment*. 18:255–267.  
455
- 456 Elliot, G., and Regan, K. 1993. Use of reflectance measurements to estimate early cereal biomass  
457 production on sandplain soils. *Australian Journal of Experimental Agriculture*. 33:179-183.  
458
- 459 Ferri, C.P., Formaggio, A.R., Schiavinato, M.A. 2004. Narrow band spectral indexes for  
460 chlorophyll determination in soybean canopies [*Glycine max* (L.) Merrill]. *Brazilian Journal of*  
461 *Plant Physiology*. 16: 131–136.  
462

- 463 Field, C.B., Randerson, J.T., Malmström, C.M. 1995. Global net primary production: combining  
 464 ecology and remote sensing. *Remote Sens. Environ.* 51(1):74–88.  
 465
- 466 Filella, I., I. Serrano, J. Serra, and J. Penuelas. 1995. Evaluating wheat nitrogen status with  
 467 canopy reflectance indices and discriminate analysis. *Crop Sci.* 35:1400–1405.  
 468
- 469 Fischer, R.A., D. Rees, K.D. Sayre, Z.M. Lu, A.G. Condon and A. Larque  
 470 Saavedra. 1998. Wheat yield progress associated with higher stomatal conductance and  
 471 photosynthetic rate, and cooler canopies. *Crop Sci.* 38:1467–1475.  
 472
- 473 Fletcher, A.L., T.R. Sinclair, and L.H. Allen, Jr. 2007. Transpiration responses to vapor pressure  
 474 deficit in well watered “slow-wilting” and commercial soybean. *Environ. Exp. Bot.* 61:145–151.  
 475
- 476 Furbank R.T., Tester, M. 2011. Phenomics - technologies to relieve the phenotyping bottleneck.  
 477 *Trends in Plant Science.* 16 (12):635-644.  
 478
- 479 Furbank, R.T. 2009. Plant phenomics: from gene to form and function. *Funct. Plant Biol.* 36:10–  
 480 11.  
 481
- 482 Gamon, J. A., Serrano, L., and Surfus, J. S. 1997. The photochemical reflectance index: an  
 483 optical indicator of photosynthetic radiation use efficiency across species, functional types and  
 484 nutrient levels. *Oecologia.* 112:492– 501.  
 485
- 486 Gamon, J.A., and J.S. Surfus. 1999. Assessing leaf pigment content and activity with a  
 487 reflectometer. *New Phytol.* 143:105–117.  
 488
- 489 Gamon, J.A., J. Penuelas, and C.B. Field. 1992. A narrow-waveband spectral index that tracks  
 490 diurnal changes in photosynthetic efficiency. *Remote Sens. Environ.* 41:35–44.  
 491
- 492 Gao, B. 1996. NDWI—A normalized difference water index for remote sensing of vegetation  
 493 liquid water from space. *Remote Sensing of Environment.* 58:257– 266.  
 494
- 495 Garbulsky, M. 2011. The photochemical reflectance index (PRI) and the remote sensing of leaf,  
 496 canopy and ecosystem radiation use efficiencies. *Remote Sensing of Environment.* 115:281-297.  
 497
- 498 Garbulsky, M.F., Penuelas, J., Papale, D., and Filella, I. 2008. Remote estimation of carbon  
 499 dioxide uptake by a Mediterranean forest. *Global Change Bio.* 14:2860-2867.  
 500
- 501 Gausman, H.W., W.A. Allen, and R. Cardenas. 1969. Reflectance of cotton leaves and their  
 502 structure. *Remote Sens. Environ.* 1:19–22.  
 503
- 504 Gitelson, A.A., and Merzlyak, M.N. 1997. Remote estimation of chlorophyll content in higher  
 505 plant leaves. *International Journal of Remote Sensing.* 18: 2691–2697.  
 506
- 507 Gitelson, A.A., and M.N. Merzlyak. 1996. Signature analysis of leaf reflectance spectra:  
 508 Algorithm development for remote sensing of chlorophyll. *J. Plant Physiol.* 148:494–500.

- 509  
510 Gitelson, A., Gritz, Y., and Merzlyak, M. 2003a. Relationships between leaf chlorophyll content  
511 and spectral reflectance and algorithms for non-destructive chlorophyll assessment in higher  
512 plant leaves. *Journal of Plant Physiology*. 160:271-282.  
513
- 514 Gitelson, A., Kaufman, Y., and Merzlyak, M. 1996a. Use of a green channel in remote sensing  
515 of global vegetation from EOS-MODIS. *Remote Sensing of Environment*. 58:289-298.  
516
- 517 Gitelson, A., M. Merzlyak, and H. Lichtenthaler. 1996b. Detection of red edge position and  
518 chlorophyll content by reflectance measurements near 700 nm. *J. Plant Physiol*. 148:501–508.  
519
- 520 Gitelson, A., Zur, Y., Chivkunova, O., & Merzlyak, M. 2002. Assessing carotenoid content in  
521 plant leaves with reflectance spectroscopy. *Photochemistry and Photobiology*. 75:272-281.  
522
- 523 Gitelson, A.A., A. Via, T.J. Arkebauer, D.C. Rundquist, G. Keydan, and B. Leavitt. 2003b.  
524 Remote estimation of leaf area index and green leaf biomass in maize canopies. *Geophys. Res.*  
525 *Lett.* 30:1248.  
526
- 527 Gitelson, A.A., and M.N. Merzlyak. 1994. Quantitative estimation of chlorophyll-a using  
528 reflectance spectra: Experiments with autumn chestnut and maple leaves. *J. Photochem.*  
529 *Photobiol.* 22:247–252.  
530
- 531 Gitelson, A.A., G.P. Keydan, and M.N. Merzlyak. 2006. Tree-band model for noninvasive  
532 estimation of chlorophyll, carotenoids, and anthocyanin contents in higher plant leaves.  
533 *Geophys. Res. Lett.* 33:111402 .  
534
- 535 Gitelson, A.A., M.N. Merzlyak, and O.B. Chivkunova. 2001. Optical properties and non-  
536 destructive estimation of anthocyanin content in plant leaves. *Photochem.Photobiol.* 74:38–45.  
537
- 538 Gitelson, A.A., Thenkabail, P.S., Lyon, J.G., Huete, A. 2011. Remote Sensing estimation of crop  
539 biophysical characteristics at various scales. Chapter 15 in *Hyperspectral Remote Sensing of*  
540 *Vegetation*. 329-358, Taylor and Francis.  
541
- 542 Gutierrez, M., Reynolds, M., Raun, W., Stone, M., and Klatt, A. 2010. Spectral water indices for  
543 assessing yield in elite bread wheat genotypes under well-irrigated, water-stressed, and high-  
544 temperature conditions. *Crop Science*. 50:197-214.  
545
- 546 Gutierrez-Rodriguez, M., Reynolds, M.P., Escalante-Estrada, J.A., Rodriguez-Gonzalez, M.T.  
547 2004. Association between canopy reflectance indices and yield and physiological traits in bread  
548 wheat under drought and well-irrigated conditions. *Australian Journal of Agricultural Research*  
549 55:1139–1147.  
550
- 551 Hansen, P.M., and Schjoering, J.K. 2003. Reflectance measurement of canopy biomass and  
552 nitrogen status in wheat crops using normalized difference vegetation indices and partial least  
553 squares regression. *Remote Sens. Environ.* 86(4):542-553.

- 554  
 555 Hansen, P.M., Jorgenson, J.R., Thomsen, A. 2002. Predicting grain yield and protein content in  
 556 winter wheat and spring barley using repeated canopy reflectance measurements and partial least  
 557 squared regression. *J. of Ag Sci.* 139:307-318.
- 558  
 559 Hatfield, J. L., Gitelson, A.A., Schepers, J.S., and Walthall, C. L. 2008. Application of Spectral  
 560 Remote Sensing for Agronomic Decisions. *Papers in Natural Resources*. Paper 257.  
 561
- 562 Hatfield, J., & Prueger, J. 2010. Value of using different vegetative indices to quantify  
 563 agricultural crop characteristics at different growth stages under varying management practices.  
 564 *Remote Sensing*, 2:562-578.
- 565 Hatfield, J.L. 1983. Remote sensing estimators of potential and actual crop yield. *Remote Sens.*  
 566 *Environ.* 13:301–311.
- 567 Hatfield, J.L., J.E. Quisenberry, and R.E. Dilbeck. 1987. Use of canopy temperatures to identify  
 568 water conservation in cotton germplasm. *Crop Sci.* 27:269–273.  
 569
- 570 Hendry, G.A.F., J.D. Houghton, and S.B. Brown. 1987. The degradation of chlorophyll-a  
 571 biological enigma. *New Phytol.* 107:255–302.  
 572
- 573 Holland, K.H., J.S. Schepers, and J.F. Shanahan. 2006. Configurable multispectral active sensor  
 574 for high-speed plant canopy assessment. In D.J.  
 575
- 576 Hong, S.Y., K.A. Sudduth, N.R. Kitchen, H.L. Palm, and W.J. Weibold. 2001. Using  
 577 hyperspectral remote sensing data to quantify within-field spatial variability [CD ROM].  
 578 *Proc. Int. Conf. on Geospatial Inf. in Agric. and Forestry*, 3rd, Denver, CO. 5–7 Nov. 2001.  
 579 Altatum, Ann Arbor, MI.  
 580
- 581 Huete, A., Didan, K., Miura, T., Rodriguez, E.P., Gao, X., Ferreira, L.G. 2002. Overview of the  
 582 radiometric and biophysical performance of the MODIS vegetation indices. *Remote Sens. Of*  
 583 *Environment*, 83:195-213.  
 584
- 585 Inman, D., Khosla, R., Reich, R., and Westfall, D. 2007. Active remote sensing and grain yield  
 586 in irrigated maize. *Precision Agriculture*. 8:241-252.
- 587 Inoue, Y., and Peñuelas, J. 2006. Relationship between light use efficiency and photochemical  
 588 reflectance index in soybean leaves as affected by soil water content. *International J. of Remote*  
 589 *Sens*, 27:5109–5114.  
 590
- 591 Jackson, R.D., S.B. Idso, R.J. Reginato, and P.J. Pinter, Jr. 1981. Canopy temperature as a crop  
 592 water stress indicator. *Water Resour. Res.* 17:1133–1138.  
 593
- 594 Jones, H.G., R. Serraj, B.R. Loveys, L. Xiong, A. Wheaton, A.H. Price. 2009. Thermal infrared  
 595 imaging of crop canopies for the remote diagnosis and quantification of plant responses to water  
 596 stress in the field. *Functional Plant Biol.* 36:978-989.

- 597  
598 Jordan, C.F. 1969. Derivation of leaf area index from quality of light on the forest floor. *Ecology*  
599 50:663–666.  
600
- 601 Kaul, M., R.L. Hill, C. Walthall. 2005. Artificial neural networks for corn and soybean yield  
602 prediction. *Agricultural Systems* 85:1-18.  
603
- 604 Kumar, R., and L. Silva. 1973. Light ray tracing through a leaf cross-section. *Appl. Optics*  
605 12:2950–2954.  
606
- 607 Lewis, J.E., Rowland, J., Nadeau, A., 1998. Estimating maize production in Kenya using NDVI:  
608 some statistical considerations. *Int. J. Remote Sens.* 13, 2609–2617.  
609
- 610 Lin, W.S., C.M. Yang, B.J. Kuo. 2012. Classifying cultivars of rice (*Oryza sativa* L.) based on  
611 corrected canopy reflectance spectra data using the orthogonal projections of latent structures (O-  
612 PLS) method. *Chemometrics and Intelligent Laboratory Systems*, 115:25-36.  
613
- 614 Ma, B.L., Dwyer, L.M., Costa, C., Cober, E.R., Morrison, M.J. 2001. Early Prediction of  
615 Soybean yield from canopy reflectance measurements. *Agron. J.* 93:1227-1234.  
616
- 617 Marti, J., Bort, J., Slafer, G., & Araus, J. 2007. Can wheat yield be assessed by early  
618 measurements of normalized difference vegetation index? *Annals of Applied Biology.* 150:253-  
619 257.
- 620 McKinney, N.V., Schapaugh, W.T., Kanemasu, E.T. 1989. Canopy temperature, seed yield, and  
621 vapor pressure deficit relationships in soybean. *Crop Sci.* 29:1038-1041.  
622
- 623 Merzlyak M.N., Gitelson A.A. 1995. Why and what for the leaves are yellow in autumn? On the  
624 interpretation of optical spectra of senescing leaves (*Acer platanoides* L.). *J Plant Physiol* 145:  
625 315–320.  
626
- 627 Merzlyak MN, Gitelson AA, Chivkunova OB, Rakitin VY. 1999. Non-destructive optical  
628 detection of pigment changes during leaf senescence and fruit ripening. *Physiologia Plantarum*  
629 106:135–141.  
630
- 631 Montes, J.M., Melchinger, A.E., Reif, J.C. 2007. Novel throughput phenotyping platforms in  
632 plant genetic studies. *Trends in Plant Sci.* 12(10):433-436.  
633
- 634 Moran, J.A., A.K. Mitchell, G. Goodmanson, and K.A. Stockburger. 2000. Differentiation  
635 among effects of nitrogen fertilization treatments on conifer seedlings by foliar reflectance: A  
636 comparison of methods. *Tree Physiol.* 20:1113–1120.  
637
- 638 Osborne, S., Schepers, J., Francis, D., and Schlemmer, M. 2002. Use of spectral radiance to  
639 estimate in-season biomass and grain yield in nitrogen- and water-stressed corn. *Crop Science*,  
640 42:165-171.

- 641 Percy, R.W., Ehleringer, J.R., Mooney, H.A., Rundel P.W. 1989. Measurement of transpiration  
642 and leaf conductance. In Percy et al. *Plant Physiological Ecology: Field methods and*  
643 *instrumentation*. 137-160.  
644
- 645 Peñuelas, J., & Filella, I. 1998. Visible and near-infrared reflectance techniques for diagnosing  
646 plant physiological status. *Trends in Plant Science*, 3:151-156.
- 647 Peñuelas, J., F. Baret, and I. Filella. 1995. Semi-empirical indices to assess  
648 carotenoids/chlorophyll a ratio from leaf spectral reflectance. *Photosynthetica* 31:221–230.  
649
- 650 Peñuelas, J., Filella, I., Biel, C., Serrano, L., & Save, R. 1993. The reflectance at the 950– 970  
651 mm region as an indicator of plant water status. *International Journal of Remote Sensing*, 14,  
652 1887–1905.  
653
- 654 Peñuelas, J., R. Isla, I. Filella, and J.L. Araus. 1997. Visible and near infrared reflectance  
655 assessment of salinity effects on barley. *Crop Sci.* 35:1400–1405. *Sci.* 37:198–202.  
656
- 657 Pimstein, A., Karnieli, A., & Bonfil, D. 2007. Wheat and maize monitoring based on ground  
658 spectral measurements and multivariate data analysis. *Journal of Applied Remote Sensing*.  
659 1:013530.
- 660 Pimstein, A., Karnieli, A., Bansal, S., & Bonfil, D. 2011. Exploring remotely sensed  
661 technologies for monitoring wheat potassium and phosphorus using field spectroscopy. *Field*  
662 *Crops Research*. 121:125-135.
- 663 Poss, J., Russell, W., & Grieve, C. 2006. Estimating yields of salt- and water-stressed forages  
664 with remote sensing in the visible and near infrared. *Journal of Environmental Quality*. 35:1060-  
665 1071.
- 666 Prasad, B., Carver, B., Stone, M., Babar, M., Raun, W., & Klatt, A. 2007a. Genetic analysis of  
667 indirect selection for winter wheat grain yield using spectral reflectance indices. *Crop Science*.  
668 47:1416-1425.
- 669 Prasad, B., Carver, B., Stone, M., Babar, M., Raun, W., & Klatt, A. 2007b. Potential use of  
670 spectral reflectance indices as a selection tool for grain yield in winter wheat under great plains  
671 conditions. *Crop Science*. 47: 1426-1440.
- 672 Price, J.C., and W.C. Bausch., 1995. Leaf area index estimation from visible and near-infrared  
673 reflectance data. *Remote Sens of Environ.* 52:55–65.  
674
- 675 Reynolds, M., Dreccer, F., and Trethowan, R. 2007. Drought-adaptive traits derived from wheat  
676 wild relatives and landraces. *J. Exp. Bot.* 58: 177–186.  
677
- 678 Reynolds, M., Manes, Y., Izanloo, A., Langridge, P. 2009. Phenotyping approaches for  
679 physiological breeding and gene discovery in wheat. *Annals of Appl. Bio.* 155(3):309-320.  
680

- 681 Reynolds, M.P., M. Balota, M.I.B. Delgado, I. Amani and R.A. Fischer. 1994. Physiological and  
 682 morphological traits associated with spring wheat yield under hot, irrigated conditions. *Aust. J.*  
 683 *Plant Physiol.* 21:717–730.
- 684  
 685 Reynolds, M.P., S. Rajaram and K.D. Sayre. 1999. Physiological and genetic changes of  
 686 irrigated wheat in the post-green revolution period and approaches for meeting projected global  
 687 demand. *Crop Sci.* 39:1611–1621.
- 688  
 689 Richards, R. A., G. J. Rebetzke, A. G. Condon, and G. D. Farquhar. 2002. Breeding  
 690 opportunities for increasing the efficiency of water use and crop yield in temperate cereals. *Crop*  
 691 *Sci.* 42: 111-121.
- 692  
 693 Richards, R.A., A. G. Condon, and G.J. Rebetzke. 2001. Traits to improve yield in dry  
 694 environments. P. 88-100. In *Application of physiology in wheat breeding*. CIMMYT, Mexico.
- 695  
 696 Richardson, A.D., S.P. Duigan, and G.P. Berlyn. 2002. An evaluation of noninvasive methods to  
 697 estimate foliar chlorophyll content. *New Phytol.* 153:185–194.
- 698  
 699 Ries, L.L., L.C. Purcell, T.E. Carter Jr., J.T. Edwards, C.A. King. 2012. Physiological traits  
 700 contributing to differential canopy wilting in soybean under drought. *Crop Sci.* 52: 272-281.
- 701  
 702 Ritchie, G., Sullivan, D., Vencill, W., Bednarz, C., & Hook, J. 2010. Sensitivities of normalized  
 703 difference vegetation index and a Green/Red ratio index to cotton ground cover fraction. *Crop*  
 704 *Science*, 50:1000-1010.
- 705  
 706 Rouse, J.W., Jr., R.H. Haas, J.A. Schell, and D.W. Deering. 1973. Monitoring vegetation  
 707 systems in the Great Plains with ERTS. p. 309–317. In *Proc. Earth Res. Tech. Satellite-1 Symp.*,  
 708 Goddard Space Flight Cent., Washington, DC. 10–14 Dec. 1973.
- 709  
 710 Royo, C., Aparicio, N., Villegas, D., Casadesus, J., Monneveux, P., & Araus, J. 2003. Usefulness  
 711 of spectral reflectance indices as durum wheat yield predictors under contrasting Mediterranean  
 conditions. *International Journal of Remote Sensing.* 24:4403-4419.
- 712  
 713 Sayre, K.D., S. Rajaram, and R.A. Fischer. 1997. Yield potential progress in short bread wheat in  
 Northern Mexico. *Crop Sci.* 37: 36–42.
- 714  
 715 Schepers, J.S., T.M. Blackmer, W.W. Wilhelm, and M. Resende. 1996. Transmittance and  
 716 reflectance measurements of corn leaves from plants with different nitrogen and water supply. *J.*  
 717 *Plant Physiol.* 148:523–529.
- 718  
 719 Serrano, L., I. Filella, and J. Peñuelas. 2000. Remote sensing of biomass and yield of winter  
 720 wheat under different nitrogen supplies. *Crop Sci.* 40:723–731.
- 721  
 722 Shanahan, J.F., J.S. Schepers, D.D. Francis, G.E. Varvel, W.W. Wilhelm, J.S. Tringe, M.R.  
 723 Schlemmer, and D.J. Major. 2001. Use of remote sensing imagery to estimate corn grain yield.  
 724 *Agron. J.* 93:583–589.



- 725  
726 Sims, D.A., and J.A. Gamon. 2002. Relationship between leaf pigment content and spectral refl  
727 ectance across a wide range species, leaf structures and development stages. *Remote Sens.*  
728 *Environ.* 81:337–354.  
729
- 730 Tanner, C.B. 1963. Plant temperature. *Agron. J.* 55:210–211.  
731
- 732 Thenkabail PS, Smith RB, De Pauw E. 2002. Evaluation of narrowband and broadband  
733 vegetation indices for determining optimal hyperspectral wavebands for agricultural crop  
734 characterization. *Photogrammetric Engineering and Remote Sensing* 68: 607–621.  
735
- 736 Thomas, J.R., and G.F. Oerther. 1972. Estimating nitrogen content of sweet pepper leaves by  
737 reflectance measurements. *Agron. J.* 64:11–13.  
738
- 739 Thomas, J.R., and H.W. Gausman. 1977. Leaf reflectance vs. leaf chlorophyll and carotenoid  
740 concentrations for eight crops. *Agron. J.* 69:799–802.  
741
- 742 Trotter, G. M., Whitehead, D., & Pinkney, E. J. 2002. The photochemical reflectance index as a  
743 measure of photosynthetic light use efficiency for plants with varying foliar nitrogen contents.  
744 *International J. of Remote Sens.* 23:1207–1212.  
745
- 746 Tucker, C. J. 1980. Remote sensing of leaf water content in the near infrared. *Remote Sensing of*  
747 *Environment*, 10:23– 32.  
748
- 749 Tucker, C. J. and Sellers, P. J. 1986. Satellite remote sensing of primary production. *International*  
750 *Journal of Remote Sensing.* 7:395-1416.  
751
- 752 Tucker, C. J., 1978. A comparison of satellite sensors for monitoring vegetation. *Photogr. E. R.*  
753 44: 1369-1380.
- 754 Tucker, C.J. 1979. Red and photographic infrared linear combinations for monitoring vegetation.  
755 *Remote Sens. Environ.* 8:127–150.  
756
- 757 Vina, A., & Gitelson, A. 2011. Sensitivity to foliar anthocyanin content of vegetation indices  
758 using green reflectance. *IEEE Geoscience and Remote Sensing Letters.* 8:464-468.
- 759 Waddington, S.R., J.K. Ransom, M. Osmanzai, and D.A. Saunders. 1986. Improvement in the  
760 yield potential of bread wheat adapted to Northwest Mexico. *Crop Sci.* 26:698–703.  
761
- 762 Walburg, G., M.E. Bauer, C.S.T. Daughtry, and T.L. Housley. 1982. Light-use efficiency of a  
763 winter wheat crop subjected to N and water deficiencies. *Agron. J.* 74:677–683.  
764
- 765 Walter, A., B. Studer, R. Ko'lliker. 2012. Advanced phenotyping offers opportunities for  
766 improved breeding of forage and turf species. *Annals of Botany.* 1-9.  
767

- 768 Weber, V.S., J.L. Araus, J.E. Cairns, C. Sanchez, A.E. Melchinger, E. Orsini. 2012. Prediction of  
769 grain yield using reflectance spectra of canopy and leaves in maize plants grown under different  
770 water regimes. *Field Crops Research*. 128: 82-90.  
771
- 772 Wessman, C. A. 1990. Evaluation of canopy biochemistry. In *Remote Sensing of Biosphere*  
773 *Functioning*. Eds R. J. Hobbs & H. A. Mooney. 135–156.  
774
- 775 White, J.W., P. Andrade-Sanchez, M.A. Gore, K.F. Bronson, T.A. Coffelt, M.M. Conley, K.A.  
776 Feldmann, A.N. French, J.T. Heun, D.J. Hunsake, M.A. Jenks, B.A. Kimball, R.L. Roth, R.J.  
777 Strand, K.R. Thorp, G.W. Wall, G. Wang. 2012. Field-Based phenomics for plant genetics  
778 research. *Field Crops Research*. 133:101-112.  
779
- 780 Wiegand, C., Richardson, A., Escobar, D., and Gerbermann, A. 1991. Vegetation indexes in crop  
781 assessment. *Remote Sensing of Environment*. 35:105-119.
- 782 Zarco-Tejada, P. J., Miller, J. R., Noland, T. L., Mohammed, G. H., and Sampson, P. H. 2001.  
783 Scaling-up and model inversion methods with narrow-band optical indices for chlorophyll  
784 content estimation in closed forest canopies with hyperspectral data. *IEEE Transactions on*  
785 *Geosciences and Remote Sensing*. 39:1491–1507.  
786
- 787 Zhao, D., K.R. Reddy, V.G. Kakani, J.J. Read, S. Koti. 2007. Canopy reflectance in cotton for  
788 growth assessment and lint yield prediction. *Europ. J. Agronomy*, 26:335-344.  
789  
790  
791  
792  
793  
794  
795  
796  
797  
798  
799  
800  
801  
802  
803  
804  
805  
806  
807  
808  
809  
810  
811

## 812 **Chapter 2 - Characterizing Changes in Soybean Spectral Response** 813 **Curves with Breeding Advancements**

### 814 **Abstract**

815 Soybean (*Glycine max* (L.) Merr.) crop yield has steadily increased in the past 60 years  
816 due in part to breeding advances. Spectral reflectance correlated to specific plant  
817 functions may help characterize the impact of breeding on soybean cultivar development.  
818 The objectives of this study were: 1) to find specific regions of the soybean spectra  
819 response curves that show genotypic differences; and 2) to determine the effect of the  
820 breeding process on spectral response curves of soybean cultivars. Spectral reflectance  
821 measurements were taken on 20 maturity group III (MGIII) and 20 maturity group IV  
822 (MGIV) soybean genotypes ranging in release year from 1923 to 2010 (arranged in a  
823 randomized complete block design) in 2011 and 2012 in Manhattan, KS. Significant  
824 genotypic differences were found between entries, especially in the green (500 nm– 600  
825 nm), red (600 nm–700 nm), and red-edge (700nm–730 nm) portions of the spectra. This  
826 study also found significant correlations with year of release (YOR) in the visible (VIS)  
827 and near-infrared (NIR) spectra. The newer released cultivars tended to have lower  
828 reflectance values in the VIS and red-edge spectra portions and higher values in the NIR  
829 portion of the spectra than older cultivars. This study concluded that breeding has most  
830 affected spectral reflectance curves by reducing the VIS portion of the spectra and  
831 extending the red-edge, resulting in a shift to lower reflectance values further into the  
832 NIR and then a sharp inflection to the NIR, with higher values in the NIR. In addition, a  
833 crossover occurs in new genotypes around 1150 nm, resulting in lower reflectance values  
834 in the transition from the NIR to the middle infrared. These results suggest that breeding

835 advancement has had an impact on spectral reflectance curves and the areas that have  
836 been changed with breeding advancement may be exploited for further advancement.

### 837 **Introduction**

838 One way to characterize plant phenotypes and function is by measuring spectral  
839 reflectance. The amount of reflectance observed is a product of the leaf tissues, cellular structure,  
840 and air-cell wall–protoplast-chloroplast interaction (Kumar and Silva, 1973). The visible (VIS)  
841 portion of the spectra (400–730 nm) have low reflectance due to the absorptive attributes of  
842 chlorophyll and other accessory pigments such as carotenoids, carotenes, and anthocyanins;  
843 however, the near-infrared portion (NIR) has a high reflectance caused by the scattering of light  
844 by cellular components and water. Many of the physiological parameters that show genotypic  
845 variation — most of which are pigment concentration and status — pertain to biochemical  
846 parameters (Reynolds et al., 2009). The photosynthetic capacity and efficiency of a plant is a  
847 function of the chlorophyll and other pigment content of the plant. Chlorophyll status can also be  
848 used to estimate biomass production and photosynthetic capacity (Curran et al., 1990; Filella et  
849 al., 1995), and, because chlorophyll content is directly influenced by nitrogen, chlorophyll status  
850 estimation can relate directly to nitrogen status (Filella et al., 1995; Moran et al., 2000). By  
851 modeling the leaf structure and content, researchers can make inferences about the plant’s health  
852 and desired attributes, such as photosynthetic capabilities and water status (Thomas and  
853 Gausman, 1977; Wessman, 1990). Researchers also have estimated yield through other plant  
854 characteristics such as chlorosis (Adams et al., 1999), green cover (Dusek et al., 1985; Daughtry  
855 et al., 2000), chlorophyll (Datt, 1999; Daughtry et al., 2000), photosynthetically active tissue  
856 (Wiegand et al., 1991), and water status (Prasad et al., 2007a, 2007b).

857 Chlorophylls have a high absorbance in the red (600–700 nm) and blue (400–500 nm)  
858 regions of the spectrum. Chlorophyll b preferentially absorbs light in the 460 and 650 nm  
859 regions, chlorophyll a absorbs in the 580, 630, and 670 nm regions of the spectrum, and 415 nm  
860 is a preferential absorption of both in soybean (Chappelle et al., 1992). Blue spectrum regions  
861 also correlate to carotenoid preferential absorption and therefore are not commonly used in  
862 chlorophyll concentration and status estimates (Sims and Gamon, 2002). The green and red  
863 regions of the spectrum—around 550 nm and 700 nm, respectively—are primarily used, due to  
864 high chlorophyll concentrations needed to saturate these wavelengths (Sims and Gamon, 2002).  
865 Shanahan et al. (2001) explained from 70 to 92% of yield variability at mid-grain fill in corn  
866 using the green region and NIR. Sims and Gamon (2002) correlated the 700 nm region to  
867 chlorophyll concentration, which is used by many researchers as a baseline for new chlorophyll  
868 indices. The ratio  $(R_{531}-R_{570})/(R_{531}+R_{570})$  has been widely used to characterize leaf pigment  
869 status in many species (Gamon et al., 1992; Peñuelas et al., 1995). Chappelle et al. (1992) found  
870 that wavebands 650, 675, and 700 nm could be used to predict chlorophyll ( $R^2 = 0.934$ ) and beta  
871 carotene ( $R^2 = 0.935$ ) in soybean leaves. Gitelson and Merzlyak (1994) used  $(R_{780}/R_{700})$  and  
872  $(R_{750}-R_{705}/R_{750}+R_{705})$  to explain as much as 98% of the variability within chlorophyll content in  
873 chestnut and maple trees. The normalized difference vegetation index (NDVI) derived by  
874 Deering (1978) and Tucker (1979) to estimate green biomass and intercepted PAR, defined as  
875  $(R_{NIR}-R_{RED}/R_{NIR}+R_{RED})$ , has been used to predict yield and other plant functions with many crops  
876 using hyperspectral and satellite imagery (Wiegand et al., 1991; Peñuelas et al. 1997; Ma et al.  
877 2001; Shanahan et al. 2001; Royo et al. 2002; Royo et al. 2003; Prasad et al. 2007a, 2007b; Marti  
878 et al. 2007). Ma et al. (2001) explained up to 80% of the yield variability in soybean using 613  
879 and 813 nm. Others have also used the 550 and 700 nm regions of the spectrum when leaves are

880 yellow-green (Gitelson and Merzlyak, 1996; Datt 1998; Gamon and Surfus, 1999; Sims and  
881 Gamon, 2002) to estimate chlorophyll status and yield, but high absorption in these regions may  
882 lead to saturation at relatively low chlorophyll concentrations. Gamon and Surfus (1999)  
883 developed a model and indices for anthocyanin concentration estimation based on a red-to-green  
884 ratio,  $R_{600}-R_{700}/R_{500}-R_{600}$ , and Viña and Gitelson (2011) used broadband wavelengths to estimate  
885 anthocyanin status ( $R^2 = 0.25 - 0.89$ ) with peak absorption around 540 to 560 nm.

886 Plant water status and stress through the preferential absorption of water and, more specifically,  
887 the hydroxyl ions within the electromagnetic spectrum also can be used to characterize plants  
888 (Peñuelas et al., 1993; Peñuelas et al., 1997; Gao, 1996; Serrano et al., 2000). The NIR (700–  
889 1300) and middle infrared (1300–2500 nm) ranges have been shown to correlate well with water  
890 status or content of plants and the wavelengths 970, 1240, 1400, and 2700 nm have been  
891 proposed as water absorption bands (Peñuelas et al., 1993; Gao, 1996; Gutierrez et al., 2010).  
892 Babar et al. (2006a, 2006b) used the wavelengths developed by Peñuelas et al. (1993) and found  
893 them useful for screening wheat genotypes for water stress and water-use efficiency. Prasad et al.  
894 (2007a, 2007b) used the wavelengths 970, 920, 900, 880, and 850 nm to screen winter wheat  
895 lines under dryland conditions and found significant correlations with yield. Gao (1996)  
896 normalized wavebands ( $R_{860}-R_{1240}/R_{860}+R_{1240}$ ) and evaluated water stress in corn and soybean,  
897 with favorable results.

898         Spectral reflectance correlated to specific plant functions may help characterize the  
899 impact of breeding on soybean cultivar development. The objectives of this study were: 1) to find  
900 specific regions of the soybean spectral response curves that show genotypic differences and  
901 could be exploited for genotype distinction; and 2) to determine the effect of the breeding  
902 process on spectral response curves of soybean cultivars released from 1923 to 2010.

## 903 **Materials and Methods**

### 904 ***Experimental and Field Design***

905 A study was conducted on soybean [*Glycine max.* (L) Merr.] at the Kansas State  
906 University Research farm south of Manhattan, KS, in 2011 and 2012. In 2011, experiments  
907 (location A) were conducted on a well-drained silt loam soil of the Eudora and Belvue types. In  
908 2012, location B was a well-drained silt loam soil of the Bismarckgrove-Kimo complex, and  
909 location C was a well-drained silt-sandy loam soil of the Belvue and Eudora types.

910 Twenty maturity group III (MGIII) and 20 maturity group IV (MGIV) soybean cultivars,  
911 ranging in release year from 1923 to 2010 (Table 1), were selected for release-year diversity out  
912 of the Soybean Genetic Gain Study coordinated by Dr. Brian Diers, University of Illinois.  
913 Selected cultivars were a mixture of private and public genotypes.

914 Replicated plots were planted on 23 May 2011 on field A, and 16 May 2012 and 4 June  
915 2012 on fields B and C, respectively. Each experimental unit consisted of 4 rows (3.4 meter  
916 long; spaced 76 cm apart). Genotypes were planted in separate well-watered and water-stressed  
917 environments arranged in a randomized complete block design with four replications. In both  
918 years, weed pressure and fertility were not limiting. Flood irrigation was applied to the well-  
919 watered environments starting at reproductive stage 1 (R1) and continued weekly until R6. In  
920 2011, no supplemental irrigation was applied to the water-stressed environments. Due to  
921 extremely dry conditions, irrigation was applied once shortly after R1 in 2012 to ensure crop  
922 development in the water-stressed environments.

### 923 ***Phenotypic Traits***

924 Maturity, height, and lodging were taken on all plots during both seasons. Maturity was  
925 calculated as the number of days past 31 August when 95% of the pods had reached mature plant

926 color. Height (cm) was measured as the distance from the base of the plant to the top of the main  
927 stem. Lodging was scored on a scale of 1 to 5, based on the amount of leaning or broken plants.  
928 Upright plants with no lean were scored as 1; other scores were 2 = 20° lean, 3 = 45° lean, 4 =  
929 60° lean, and 5 = flat on the ground. The center two rows of each plot were mechanically  
930 harvested using a 2-row plot combine. Seed yield was recorded as  $\text{kg ha}^{-1}$ , adjusted to uniform  
931 moisture.

### 932 *Canopy Reflectance Measurements*

933 Canopy reflectance measurements were conducted using an ASD FieldSpec 3  
934 spectroradiometer (Analytical Spectral Devices, Boulder, CO). Solar radiation reflecting back  
935 from the plant canopy was captured from 350 to 2500 nm in the electromagnetic spectrum using  
936 fiber optics with a 25° field of view and sampling intervals of 1.4 nm between 350 and 1050 nm  
937 and 2 nm between 1050 and 2500 nm. Moving averages were calculated automatically to achieve  
938 1-nm-width continuous bands. A white calibration disk ( $\text{BaSO}_4$ ) was used to achieve reflectance  
939 percentages and to calibrate the spectroradiometer with a dark current and white reference every  
940 40 plots or when needed (ranging from every plot to 40 plot intervals, depending on field  
941 conditions). The sensor was mounted on an adjustable monopod pole and held vertically 1 m  
942 above the canopy to achieve a 50-cm circumference collection area. Two measurements were  
943 taken per plot on rows 2 and 3, excluding the first meter of each plot to eliminate border effect.  
944 Each measurement was the average of 10 scans, which was calculated automatically. Spectral  
945 data were collected on nearly cloud-free days within  $\pm 2$  hours of solar noon. Measurements were  
946 collected weekly from R3–R6 in 2011 and R2–R6 in 2012 (Fehr and Caviness, 1977), totaling  
947 three and four collection dates for the water-stressed and well-watered environments in 2011,  
948 respectively. In 2012, there were five collection dates for the well-watered MGIV environment



949 on field B and four collection dates for the well-watered MGIII experiment on field B and well-  
950 watered MGIII and MGIV experiments on field C. There were three collection dates for the  
951 water-stressed experiment on field B, but only two collection dates for the water-stressed  
952 environment on field C for each maturity group.

### 953 *Data Pretreatment*

954 Hyperspectral data were initially trimmed from 350–2500 nm to 400–1310 nm, which  
955 was necessary to eliminate noise from atmospheric absorption regions focused around the water  
956 absorption bands in the infrared and atmospheric scatter of blue color in the ultraviolet portion of  
957 the spectrum. Before averages were calculated for observation day and season totals, initial  
958 outlier control was implemented on each observation day's raw data. After outliers were  
959 identified and excluded from analysis, data were combined to form 10-nm-wide band regions to  
960 reduce the dataset size and eliminate some of the collinearity associated with bands in close  
961 proximity (Naes et al., 2004). Combined bands have been determined to contain less variation  
962 from sample to sample than single-band measurements (Lin et al., 2012).

### 963 *Statistical Analyses*

964 All data were analyzed using SAS 9.2 (SAS Institute, 2008). The GLIMMIX procedure  
965 of SAS (SAS Institute, 2008) was used for analysis of variance (ANOVA) of yield. Cultivar and  
966 experiment were treated as fixed effects and replication nested within the experiment was treated  
967 as a random effect. PROC GLM was used for ANOVA of the wavebands. Spectral data were  
968 analyzed for significant difference between genotypes using the genotype  $\times$  environment  
969 interaction as the error term. PROC CORR was used to characterize the relationship between  
970 YOR and each waveband.

971

## Results and Discussion

### *Genotypic Performance for Yield and Reflectance Data*

972  
973  
974 Genotypes differed significantly in average seed yield across the six environments in both  
975 maturity groups (Table 2.1). Seed yield ranged from 2.32 to 4.63 t ha<sup>-1</sup> and 1.97 to 4.26 t ha<sup>-1</sup> for  
976 the MGIII and MGIV experiments, respectively. Seed yield increased with year of release by  
977 0.0238 and 0.0255 t ha<sup>-1</sup> year<sup>-1</sup> and had coefficient of determination values of 82 and 86%  
978 between yield and YOR in MGIII and MGIV, respectively (Figure 2.1). Yield increases are  
979 consistent with observations of short-season soybean covering 58 years of cultivar development  
980 (Morrison et al., 1999). Significant differences between genotypes, environments, and genotype  
981 × environment interaction were observed for seed yield ( $P < 0.0001$ ) in both maturity groups  
982 (Table 2.2). The genotype × environment interactions were quite low compared with the total  
983 phenotypic variation of each maturity group experiment because the genotypes tested were  
984 genetically diverse with a large gradient between high-yielding and low-yielding genotypes.

985 Significant differences ( $P < 0.05$ ) were detected between genotypes for individual band  
986 regions in both maturity groups, with the exception of 905 nm in MGIII (Table 2.3). In the  
987 MGIII experiment, Illini was eliminated from spectral analysis due to spectral inconsistencies  
988 from lodging and soil confounds. The VIS portion of the spectrum (405–695 nm) had greater  
989 genotypic differences than the NIR (705–1305 nm) in both maturity groups. The highest  
990 genotypic differences (based on F values) were observed in the green and red portions of the  
991 spectrum in both maturity groups. In the MGIII and MGIV experiments, the 735 to 1135 nm  
992 region was the least significant portion of the spectrum. Large G × E interactions and high  
993 variability in the NIR from cellular scatter can account for the decreased genotypic differences  
994 observed for this region. The MGIV experiment had higher genotypic differences observed than

995 the MGIII experiment because  $G \times E$  interactions constituted less of the total phenotypic  
996 variation.

997         Spectral responses varied based on YOR in both maturity groups. The earliest released  
998 cultivars tended to have higher values in the VIS portion of the spectrum and lower values in the  
999 NIR than the latest released cultivars (Figures 2.2 and 2.3). Maturity group spectral curves were  
1000 similar in magnitude. High values for group VIS suggests that chlorophyll and other associated  
1001 pigments are not as plentiful or efficient in the earlier cultivars, and higher values in the green  
1002 correlates with more yellow pigment and therefore more foliar diseases or issues contributing to  
1003 decreased plant function. These results are consistent with trends observed in soybean (Ma et al.,  
1004 2001), corn (Chang et al., 2003; Weber et al., 2012), wheat (Hansen et al., 2002), and rice (Lin et  
1005 al., 2012). Higher reflectance in the NIR suggests more biomass production or denser canopy  
1006 and cellular structure in the later cultivars (Sims and Gamon, 2003; Royo et al., 2003). In the  
1007 MGIV experiment, greater separation was observed between cultivars in the 735– 1095 nm—an  
1008 area correlated with brown pigmentation, biomass production, and water status—than in the  
1009 MGIII experiment (Figure 2.3). Observed results suggest that foliar diseases and maturity play a  
1010 larger role in MGIV than in MGIII. The MGIII experiment genotypes separate much more in the  
1011 1155–1305 nm regions (Figure 2.2), which have been associated with biomass production, water  
1012 content, and water status. In both experiments, genotypes tended to be stable in the VIS and NIR:  
1013 entries exhibited high reflection in the VIS but lower NIR reflection values. Weber et al. (2012)  
1014 found a crossover in the water content region and concluded that lower values in this region  
1015 correlated with high-yielding corn cultivars. A water-content region crossover was also observed  
1016 in this experiment, which validates Weber et al.’s assertion for soybean and suggests that the  
1017 crossover region may be a candidate for genotypic differentiation.

### 1018 *Correlation of Spectral Reflectance Data to Year of Release*

1019 Many of the genotypic differences in spectral reflectance were significantly correlated (r)  
1020 to YOR (Figure 2.4). Compared with the NIR portion of the spectrum, highest r values were  
1021 observed in the VIS portion in both experiments. The green (505-595 nm), red (605–695 nm),  
1022 and red-edge (705–735 nm) regions of spectrum ( $r = -0.79$  to  $-0.83$ ,  $r = -0.76$  to  $-0.85$ , and  $r = -$   
1023  $0.76$  to  $-0.88$  respectively) exhibited the highest correlations with YOR in both MG genotypes  
1024 (Figure 4). The NIR was not as consistent between maturity groups: the 1155–1305 nm had  
1025 significant association with YOR in the MGIII experiment and the 765–1125 nm regions in the  
1026 MGIV experiment.

1027 For the MGIII experiment, r values ranging from  $-0.88$  to  $0.6$  were observed for  
1028 waveband to YOR correlation. For the MGIV experiment, r values ranged from  $-0.93$  to  $0.60$ .  
1029 The green and red regions correlate with the green reflection and red absorption by chlorophyll  
1030 and other photosynthetic pigments. The blue portion of the spectrum (405–495) also had  
1031 significant correlation with YOR ( $r = -0.61$  to  $-0.77$ ) in the MGIII and MGIV ( $r = -0.53$  to  $-0.93$ )  
1032 because of absorption peaks in chlorophyll a and b and beta carotene within soybean leaves in  
1033 this region (Chappelle et al., 1992). Wavebands in the blue also have been associated with  
1034 canopy temperature measurements. Canopy temperature has been shown to have a significantly  
1035 negative correlation with soybean YOR and yield. The blue region in field-based research tends  
1036 to be unreliable, however, due to atmospheric scatter of blue light; hence,  $r = -0.93$  in the MGIV  
1037 experiment seems like an unlikely result. Abnormally high reflectance values were obtained in  
1038 the 405 waveband region from some of the earlier-released cultivars. This result may be due to  
1039 atmospheric scatter or the tendency for older cultivars to lodge and allow soil confounds to  
1040 influence the spectra more.

1041           The red inflection region (705–735 nm) was highly significantly correlated with YOR in  
1042 the MGIII ( $r = 0.65$ – $0.84$ ) and MGIV ( $r = 0.79$ – $0.88$ ) experiments (Figure 2.4). In the MGIII  
1043 experiment, the 705-nm region had the highest correlation with year, but in the MGIV  
1044 experiment, the 715-nm region had the most significant correlation. Filella and Peñuelas (1994)  
1045 characterized the red-edge inflection point as the transition region between red and NIR, where a  
1046 sharp increase in reflection values are observed. They found that the region correlated well with  
1047 overall leaf health, in which the magnitude of the difference between the reflection values  
1048 between the red and NIR is a function of chlorophyll content and health, plant nitrogen status,  
1049 and plant water status. Plants with a steeper increase in reflection values between the two regions  
1050 have high chlorophyll content, high leaf area, and overall healthier vegetation. Weber et al.  
1051 (2012) found that the red-edge region contributed significantly to yield estimation, which  
1052 explains a significant portion of yield variation in corn cultivars. This study found negative  
1053 correlations between YOR and reflection values in this region. Compared with other cultivars, a  
1054 decrease in reflection is associated with a shift of the red edge to longer wavelengths, which  
1055 occurs because of increased chlorophyll content and increased biomass production (Filella and  
1056 Peñuelas, 1994).

1057           Near-infrared measurements were not as well correlated with YOR as the VIS spectrum,  
1058 but significant correlations were found between YOR and the NIR plateau (745–895 nm), as well  
1059 as the small water absorption region (915–1065 nm) in the MGIV entries. Decreased spectral  
1060 reflectance in the plateau region correlates with brown pigment (senescence), and significant  
1061 correlations ( $r = 0.32$  to  $0.60$ ) suggest that maturity and a higher incident of foliar diseases  
1062 occurred in the later (rather than the earlier) MGIV cultivars. The maturity factor may be due to  
1063 the extremely hot and dry conditions in 2011 and 2012 and an early frost in 2012, which

1064 prevented some MGIV cultivars from reaching full maturity. Visual observations indicated that  
1065 earlier-released MGIV cultivars tended to have more foliar issues leading to early senescence  
1066 and less green tissue due to insects and disease than earlier-released MGIII genotypes. The  
1067 plateau region has been shown to be associated with total biomass production, which suggests  
1068 that total biomass may have increased with YOR. As in the plateau region, the small water  
1069 absorption region had a positive relationship between YOR, and these band regions may suggest  
1070 that total water content has increased as breeders have made selections based on other  
1071 characteristics.

1072         This experiment found significant correlations with YOR in the 1100–1305-nm regions  
1073 in the MGIII entries but not in the MGIV genotypes. The 1100–1305-nm regions have been  
1074 associated with plant water status with high absorption and lower reflection of light by water  
1075 leading to greater water content within the plant leaf (Sims and Gamon, 2003). In this  
1076 experiment, later- released genotypes had a higher reflection in these regions than earlier-  
1077 released genotypes. Sims and Gamon (2003) concluded that thick canopies (such as those seen in  
1078 the newer-released cultivars) tend to confound water absorption regions, leading to increased  
1079 reflection values. The greater reflectance values would be expected because less light penetrates  
1080 thicker vegetation than thinner vegetation (Bull, 1991). Asrar et al. (1983) found that NIR and  
1081 red reflectance could be used for leaf area index (LAI) calculation (which measures  
1082 photosynthetically active tissue) and concluded that high reflectance in the NIR was associated  
1083 with higher LAI values in wheat. However, LAI values are highly influenced by soil  
1084 backgrounds, which could be an influence in the spectra obtained in this study. As visual  
1085 observations and observed higher values in the NIR have shown, a conclusion can be made that



1109 portion of the spectra and extending the red-edge, resulting in a shift to lower reflectance values  
1110 further into the NIR and then a sharp inflection to the NIR, with higher values in the NIR. In  
1111 addition, a crossover occurs in new genotypes around 1150 nm, resulting in lower reflectance  
1112 values in the transition from the NIR to the middle infrared. These results suggest that breeding  
1113 advancement has had an impact on spectral reflectance curves and the areas that have been  
1114 changed with breeding advancement may be exploited for further advancement. Caution should  
1115 be applied to certain aspects of spectral data because weather and soil confounds may lead to  
1116 inconsistent spectra. Nevertheless, spectral reflectance data may provide an indirect selection  
1117 tool for increasing genetic gain in yield of soybean cultivars.

## 1118 **References**

- 1119 Adams, M.L., W.D. Philpot, and W.A. Norvell. 1999. Yellowness index: an application of  
1120 spectral 2nd derivatives to estimate chlorosis of leaves in stressed vegetation. *Int. J. of*  
1121 *Remote Sensing* 20:3663–3675.
- 1122 Ashley, D.A., and H.R. Boerma. 1989. Canopy photosynthesis and its association with seed yield  
1123 in advanced generations of a soybean cross. *Crop Sci.* 29:1042–1045.
- 1124 Asrar, G., M. Fuchs, E.T. Kanemasu, and J.L. Hatfield. 1983. Estimating absorbed  
1125 photosynthetic radiation and leaf area index from spectral reflectance in wheat. *Agron. J.*  
1126 76:300–306.
- 1127 Austin, R.B. 1999. Yield of Wheat in the United Kingdom: Recent advances and prospects. *Crop*  
1128 *Sci.* 39:1604–1610.
- 1129 Babar, M., M. Reynolds, M. van Ginkel, A. Klatt, W. Raun, and M. Stone. 2006a. Spectral  
1130 reflectance indices as a potential indirect selection criteria for wheat yield under  
1131 irrigation. *Crop Sci.* 46(2):578–588.



- 1132 Babar, M., M. Reynolds, M. van Ginkel, A. Klatt, W. Raun, and M. Stone. 2006b. Spectral  
1133 reflectance to estimate genetic variation for in-season biomass, leaf chlorophyll, and  
1134 canopy temperature in wheat. *Crop Sci.* 46(3):1046–1057.
- 1135 Bull, C.R. 1991. Wavelength selection for near-infrared reflectance moisture meters. *J. Agric.*  
1136 *Eng. Res.* 49:113–125.
- 1137 Buttery, B.R., R.I. Buzzell, and W.I. Findlay. 1981. Relationships among photosynthetic rate,  
1138 bean yield and other characters in field grown cultivars of soybean. *Can. J. Plant Sci.*  
1139 61:191–198.
- 1140 Calderini, D.F., M.F. Dreccer, and G.A. Slafer. 1995. Genetic improvement in wheat yield and  
1141 associated traits. A re-examination of previous results and the latest trends. *Plant Breed.*  
1142 114:108–112.
- 1143 Chang, J., D.E. Clay, K. Dalsted, S. Clay, and M. O'Neill. 2003. Corn (*Zea Mays* L.) yield  
1144 prediction using multispectral and multivariate reflectance. *Agron. J.* 95:1447–1453.
- 1145 Chappelle, E.W., M.S. Kim, and J.E. McMurtrey, III. 1992. Ratio analysis of reflectance spectra  
1146 (RARS): An algorithm for the remote estimation of the concentrations of chlorophyll a,  
1147 chlorophyll b, and carotenoids in soybean leaves. *Remote Sens. Environ.* 39:239–247.
- 1148 Clevers, J.G.P.W. 1997. A simplified approach for yield prediction of sugar beet based on optical  
1149 remote sensing data. *Remote Sens. Environ.* 61:221–228.
- 1150 Curran, P.J., J.L. Dungan, and H.L. Gholz. 1990. Exploring the relationship between reflectance  
1151 red edge and chlorophyll content in slash pine. *Tree Physiol.* 7:33–48.
- 1152 Datt, B. 1998. Remote sensing of chlorophyll a, chlorophyll b, chlorophyll a+b, and total  
1153 carotenoid content in eucalyptus leaves. *Remote Sens. Environ.* 66:111–121.

- 1154 Datt, B. 1999. Remote sensing of water content in Eucalyptus leaves. *Australian Journal of*  
1155 *Botany*. 47:909–923.
- 1156 Daughtry, C.S.T., C.L. Walthall, M.S. Kim, E. Brown de Colstoun, and J.E. McMurtrey, III.  
1157 2000. Estimating corn leaf chlorophyll content from leaf and canopy reflectance. *Remote*  
1158 *Sens. Environ.* 74:229–239.
- 1159 Deering, D.W. 1978. Rangeland reflectance characteristics measured by aircraft and spacecraft  
1160 sensors. Ph.D. diss., Texas A&M Univ., College Station.
- 1161 Dusek, D.A., R.D. Jackson, and J.T. Musick. 1985. Winter wheat vegetation indices calculated  
1162 from combinations of seven spectral bands. *Remote Sensing of Environment* 18:255–267.
- 1163 Fehr, W.R., and C.E. Caviness. 1977. Stages of soybean development. Spec. Rep. 80. Iowa  
1164 Agric. Home Econ. Exp. Stn., Iowa State Univ., Ames.
- 1165 Filella, I., I. Serrano, J. Serra, and J. Peñuelas. 1995. Evaluating wheat nitrogen status with  
1166 canopy reflectance indices and discriminate analysis. *Crop Sci.* 35:1400–1405.
- 1167 Filella, I., and J. Peñuelas. 1994. The red edge position and shape as indicators of plant  
1168 chlorophyll content, biomass, and hydric status. *Int. J. of Remote Sensing*. 15(7):1459-  
1169 1470.
- 1170 Gamon, J.A., J. Peñuelas, and C.B. Field. 1992. A narrow-waveband spectral index that tracks  
1171 diurnal changes in photosynthetic efficiency. *Remote Sens. Environ.* 41:35–44.
- 1172 Gamon, J.A., and J.S. Surfus. 1999. Assessing leaf pigment content and activity with a  
1173 reflectometer. *New Phytol.* 143:105–117.
- 1174 Gao, B.C. 1996. NDWI—a normalized difference water index for remote sensing of vegetation  
1175 liquid water from space. *Sens. Environ.* 58:257-266.

- 1176 Gitelson, A., and M.N. Merzlyak. 1996. Signature analysis of leaf reflectance spectra: Algorithm  
1177 development for remote sensing of chlorophyll. *J. Plant Physiol.* 148:494–500.
- 1178 Gitelson, A.A., and M.N. Merzlyak. 1994. Quantitative estimation of chlorophyll-a using  
1179 reflectance spectra: Experiments with autumn chestnut and maple leaves. *J. Photochem.*  
1180 *Photobiol.* 22:247–252.
- 1181 Gutierrez, M., M. Reynolds, W. Raun, M. Stone, and A. Klatt. 2010. Spectral water indices for  
1182 assessing yield in elite bread wheat genotypes under well-irrigated, water-stressed, and  
1183 high-temperature conditions. *Crop Sci* 50:197–214.
- 1184 Hanson, P.M., J.R. Jorgenson, A. Thomsen. 2002. Predicting grain yield and protein content in  
1185 winter wheat and spring barley using repeated canopy reflectance measurements and  
1186 partial least squares regression. *J. of Ag Sci.* 139:307-318.
- 1187 Kumar, R., and L. Silva. 1973. Light ray tracing through a leaf cross-section. *Appl. Optics*  
1188 12:2950–2954.
- 1189 Lin, W.S., C.M. Yang, and B.J. Kuo. 2012. Classifying cultivars of rice (*Oryza sativa* L.) based  
1190 on corrected canopy reflectance spectra data using the orthogonal projections of latent  
1191 structures (O-PLS) method. *Chemometrics and Intelligent Laboratory Systems.* 115:25–  
1192 36.
- 1193 Ma, B.L., L.M. Dwyer, C. Costa, E.R. Cober, and M.J. Morrison. 2001. Early Prediction of  
1194 Soybean yield from canopy reflectance measurements. *Agron. J.* 93:1227–1234.
- 1195 Marti, J., J. Bort, G. Slafer, and J. Araus. 2007. Can wheat yield be assessed by early  
1196 measurements of normalized difference vegetation index? *Annals of Applied Biology*  
1197 150:253–257.
- 1198 Moran, J.A., A.K. Mitchell, G. Goodmanson, and K.A. Stockburger. 2000. Differentiation

- 1199 among effects of nitrogen fertilization treatments on conifer seedlings by foliar  
1200 reflectance: A comparison of methods. *Tree Physiol.* 20:1113–1120.
- 1201 Morrison, M.J., H.D. Voldeng, and E.R. Cober. 1999. Physiological changes from 58 years of  
1202 genetic improvement of short-season soybean cultivars in Canada. *Agron. J.* 91:685–689.
- 1203 Moss, D.N., and R.B. Musgrave. 1971. Photosynthesis and crop production. *Adv. Agron.*  
1204 23:317–336.
- 1205 Naes, T., T. Isaksson, T. Faern, and T. Davis. 2004. A user-friendly guide to multivariate  
1206 calibration and classification. NIR Publ., Chichester, UK.
- 1207 Peñuelas, J., F. Baret, and I. Filella. 1995. Semi-empirical indices to assess  
1208 carotenoids/chlorophyll a ratio from leaf spectral reflectance. *Photosynthetica.* 31:221–  
1209 230.
- 1210 Peñuelas, J., I. Filella, C. Biel, L. Serrano, and R. Save. 1993. The reflectance at the 950– 970  
1211 mm region as an indicator of plant water status. *International Journal of Remote Sensing.*  
1212 14:1887–1905.
- 1213 Peñuelas, J., R. Isla, I. Filella, and J.L. Araus. 1997. Visible and near infrared reflectance  
1214 assessment of salinity effects on barley. *Crop Sci.* 35:1400–1405.
- 1215 Prasad, B., B. Carver, M. Stone, M. Babar, W. Raun, and A. Klatt. 2007a. Genetic analysis of  
1216 indirect selection for winter wheat grain yield using spectral reflectance indices. *Crop*  
1217 *Sci.* 47:1416–1425.
- 1218 Prasad, B., B. Carver, M. Stone, M. Babar, W. Raun, and A. Klatt. 2007b. Potential use of  
1219 spectral reflectance indices as a selection tool for grain yield in winter wheat under great  
1220 plains conditions. *Crop Sci.* 47:1426–1440.

- 1221 Reynolds, M., Y. Manes, A. Izanloo, and P. Langridge. 2009. Phenotyping approaches for  
1222 physiological breeding and gene discovery in wheat. *Annals of Appl. Bio.* 155(3):309–  
1223 320.
- 1224 Reynolds, M.P., S. Rajaram, and K.D. Sayre. 1999. Physiological and genetic changes of  
1225 irrigated wheat in the post-green revolution period and approaches for meeting projected  
1226 global demand. *Crop Sci.* 39:1611–1621.
- 1227 Ries, L.L., L.C. Purcell, T.E. Carter Jr., J.T. Edwards, and C.A. King. 2012. Physiological traits  
1228 contributing to differential canopy wilting in soybean under drought. *Crop Sci.* 52:272–  
1229 281.
- 1230 Royo, C., N. Aparicio, D. Villegas, J. Casadesus, P. Monneveux, and J. Araus. 2003. Usefulness  
1231 of spectral reflectance indices as durum wheat yield predictors under contrasting  
1232 Mediterranean conditions. *Int. J. of Remote Sensing* 24:4403–4419.
- 1233 Royo, C., D. Villegas, L.F. Garc'ia del Moral,, S. El Hani, N. Aparicio, Y. Rharrabti, and J.L.  
1234 Araus. 2002. Comparative performance of carbon isotope discrimination and canopy  
1235 temperature depression as predictors of genotype differences in durum wheat yield in  
1236 Spain. *Aust. J. Agr. Res.* 53:561–569.
- 1237 Sayre, K.D., S. Rajaram, and R.A. Fischer. 1997. Yield potential progress in short bread wheat in  
1238 Northern Mexico. *Crop Sci.* 37:36–42.
- 1239 Serrano, L., I. Filella, and J. Peñuelas. 2000. Remote sensing of biomass and yield of winter  
1240 wheat under different nitrogen supplies. *Crop Sci.* 40:723–731.
- 1241 Shanahan, J.F., J.S. Schepers, D.D. Francis, G.E. Varvel, W.W. Wilhelm, J.S. Tringe, M.R.  
1242 Schlemmer, and D.J. Major. 2001. Use of remote sensing imagery to estimate corn grain  
1243 yield. *Agron. J.* 93:583–589.

- 1244 Shibles, R. 1978. Adaptation of soybeans to different seasonal durations. In: R. J. Summerfield  
1245 and A. H. Bunting, editors, *Advances in Legume Science*. Royal Botanic Gardens,  
1246 University of Michigan. p. 279–285.
- 1247 Sims, D.A., and J.A. Gamon. 2002. Relationship between leaf pigment content and spectral  
1248 reflectance across a wide range species, leaf structures and development stages. *Remote*  
1249 *Sens. Environ.* 81:337–354.
- 1250 Sinclair, T. R., L.C. Purcell, and C.H. Sneller. 2004. Crop transformation and the challenge to  
1251 increase yield potential. *Trends Plant Sci.* 9:70–75.
- 1252 Thomas, J.R., and H.W. Gausman. 1977. Leaf reflectance vs. leaf chlorophyll and carotenoid  
1253 concentrations for eight crops. *Agron. J.* 69:799–802.
- 1254 Tucker, C.J. 1979. Red and photographic infrared linear combinations for monitoring vegetation.  
1255 *Remote Sens. Environ.* 8:127–150.
- 1256 Vina, A., and A. Gitelson. 2011. Sensitivity to foliar anthocyanin content of vegetation indices  
1257 using green reflectance. *IEEE Geoscience and Remote Sensing Letters* 8:464–468.
- 1258 Waddington, S.R., J.K. Ransom, M. Osmanzai, and D.A. Saunders. 1986. Improvement in the  
1259 yield potential of bread wheat adapted to Northwest Mexico. *Crop Sci.* 26:698–703.
- 1260 Weber, V.S., J.L. Araus, J.E. Cairns, C. Sanchez, A.E. Melchinger, and E. Orsini. 2012.  
1261 Prediction of grain yield using reflectance spectra of canopy and leaves in maize plants  
1262 grown under different water regimes. *Field Crops Research* 128:82–90.
- 1263 Welles, J. M., and J.M. Norman. 1991. Instrument for indirect measurement of canopy  
1264 architecture. *Agron. J.* 83:818–825.
- 1265 Wessman, C. A. 1990. Evaluation of canopy biochemistry. In: R. J. Hobbs and H. A. Mooney,  
1266 editors, *Remote Sensing of Biosphere Functioning*. 135–156.

1267 Wiegand, C., A. Richardson, D. Escobar, and A. Gerbermann. 1991. Vegetation indexes for crop  
1268 assessment. *Remote Sensing of Environment* 35:105–119.

1269

1270

1271

1272

1273

1274

1275

1276

1277

1278

1279

1280

1281

1282

1283

1284

1285

1286

1287

1288

1289

1290

1291

1292

1293

1294

1295 **Table 2.1. Cultivars used for spectral data evaluation with year of release and two-year**  
 1296 **yield averages.**

Cultivar	Year of Release	Yield t ha <sup>-1</sup>	Cultivar	Year of Release	Yield t ha <sup>-1</sup>
MGIII			MGIV		
AK (Harrow)	1928	2.67	Boone	1935	2.34
Calland	1968	2.95	Chief	1940	1.97
Dunfield	1923	2.32	Clark	1953	2.70
IA 3010	1998	4.30	Cutler	1968	2.74
Illini	1927	2.72	Douglas	1980	2.76
Lincoln	1943	2.51	Flyer	1988	3.48
MACON	1995	3.86	KS4694	1993	3.24
NE3001	2004	3.59	LD00-3309	2005	4.09
Private 3- 1	1978	3.80	Macoupin	1930	2.29
Private 3- 8	2002	4.08	Private 4- 1	1985	3.54
Private 3- 9	1989	4.03	Private 4- 4	2001	3.86
Private 3-12	1997	4.11	Private 4- 6	1980	3.56
Private 3-13	2004	4.44	Private 4-11	2000	4.04
Private 3-14	2007	4.63	Private 4-12	1973	2.92
Private 3-15	1983	2.99	Private 4-13	1984	3.60
Private 3-21	2001	4.30	Private 4-19	2006	3.68
Private 3-23	2006	4.49	Private 4-20	2008	4.21
Shelby	1958	2.81	Private 4-21	2010	4.26
Wayne	1964	2.92	Private 4-22	2000	3.68
Williams	1971	3.44	Sparks	1981	2.98

1297

1298

1299

1300

1301

1302

1303

1304

1305

1306

1307

1308

1309

1310

1311



1312 **Table 2.2. Analysis of variance for seed yield of MGIII and IV experiments.**

1313  
1314  
1315  
1316  
1317  
1318  
1319  
1320  
1321  
1322  
1323  
1324  
1325  
1326  
1327  
1328  
1329  
1330  
1331  
1332  
1333  
1334  
1335  
1336  
1337  
1338  
1339  
1340

Source	D.F.	F Value	Pr > F
MGIII			
Genotype (G)	18	111.57	< 0.01
Environment (E)	5	109.10	< 0.01
G x E	94	3.11	< 0.01
MGIV			
Genotype (G)	19	95.98	< 0.01
Environment (E)	5	82.76	< 0.01
G x E	95	3.90	< 0.01

1341 **Table 2.3 Band regions with genotypic differences from analysis of variance (N=20), for**  
 1342 **MGIII and MGIV experiments.**

Band	MGIII	MGIV
	F Value	F Value
405	20.61**	13.47**
415	19.96**	13.63**
425	17.41**	12.54**
435	15.80**	11.41**
445	15.26**	10.85**
455	15.11**	10.68**
465	15.41**	10.59**
475	15.78**	10.58**
485	16.09**	10.56**
495	16.90**	10.88**
505	18.66**	13.60**
515	22.73**	15.00**
525	29.10**	17.86**
535	32.83**	18.87**
545	34.42**	19.32**
555	34.77**	19.46**
565	33.83**	19.62**
575	31.08**	19.27**
585	28.34**	18.63**
595	26.62**	18.02**
605	25.23**	17.53**
615	22.78**	16.52**
625	21.12**	15.64**
635	20.46**	15.22**
645	19.29**	13.82**
655	17.94**	12.44**
665	17.11**	11.12**
675	17.33**	10.61**
685	17.52**	11.48**
695	22.96**	17.13**
705	37.14**	20.73**
715	38.07**	18.55**
725	22.66**	12.10**
735	8.69**	5.41**
745	3.12**	3.13**
755	1.96*	3.19**
765	1.85*	3.41**

775	1.96*	3.61**
785	1.99*	3.68**
795	2.00*	3.70**
805	2.01*	3.73**
815	1.97*	3.71**
825	2.00*	3.74**
835	2.04**	3.80**
845	2.10**	3.85**
855	2.12**	3.89**
865	2.15**	3.92**
875	2.17**	3.95**
885	2.16**	3.97**
895	1.97*	3.95**
905	1.59	3.96**
915	1.73*	3.96**
925	1.87*	4.01**
935	2.05*	3.84**
945	2.11**	3.93**
955	2.23**	4.01**
965	2.41**	4.14**
975	2.56**	4.23**
985	2.63**	4.30**
995	2.67**	4.34**
1005	2.67**	4.66**
1015	2.66**	4.68**
1025	2.65**	4.69**
1035	2.64**	4.70**
1045	2.64**	4.70**
1055	2.63**	4.70**
1065	2.61**	4.70**
1075	2.58**	4.70**
1085	2.34**	4.70**
1095	2.08**	4.69**
1105	2.39**	4.67**
1115	2.57**	4.61**
1125	2.60**	4.51**
1135	2.90**	4.65**
1145	3.38**	4.81**
1155	4.26**	5.08**
1165	4.56**	5.24**
1175	4.74**	5.32**
1185	4.86**	5.37**

1195	4.94**	5.41**
1205	4.95**	5.42**
1215	4.90**	5.41**
1225	4.84**	5.38**
1235	4.78**	5.37**
1245	4.73**	5.35**
1255	4.68**	5.34**
1265	4.65**	5.32**
1275	4.68**	5.34**
1285	4.75**	5.37**
1295	4.89**	5.38**
1305	5.00**	5.41**

\* =  $P \leq 0.05$

\*\* =  $P \leq 0.01$

1343

1344

1345

1346

1347

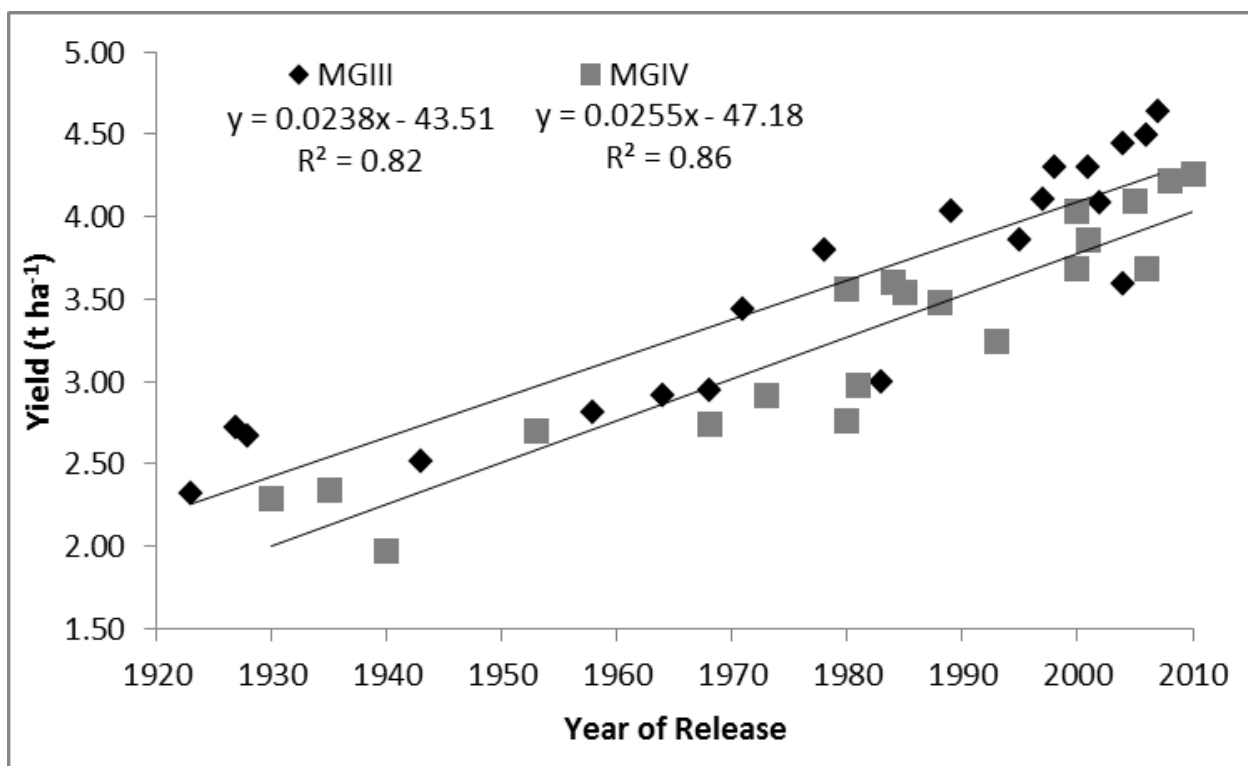
1348

1349

1350

1351

1352



1353

1354

1355

1356 **Figure 2.A. Relationship between year of release and two-year yield**

1357 **means for MGIII and MGIV experiments. Least square line with**

1358 **equation and coefficient of determination ( $R^2$ ) represented at the top**

1359

1360 **of the figure.**

1361

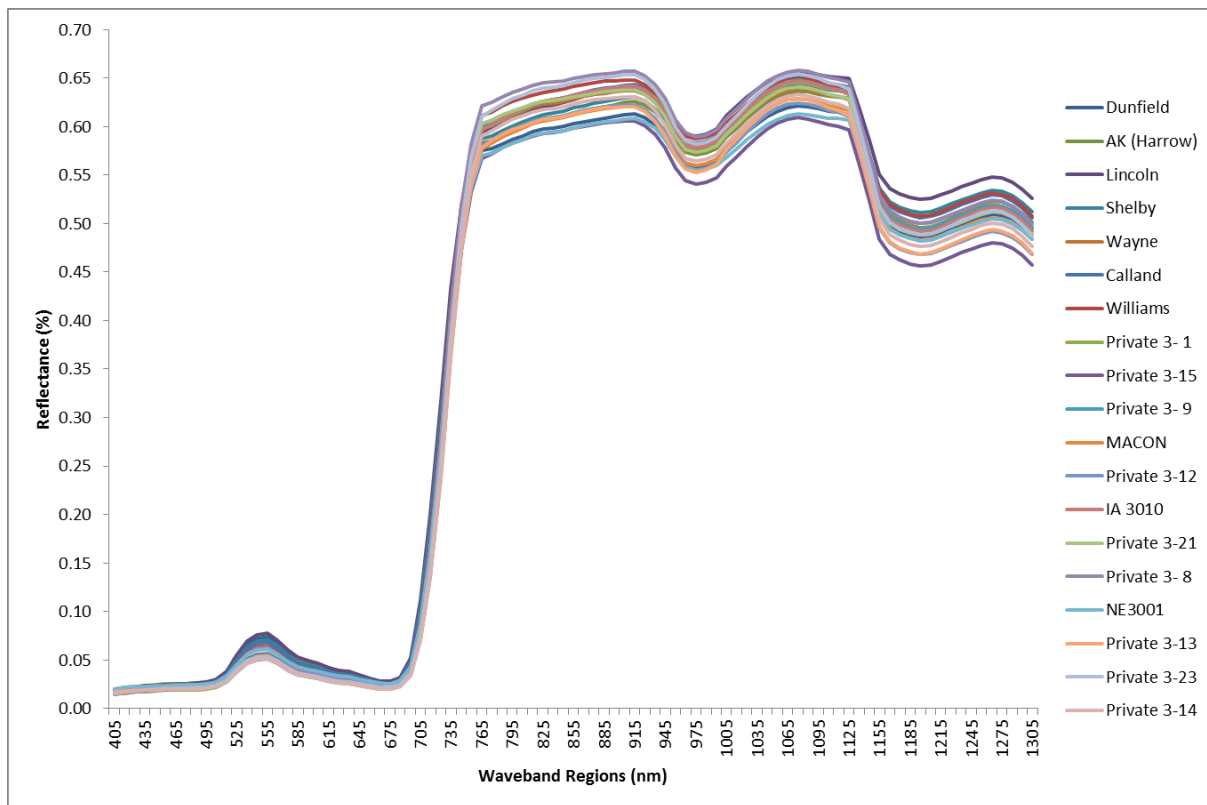
1362

1363

1364

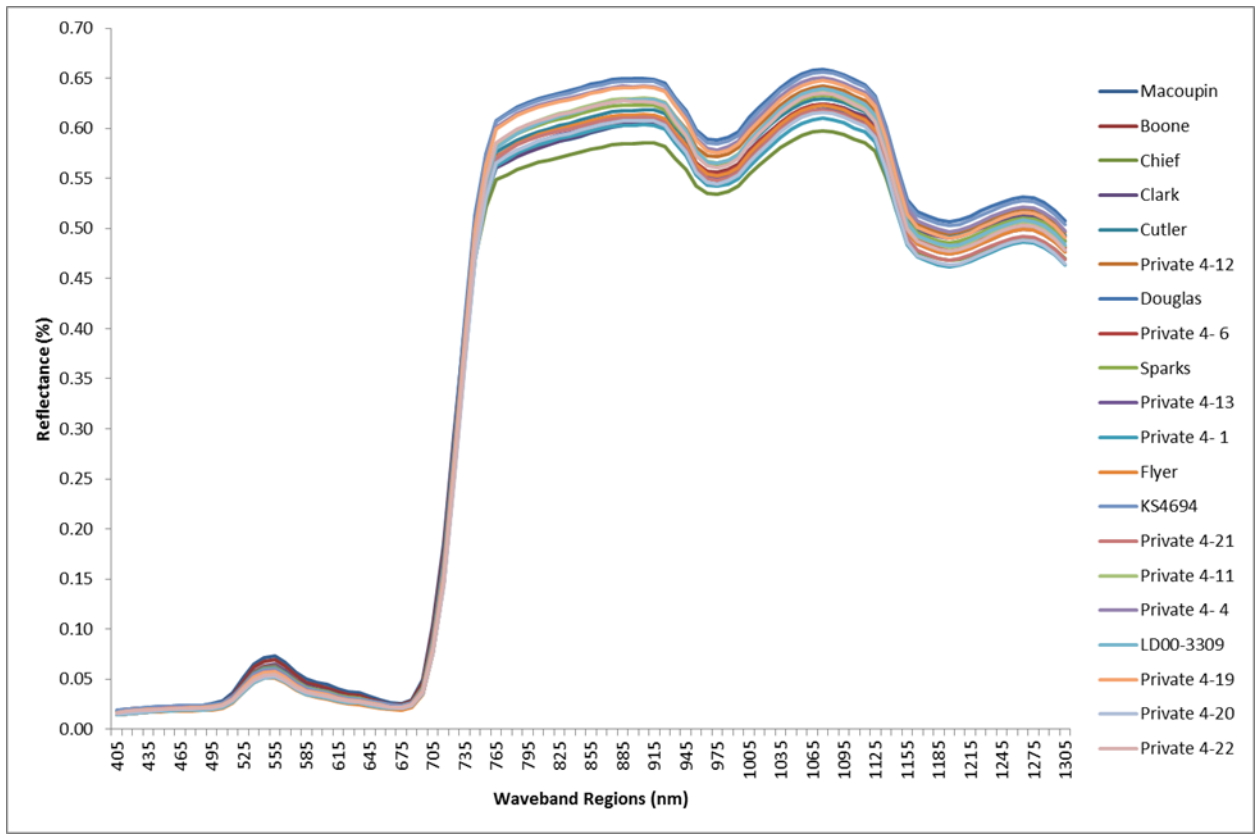
1365

1366



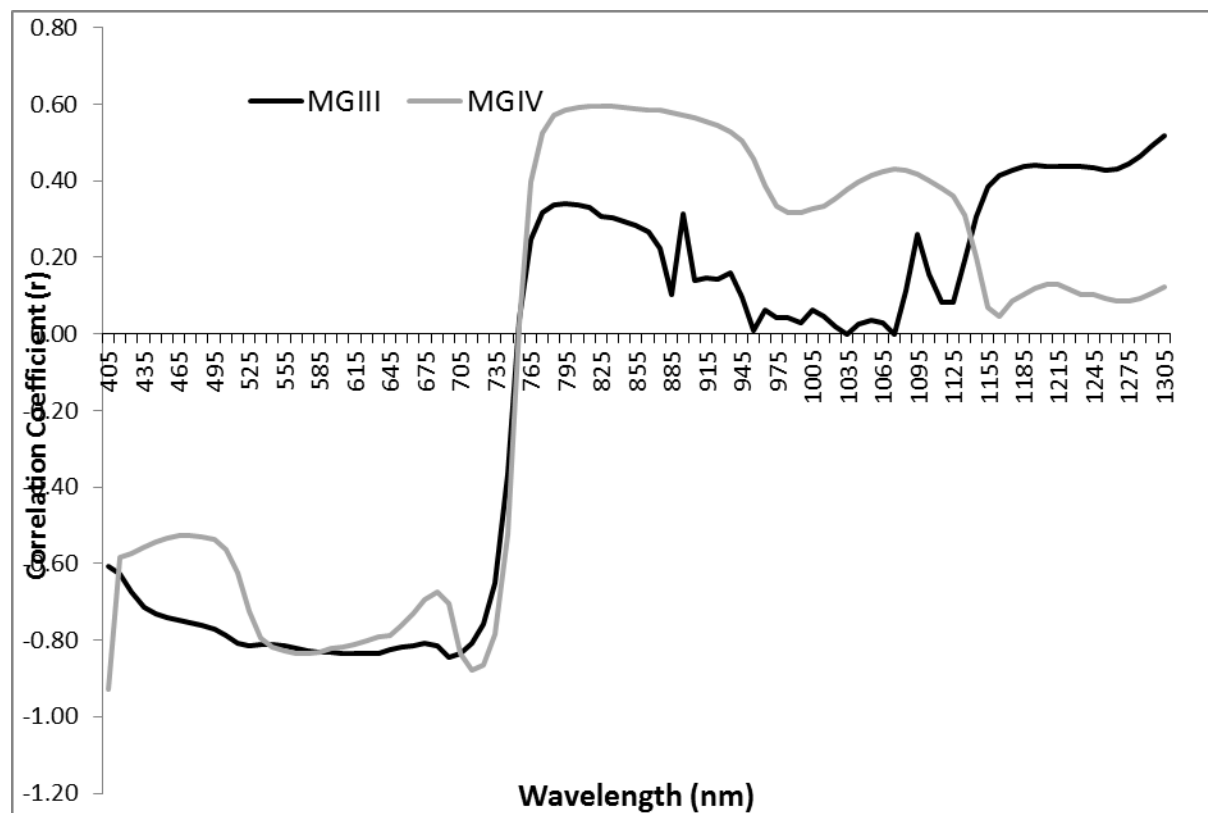
1367  
1368

**Figure 2.B. Mean spectral response curves of MGIII genotypes (without ‘Illini’). Wavebands are 10nm intervals and reflectance is the percentage of a white reference panel.**



1369  
1370  
1371  
1372  
1373  
1374

**Figure 2.C. Mean spectral response curves of MGIV genotypes. Wavebands are 10nm intervals and reflectance is the percentage of a white reference panel.**



1375  
 1376 **Figure 2.D. Correlation coefficient (r) values between wavelength (nm) and year of release**  
 1377 **for MGIII and MGIV two-year mean reflectance values. An r value  $\geq \pm 0.37$  is significant at**  
 1378 **the  $Pr \leq 0.05$  level, and an r value  $\geq \pm 0.56$  is significant at the  $Pr \leq 0.01$ .**  
 1379



# Chapter 3 - Characterizing Soybean Seed Yield Using Optimized Phenotyping with Canopy Reflectance

## Abstract

Genotyping and phenotyping technologies that increase the amount of genetic material in the breeding program and increase the efficiency of cultivar development are necessary to accomplish the genetic gains needed to meet food demand. Optimized phenotyping using canopy reflectance measurements may provide a logical solution. The objectives of this study were: 1) to determine if canopy reflectance is useful in characterizing soybean seed yield; 2) to build yield estimation models for use as a screening tool; 3) to determine which wavebands contribute most to soybean yield estimation; and 4) to determine which spectral reflectance observations at specific growth stages contribute most to soybean seed yield. Canopy reflectance and seed yield were measured on 20 maturity group III (MGIII) and 20 maturity group IV (MGIV) soybean cultivars released from 1923 to 2010. Measurements were conducted on six irrigated and water-stressed environments in 2011 and 2012. Spectral band regions significantly contributing to seed yield prediction were selected through partial least squares regression, and yield estimation models were created using selected band regions through multiple linear regression. Significant differences were detected between genotypes, environments, and genotype  $\times$  environment interactions for yield and band regions. Yield prediction models created using the red edge and portions of the near-infrared spectrum explained much of the variation in seed yield among genotypes. No significant trend was found for specific growth stages contributing more to yield estimation modeling or between water regimes. Yield estimation models using canopy reflectance measurements may be a useful selection tool in breeding programs.

## Introduction

Due to the complex genetic basis of soybean yield, classic breeding approaches are still utilized to assess yield potential and improvement. In these approaches, crosses are made with elite lines and progeny and then selected based on attributes favorable to specific target environments. Superior genotypes are moved through the process, with seed yield used as a main selection criterion (Loss and Siddique, 1994). This selectivity has decreased genotypic diversity because many parental lines have similar backgrounds. Mechanized harvesters are utilized to make the process of obtaining seed yield faster, but this method is expensive, laborious, and time-consuming. Field evaluation of plots under normal growing conditions will always be necessary, but if specific regions of the electromagnetic spectrum can consistently account for a large portion of seed yield variability between genotypes and across environments, the technology may be a useful indirect selection criterion for breeding programs.

Most of the field-based research conducted on yield estimation models using canopy reflectance are focused on one-, two-, or three-band indices, which can be highly variable and inconsistent (Babar et al., 2006a, 2006b). Some of these indices have been useful in estimating yield through other plant characteristics, such as chlorosis (Adams et al., 1999), green cover (Dusek et al., 1985; Daughtry et al., 2000), chlorophyll (Datt, 1999; Daughtry et al., 2000), and photosynthetically active tissue (biomass) (Wiegand et al., 1991). These indices have had varying degrees of success, but none have fully captured the underlying physiological and environmental factors behind consistent phenotypic yield estimation.

Studies focusing on utilizing full-spectrum instruments and models for various parameters have been published in recent years in wheat (Hansen et al., 2002; Pimstein et al., 2007, 2011), corn (Hong et al., 2001; Weber et al., 2012), rice (Lin et al., 2012), and cotton (Zhao et al., 2006) in optimal and drought environments. Additional studies have characterized

1 and explored how to incorporate these new models into high-efficiency platforms (Walter et al.,  
2 2012; White et al., 2012).

3 Most of the indices created correlate plant health parameters such as pigment status to  
4 grain yield. Indices such as the simple ratio (SR), first used by Jordan (1969) and Rouse et al.  
5 (1973) and described by the equation  $[R_{\text{NIR}}/R_{\text{RED}}]$ , capture the ratio of NIR reflectance to red  
6 reflectance. SR has been shown to correlate well with biomass, leaf area index (LAI), fractional  
7 photosynthetically active radiation (FPAR), ground cover, and wheat and soybean yield  
8 (Hatfield, 1983; Wiegand et al., 1991; Ball and Konzak, 1993; Price and Bausch, 1995; Ma et al.,  
9 2001; Royo et al., 2003; Hatfield and Prueger, 2010). The normalized difference vegetation  
10 index (NDVI) (derived by Deering (1978) and Tucker (1979) to estimate green biomass and  
11 intercepted PAR; defined as  $[R_{\text{NIR}}-R_{\text{RED}}/R_{\text{NIR}}+R_{\text{RED}}]$ ) has been used to predict yield and other plant  
12 functions with many crops using hyperspectral and satellite imagery (Wiegand et al., 1991;  
13 Peñuelas et al., 1997; Ma et al., 2001; Shanahan et al., 2001; Royo et al., 2002; Royo et al., 2003;  
14 Prasad et al., 2007a, 2007b; Marti et al., 2007). Gittelsohn et al. (1996a) proposed the Green  
15 NDVI as a substitute for the high saturation point of the NDVI's red region. Shanahan et al.  
16 (2001) have successfully predicted yields in corn under normal growing conditions in Nebraska  
17 using the Green NDVI. Researchers found that normalizing the green and NIR relationship was  
18 highly correlated with grain yield, explaining 70 to 92% of yield variability at mid-grain fill  
19 (Shanahan et al., 2001). Ma et al. (2001) used the Green NDVI  $(R_{613}-R_{559}/R_{613}+R_{559})$  to predict  
20 soybean yield and found a high correlation with soybean yields under irrigated conditions, which  
21 explained up to 80% of the variation within yield. The photochemical reflectance index (PRI),  
22 which is defined by the equation  $(R_{550} - R_{531})/(R_{550} + R_{531})$ , captures the normalized difference  
23 between the major green wavelength reflectance of the plant canopy and leaves, which can be

1 used to quantify radiation use efficiency (Gamon et al., 1992). Trotter et al. (2002) and  
2 Garbulsky (2011) used the PRI to assess nitrogen use efficiency and radiation use efficiency to  
3 distinguish genotypes that were superior to checks. These indices have been used estimate yield  
4 varying environments on many platforms.

5 Other indices focus on the biophysical parameters, such as water content and leaf area.  
6 Leaf area index (first illustrated by Tucker and Sellers, 1986) was developed to predict  
7 vegetation parameters such as green biomass and green leaf area (Babar et al., 2006a, 2006b).  
8 The LAI captures the genotypic differences between photosynthetically active radiation (PAR)  
9 either being absorbed by leaves with more area or being able to monitor important crop variables  
10 throughout the growing season (Clevers, 1997). Aparicio et al. (2002) have determined that LAI  
11 plays a large part in plant function and correlates well with yield prediction. Many water indices  
12 have been developed to relate reflectance measurements with success in the 850 and 970 nm  
13 regions with bread and durum wheat yield (Royo et al., 2003; Gutierrez et al., 2010). The water  
14 indices focus on the minor water absorption bands within the spectrum and capture relative water  
15 content based on absorption strength of water within the plant leaves. Capturing biophysical  
16 properties can mean discovering properties that influence yield production of field crops. These  
17 indices are easy to calculate and give researchers a way to easily handle the large amounts of  
18 data associated with such research; however, indices tend to be environment-specific and have a  
19 low correlation with yield outside of wheat (Ma et al., 2001; Gutierrez-Rodrigues et al., 2004;  
20 Prasad et al., 2007a; Gutierrez et al., 2010). Therefore, more complex models that use more of  
21 the spectrum need to be developed to capture the necessary variation within yield across different  
22 environments and crops (Pimstein et al., 2007 and 2011; Weber et al., 2012).

1 High-yielding cultivars tend to have high biophysical and biochemical properties that  
2 make distinguishing these genotypes using spectral indices unreliable (Baret and Guyot, 1991;  
3 Aparicio et al., 2002; Pimstein et al., 2007). Due to confounds such as biomass saturation, dense  
4 cover, high LAI, and high chlorophyll levels, full-spectrum models have been considered for  
5 yield estimation. These models have not been utilized, however, because of over-fitting and  
6 collinearity concerns from the large number of predictors and typically small sample size  
7 associated with spectral research (Pimstein et al., 2007). The main approaches used to meet the  
8 challenges of hyperspectral data analysis focus on reducing the correlation between predictor  
9 variables, causing multicollinearity and normalizing the variability within predictor variables  
10 from sample to sample. Researchers also use these new techniques to make the spectral response  
11 curves into meaningful spectral waveband regions.

12 Principal component analysis (PCA) has been used by researchers to build yield  
13 prediction models that explain 70 to 90% of the yield variability in maize (Hong et al., 2001;  
14 Chang et al., 2003) and 39% of the yield variability among soybean genotypes (Hong et al.,  
15 2001). Using six bands, regression explained almost 95% of the variability within maize yield.  
16 Artificial Neural Network Analysis has also been used in soybean to build prediction models that  
17 explain between 46 and 81% of the yield variability in soybean and 42 to 77% in corn (Kaul et  
18 al., 2005). Researchers also determined that reducing the dataset to 10-nm intervals reduced the  
19 noise within the spectra (Lin et al., 2012). Utilizing multivariate analysis is new to precision  
20 phenotyping research but has the potential to create yield prediction models and explain other  
21 important phenotypic parameters.

22 Partial Least Squares (PLS) was used for initial data pre-treatment and variable reduction  
23 before multiple linear regression techniques (Wold, 1966). Partial least squares was selected for

1 analysis due to the high redundancy in spectral data and subsequent multicollinearity between  
2 bands and “large p small n” phenomenon associated with spectral data analysis. Like PCA, PLS  
3 extracts successive linear predictors of y called latent variables or factors. The new variables aim  
4 to explain response variation and predictor variation; models are selected based on balancing  
5 these two goals. Hansen et al. (2002) compared three different PLS methods and concluded the  
6 N-PLS was the most consistent for yield and protein content estimation in wheat and barley,  
7 which explained up to 75% of the variation in protein content and up to 97% of the yield  
8 variation. Using different water regimes, Weber et al. (2012) similarly found that PLS explained  
9 a maximum of 40% of the variability within corn yield and prediction models explained more  
10 variability in water-limited environments than non-water-limited environments. Lin et al. (2012)  
11 used orthogonal projections to latent structure PLS in rice and distinguished three cultivars with  
12 90% accuracy, but this result dropped to 80% when distinguishing one cultivar.

13         The goal of this study was to develop statistical models for soybean yield estimation  
14 using canopy reflectance measurements. The specific objectives were to assess canopy  
15 reflectance as a tool for soybean yield estimation, identify specific growth stages significantly  
16 contributing to yield estimation, and test the stability and utility of yield estimation models  
17 across varying environments.

## Materials and Methods

### *Experimental and Field Design*

A study was conducted on soybean [*Glycine max* (L) Merr.] in 2011 and 2012 at the Kansas State University Research farm (south of Manhattan, KS). In 2011, experiments (location A) were conducted on a well-drained silt loam soil of the Eudora and Belvue types. In 2012, location B was a well-drained silt loam soil of the Bismarckgrove-Kimo complex and location C was a well-drained silt-sandy loam soil of the Belvue and Eudora types.

Twenty maturity group III (MGIII) and 20 maturity group IV (MGIV) soybean cultivars, ranging in release year from 1923 to 2010, were selected for release year diversity out of the Soybean Genetic Gains Study, which contained 60 MGIII and 54 MGIV genotypes. Selected cultivars were a mixture of private and public released cultivars.

The experiment was planted in a randomized complete plot design with 4 replications in 2011 and 2012. Replicated plots were planted on 23 May, 2011 on field A, and 16 May, 2012 and on 4 June, 2012 on fields B and C respectively. Each experimental unit consisted of 4 rows, 3.4 meter long, and spaced 76 cm apart. Genotypes were planted in separate irrigated (IRR or I) and water stressed (DRY or D) environments. In both years, weed pressure and fertility were not limiting. In 2011 and 2012, flood irrigation was applied to the irrigated plots starting at reproductive stage 1 (R1), and continued weekly until R6 (Fehr and Caviness, 1977). In 2011, no supplemental irrigation was applied to the water-stressed environments whereas in 2012, due to the extremely dry conditions, one irrigation of approximately 5 cm was applied to the DRY plots on fields B and C shortly after R1 to ensure crop development. No further irrigation was applied to the DRY plots on field B. Weekly irrigation continued in the IRR plots. Later in the growing season on Field C, an irrigation malfunction occurred during seed fill, and the water-stressed

1 environment received an additional 5 to 6 cm of water. This irrigation occurred after all of the  
2 spectral readings had been taken. Because of this late-season irrigation, the water treatments for  
3 Field C are designated irrigation 1 (IRR1, or I1) and irrigation 2 (IRR2 or I2), rather than IRR  
4 and DRY.

### 5 *Phenotypic Traits*

6 Maturity, height, and lodging were taken on all plots during both seasons. Maturity was  
7 calculated as the number of days past 31 August when 95% of the pods had reached mature  
8 color. Height was measured as the average length (in cm) of mature plants from the ground to the  
9 tip of the main stem. Lodging was scored on a scale of 1 to 5 based on the number of plants  
10 leaning or broken. Upright plants with no lean were scored a 1, 2 = 20° lean, 3 = 45° lean, 4 =  
11 60° lean, and 5 = flat on the ground. Plots were mechanically harvested using a two-row plot  
12 combine, with rows two and three used to calculate seed yield of the plot. Seed yield was  
13 calculated as the total mass of seed obtained and was adjusted to uniform moisture.

### 14 *Data Analysis*

#### 15 *Analysis of Variance*

16 The GLIMMIX procedure in SAS 9.2 (SAS Institute, 2008) was used for analysis of  
17 variance (ANOVA). Cultivar and experiment were treated as fixed effects, and replication nested  
18 within the experiment was treated as a random effect for yield and agronomic traits. For  
19 hyperspectral data, replication nested within experiment and subsamples were treated as random  
20 effects for full-season analysis. For observation-day analysis, the repeated statement for repeated  
21 sampling data was used and treated as a random effect. Environment was classified as year, field,  
22 and water treatment. The Brown-Forsythe homogeneity of variance test was implemented in all



1 ANOVA analyses, and residuals were used to determine outliers that were excluded from further  
2 statistical analysis.

### 3 *Partial Least Squares (PLS)*

4 PROC PLS in SAS 9.2 with the non-linear iterative partial least squares (N-PLS)  
5 algorithm, random k-fold = 10-cross validation, and factor levels set at 15 was used for outlier  
6 identification, pre-treatment, and predictor variable selection on 2011 and 2012 data. The  
7 predicted residual sums of squares (PRESS) were used for model selection. The NIPALS  
8 algorithm was chosen over the SIMPLS algorithm (De Jong, 1993) because of the high  
9 dimensionality and non-linear nature of the hyperspectral data. Random k-fold = 10-cross  
10 validation was chosen because of the small sample size compared with the number of predictors  
11 and the lack of a true validation dataset for validating built models. Max factor number was set at  
12 15, which is the max factor number allowed by SAS for the dataset used. Optimized factor  
13 number was selected when the PRESS statistic was minimized most (Wold, 1966).

### 14 *Outlier Identification and Data Synthesis*

15 Hyperspectral data were initially trimmed from 350 to 2500 nm to 400 to 1310 nm to  
16 eliminate noise from atmospheric absorption regions focused around the water absorption bands  
17 in the near-infrared and atmospheric noise in the ultra-violet areas of the spectrum. For each  
18 observation day, initial outlier control on raw data was implemented before averages were  
19 calculated for observation day and season totals. After outliers were identified and excluded from  
20 analysis, data were combined to form 10-nm band regions to reduce the dataset size and  
21 eliminate some of the collinearity associated with bands in close proximity (Naes et al., 2004). It  
22 was also determined that combined bands would have less variation from sample to sample than  
23 single band measurements (Lin, et al., 2012).

1

***Pre-treatment Before Modeling***

2 Because modeling assumptions of normality were not met, it was necessary to auto-scale  
3 spectral data and dependent variable before PLS analysis (Harshman and Lundy, 1984). The data  
4 were mean-centered and auto-scaled separately for each individual experiment analysis and then  
5 across experiments when datasets were combined. Mean-centering and scaling eliminates bias  
6 within the bands to ensure even weighting of band magnitude, so the analysis is focused on the  
7 variance (Hansen et al., 2002). Auto-scaling is calculated as the inverse of the standard deviation  
8 for each variable [ $1/(SDev)$ ].  
9

10

***Predictor Variable Selection***

11 Hyperspectral band regions from 2-yr means and individual environments that most  
12 significantly contributed to yield estimation were determined using partial least squares  
13 regression (PLSR). In total, 91 band regions from 400 to 1310 nm were analyzed for variable  
14 importance and selected for further analysis through traditional least squares multiple linear  
15 regression (MLR). This procedure was done to extract exact band regions contributing to yield  
16 estimation, which is not possible in PLS models; therefore, custom sensors based on specific  
17 bands could be built for further research studies. Variables were determined to be important  
18 through variable importance within projection plots (VIP), which were created through a macro  
19 in SAS. Wold's criterion limit of 0.8 was used as a cutoff point to indicate variables that  
20 contributed significantly to yield estimation (Wold, 1966). Band regions were selected within  
21 peaks and over Wold's threshold. Due to collinearity issues, band regions that significantly  
22 contributed to yield estimation and were close to each other were combined for final analysis.  
23



1 genotypes, respectively. Mean yields and yield ranges and differences between water regimes  
2 varied highly between locations (Table 3.1). For yield, highly significant genotypic,  
3 environment, and genotype  $\times$  environment ( $G \times E$ ) interaction differences were detected in both  
4 maturity groups (Table 3.2). In fields A and B, where the water regimes were maintained  
5 throughout the growing season, seed yields were significantly higher in the irrigated treatments  
6 than in the water-stressed treatments. In Field C, where the breakdown of the water regimes  
7 occurred, the irrigated and water-stressed yields were not statistically different.

8         Analysis of 10-nm hyperspectral band regions revealed genotype and environmental  
9 differences among many waveband regions. The regions that were significant for genotype,  
10 environment, or  $G \times E$  are listed in Table 3.2. Maturity exhibited significant genotypic,  
11 environment, and  $G \times E$  interaction differences in both maturity groups (Table 3.2). The  $G \times E$   
12 interaction did not account for a large portion of the total phenotypic variation, which suggests  
13 that genotypic means observed in a single environment could be replicated across environments  
14 with minimal interaction influence. Looking at individual growth stage observations, the visible  
15 VIR and red-edge bands were more consistent across growth stages and environments for  
16 genotypic differences in both maturity groups (Table 3.3). In the MGIII and MGIV genotypes,  
17 wavebands at 415 to 715 nm exhibited highly significant ( $Pr > 0.01$ ) and significant ( $Pr > 0.05$ )  
18 genotypic differences in all environments and growth stages; however, no wavebands in the NIR  
19 had significant genotypic differences in all environments and growth stages in both maturity  
20 groups.

21         For the MGIII genotypes, the later growth stages are more consistent than earlier growth  
22 stages for genotypic differences for all wavebands; however, in the MGIV genotypes, no such  
23 trend is observed, with early and late growth stages exhibiting genotypic differences. As seen,

1 the  $G \times E$  in the VIR and red-edge wavebands is minimal, whereas in the NIR, the  $G \times E$  is  
2 greater in both maturity groups. Lin et al. (2012) observed greater genotypic differences in the  
3 NIR compared with the VIR in rice. This could be due to the high biomass variability in their  
4 study, which mainly affects the NIR. The small contribution that the  $G \times E$  interaction  
5 contributes to the total phenotypic variation suggests that spectral data may be robust across  
6 environments, making it a strong candidate for an indirect selection technique. Reynolds et al.  
7 (2009) suggested that  $G \times E$  stability is one of the major factors for evaluating any new  
8 phenotyping technique.

### 9 ***Waveband Region Selection***

10 Using PLSR portions of the 2011 and 2012 mean spectra significantly contributed to  
11 yield estimation within the MGIII and MGIV experiments (Figures 3.1A and 3.1H). The VIR  
12 (400 to 700 nm) and red edge (701 to 730 nm) contributed significantly to yield estimation, with  
13 the red and red-edge portions of the spectra exhibiting the most significant projection to yield  
14 estimation in both maturity groups. Most of the NIR portion of the spectra did not contribute  
15 significantly to yield estimation for either maturity group; however, in both maturity groups, the  
16 1290- to 1310-nm regions of the spectra were slightly above the 0.8 threshold, which suggests  
17 increased significance for yield estimation in these regions.

18 For 2011 Field A irrigated and water-stressed environments, both MGIII and MGIV  
19 mean spectra exhibited high variable importance values in the VIR and red-edge portions of the  
20 spectra (Figures 3.1B, 3.1C, 3.1I, and 3.1J. For the MGIII environments (A-I), visible and red  
21 edge portions had the highest significances for yield estimation, with a sharp decrease at the  
22 beginning of the NIR and a significant increase from 775 to 955 nm (Figure 3.1b). For the A-D  
23 environment, variable importance was similar to that of the A-I environment, but a decrease in

1 the blue (400 to 500 nm) portion of the spectra was observed, and there were significant peaks  
2 from 1035 to 1095 nm (Figure 3.1C).

3 For Field B, the VIR and red edge were highly significant in 2012, similar to that of Field  
4 A and the 2-yr averages for both maturity groups. For environment MGIII B-I, the VIR and NIR  
5 had highly significant portions of the spectra for yield estimation (Figure 3.1D). The red edge  
6 was the most significant, followed by the green and red. A spike in the NIR was observed around  
7 the 915-, 1100-, and 1165-nm regions, as was a sharp peak in the early blue portion of the  
8 spectra. For the MGIII B-D environment the VIR and NIR had highly significant regions above  
9 Wold's 0.8 threshold, with a sharp decrease in the NIR portion until 1165 to 1305 nm. The red  
10 edge portion was the most significant, as in the A-I environment (Figure 3.1E).

11 In 2012, neither maturity group in Field C was as consistent as in the other two fields;  
12 there was an irrigation malfunction, no spectral data was collected on IRR1 after the irrigation  
13 malfunction, and yield values were higher than expected. In addition, after the irrigation  
14 malfunction, plants were highly lodged, which could have contributed to inconsistent spectra  
15 influenced by soil background and sensing of under-leaf or stem reflectance. As in the other  
16 fields and environments, however, the VIR and red edge portions were the most useful for yield  
17 estimation (Figures 3.1F, 3.1G, and 3.1M).

18 The MGIII C-I environment had high peaks of significance in the VIR, but these peaks  
19 were not as strong as those in locations A and B (Figure 3.1F). There was a sharp increase in the  
20 red edge and slight peaks in the 915- to 1005-nm region, as well as in the 1165- to 1305-nm  
21 regions of the NIR. The C-I 2 environment mostly mirrors the C-I 1 environment, with a sharp  
22 peak in the green in the 550-nm region (Figure 3.1G). Compared with the C-I 1 environment, the

1 C-I 2 environment saw a sharp increase in the early blue, and the red edge was the most  
2 significant for yield estimation (Figure 3.1G).

3 In the MGIV A-I environment, a low significance in the blue region and a sharp increase  
4 in the green region was observed, with 550 nm being the highest significance for yield estimation  
5 in the green (Figure 3.1I). The red portion of the spectra was not as significant as the green or as  
6 in the MGIII environments; overall, however, the red-edge was the most significant region for  
7 yield estimation, similar to the MGIII environments. There was also a sharp decrease in the  
8 beginning of the NIR, with the rest of the plateau region (735 to 910 nm) being significant. The  
9 MGIV A-D environment had an increase in the blue region compared to the A-I environment,  
10 with the green being the most significant region of the VIR, similar to the A-I environment  
11 (Figure 3.1J). The red edge was significant, as in the MGIII and MGIV A-I environment;  
12 however, no significant regions of the NIR were observed.

13 In the MGIV B-I and B-D environments, significant portions of the spectra in the blue,  
14 green, red, and red edge were observed, as well as some portions of the NIR (Figures 3.1K,3.1  
15 L). For the B-I environment, the early blue, green, red, and red edge were the most highly  
16 significant for yield estimation, as well as a slight peak in the 1305-nm region (Figure 3.1K). For  
17 the B-D environment, the early blue, green, and red edge were the most highly significant,  
18 similar to the B-I environment (Figure 3.1L); however, the red portion of the spectra and the NIR  
19 had different significant levels than the B-I environment. In the NIR, peaks in the 765 to 945 nm  
20 and a slight peak from 1065 to 1105 nm were observed, which were not observed in the B-I  
21 environment. These regions have been correlated with biomass production as well as plant  
22 water content; this correlation suggests that genotypes in the water-stressed environment may be  
23 differentiating in total biomass and water content, which leads to differences in yield.

1 For the MGIV environments in Field C, no optimized model was found for the C-I 2  
2 environment because of higher than expected yield and inconsistent spectra from irrigation  
3 issues. The C-I 1 environment, however, had significant regions in the VIR and red edge, as well  
4 as most of NIR (with the exception of 1005 to 1125 nm) (Figure 3.1M). Overall, for the MGIV  
5 experiments, Field C was the most inconsistent and had the most variability between regions  
6 significant for yield estimation.

7 Different wavebands between maturity group mean spectra were detected for yield  
8 estimation. The differences in spectral regions correlated to yield could be due to morphological  
9 characteristics of the maturity groups. Other spectral regions exhibited variable importance  
10 values over Wold's criterion but were not selected due to fears of high multicollinearity between  
11 bands and over-fitting due to more predictor variables than the sample size ( $N = 20$ ).  
12 Overall, the most significant portions of the spectra across all experiments were the visible and  
13 red-edge portions of the spectra. The green around the 550-nm region and red around the 675–  
14 695-nm regions were the most significant portions of the visible spectra. In the red edge, the  
15 705–715-nm regions were the most significant. The NIR was highly influenced by  
16 environmental factors and was inconsistent in significance for yield estimation across  
17 environments. This result is most likely due to atmospheric scatter and observational day  
18 conditions influencing the spectra. Band regions for final yield modeling were selected based on  
19 significance to yield estimation through importance in projection values in all environments in  
20 both maturity groups. Selected portions of the spectra that were close to each other were  
21 combined to form 11 spectral regions used for further yield modeling. The final bands used for  
22 modeling were 415 (400–430 nm), 550 (530–570 nm), 680 (670–690nm), 715 (700–730 nm),  
23 915 (910–920 nm), 940 (930–950 nm), 990 (980–1000 nm), 1100 (1090–1110 nm), 1140 (1120–



1 1160 nm), 1245 (1240–1250 nm), and 1300 (1290–1310 nm). The 405–435-nm regions have  
2 been correlated with high chlorophyll a and b as well as beta-carotene absorption, resulting in  
3 low reflectance values in soybean (Chappelle et al., 1992). Lower reflection values in this region  
4 are due to high absorption of light by the chlorophylls and beta-carotene. Peñuelas et al. (1995)  
5 also created a normalized phaeophytinization index (NPQI) that related senescence to reflectance  
6 in the 415- and 435-nm regions.

7         The 535–565-nm regions of the spectra are in the visible green region of the spectra,  
8 which has high reflection due to chlorophyll a and b reflecting green light. Chappelle et al.  
9 (1992) found that chlorophyll a and b of soybean leaves reflected the 550-nm region the most  
10 and could be used in a ratio with 675 nm to explain 93% of the variation within chlorophyll  
11 content between soybean leaves and could then be related directly to photosynthetic capacity.  
12 Also, 550 nm has been used to explain 92% of yield variability in wheat yield (Royo et al.,  
13 2003). Ma et al. (2001) also used 559 nm by itself as well as in a ratio with 613 nm to explain  
14 from 13 to 80% of the variation within yield in soybean genotypes.

15         The 675–685-nm regions of the spectra are in the middle of the red depression region of  
16 the spectra and have been correlated with chlorophyll absorption in soybean (Chappelle et al.,  
17 1992). The lower yielding varieties had a higher reflection value in this region, suggesting a  
18 lower amount of chlorophyll or inefficiency of the chlorophyll, resulting in lower yields in  
19 soybean (Ma et al., 2001), corn (Weber et al., 2012), and wheat (Royo et al., 2003).

20         The 705-745nm region encompasses the end of the red and start of the red-edge  
21 inflection point. The red-edge inflection point is the sharp increase in reflection values, due to  
22 the transition from the visible red region to the high-reflection NIR portion due to cellular

1 scatter. This inflection point has been used to distinguish plants for health and yield, with  
2 healthier plants having a large contrast between red and NIR (Gitelson et al., 2011).

3         The 915-nm waveband regions had a high reflection value in the spectra and have been  
4 associated with chlorophyll content measurements. Zhao et al. (2006) found that ratios using 551  
5 and 915 nm as well as 708 and 915 nm accounted for 67–76 % of the variability within  
6 chlorophyll content between cotton genotypes; however, Gitelson et al. (2003 and 2005) found  
7 that the best wavebands for estimating chlorophyll in higher plants were from 525 to 585 nm and  
8 695 to 725 nm. 915 nm also has been used for total biomass prediction in bermudagrass,  
9 accounting for 29.8 to 44.3% of the biomass variation (Stark et al., 2006). Marti et al. (2007)  
10 found that total biomass had a strong correlation with wheat yield ( $r = 0.97$ ).

11         Reflection in the 940-nm region has been used in chlorophyll meters (Minolta Osaka Co.,  
12 Ltd., Japan) to capture nitrogen status and chlorophyll content of crops (Blackmer et al., 1994).  
13 Vollmann et al. (2011) found a significant correlation with SPAD-502 readings (ratio between  
14 650 nm and 940 nm) and 1000-seed weight in soybean cultivars. High reflection values were  
15 also observed in the 985–995-, 1105-, and 1135–1155-nm regions, with higher yielding  
16 genotypes tending to have higher reflection (data not shown). Wenjiang et al. (2004) found that  
17 wavebands selected through regression techniques for winter wheat total foliar nitrogen content  
18 were in the 1000–1140-nm ( $r = 0.8325$ ) and 1200–1300-nm ( $r = 0.5138$ ) regions.

19         The 1240-nm region of the spectra has been correlated with water content of the leaf in  
20 many crops (Peñuelas et al., 1993; Gao, 1996; Datt et al., 2003; Gutierrez et al., 2010).  
21 Moreover, lower values in the 1150–1260-nm region have been associated with higher water  
22 content (Sims and Gamon, 2003); Prasad et al. (2007b) concluded that indices using water  
23 content bands had higher heritability and could distinguish higher yielding genotypes more

1 consistently than vegetation based indices in wheat. The 1095-nm and 1295–1300-nm regions of  
2 the spectra are in the NIR portion, and higher values in these regions correlate to higher yielding  
3 varieties in corn, but no physiological characteristics have been associated with these waveband  
4 regions (Weber et al., 2012).

### 5 *Correlation Between Parameters*

6 Significant correlations were found between yield, maturity, and wavebands (Table 3.4).  
7 There was a significant positive correlation ( $r = 0.68$ ) between yield and maturity in the MGIV  
8 experiment, but no significant correlation ( $r = 0.35$ ) was found between yield and maturity in the  
9 MGIII genotypes. This result may have been mainly due to premature death of some MGIV  
10 entries in 2011 and an early frost in 2012 that did not allow these genotypes to develop fully.  
11 When the top five maturing cultivars were eliminated from analysis, no significant correlation  
12 was observed between yield and maturity in the MGIV genotypes (data not shown). In both  
13 maturity groups, the VIR wavebands had a negative and more significant correlation with yield  
14 than the NIR wavebands with the exception of 915 in the MGIV ( $r = 0.46^*$ ). The NIR portion  
15 had a positive correlation with yield, with the exception of 1245 and 1300 in both experiments.  
16 Chang et al. (2003) found similar patterns in correlation between VIR and NIR bands to corn  
17 yield; however, they found that in early sampling dates, the NIR had a negative correlation with  
18 yield. They concluded that negative correlations were due to soil reflectance confounds, similar  
19 to observations by Ryerson and Curran (1997). For the MGIII entries, 715 ( $r = -0.83^{**}$ ) had the  
20 most significant correlation with yield, and 1140 ( $r = 0.06$ ) exhibited the least association (Table  
21 3.4). In the MGIV experiment, 680 ( $r = -0.78^{**}$ ) was the most significantly correlated with yield,  
22 and 1140 ( $r = 0.03$ ) was the least correlated.

1 Significant correlation coefficients were identified between maturity and the wavebands  
2 in both maturity groups (Table 3.4). For the MGIII genotypes, no significant correlations were  
3 identified in the VIR, but significant positive correlations were identified in the NIR ( $r = 0.51^*$  to  
4  $0.73^{**}$ ). For the MGIV genotypes, significant correlations between maturity and wavebands  
5 were found in the VIR ( $r = -0.48^*$  to  $-0.59^{**}$ ) and NIR ( $r = 0.46^*$  to  $0.57^{**}$ ) portions of the  
6 spectrum. Due to the NIR's association with cell structure, earlier maturing varieties would have  
7 cellular degradation due to senescence sooner than later maturing varieties and would be  
8 distinguished due to low NIR values.

9 In both maturity groups, wavebands in the VIR portion were significantly correlated with  
10 each other ( $r = 0.77^{**}$  to  $0.99^{**}$ ), and the NIR wavebands were significantly correlated with  
11 each other ( $r = 0.69^{**}$  to  $1.00^{**}$ ). In the MGIII and MGIV genotypes, wavebands close in  
12 proximity were highly correlated with each other, and 1245 and 1300 had a correlation  
13 coefficient of 1.00. In both maturity groups, 1245 and 1300 tended to be significantly correlated  
14 with other bands, suggesting multicollinearity between these bands that could confound  
15 regression analysis. The high correlation between wavebands suggests that these wavebands are  
16 not independent information and techniques need to be employed to detect multicollinearity in  
17 regression analysis to reduce the risk of over-fitting yield estimation models.

### 18 *Growth Stage Selection*

19 Yield estimation models based on growth stages that explained a significant proportion of  
20 the yield variation were created for both maturity groups (Tables 3.5 and 3.6; growth stage  
21 observations selected for further analysis are bolded). Overall, some observation days were  
22 significantly better than other observation days. Weather and other environmental conditions  
23 seemed to affect the spectral response curves from observation day to observation day, leading to

1 some observations being inconsistent and showing lack of fit, whereas others significantly  
2 contribute to yield estimation. Also, expanding upon the intensity of observations to alleviate  
3 some of these problems may be necessary. The results seem to suggest that singular observation  
4 days are not consistent enough for yield estimation across different environments and  
5 recommendations for best growth stages for yield estimation cannot be concluded. Although not  
6 recorded in this study, these inconsistencies across days and environments could be due to  
7 changing air temperature, sun angle, and humidity levels affecting spectral reflectance values.  
8 Environments A-I and B-D tended to have the most consistent models, with all observation days  
9 in both maturity groups selected for final model building. Irrigated environment models tended  
10 to explain a greater portion of yield among genotypes than water-stressed environments, which is  
11 most likely due to genotypes being easier to distinguish in high-yielding environments than low-  
12 yield potential environments. No real trend for early or later growth stages was observed in this  
13 study, which is inconsistent with observations made by Ma et al. (2001), who found that late  
14 seed fill (R6) accounted for the most yield variability in soybean cultivars and that reproductive  
15 stages were better for yield estimation than vegetation stages. A study by Ma et al. (2001),  
16 however, was conducted using the Green NDVI, which may be more consistent in later growth  
17 stages than earlier growth stages due to greater genotypic differences in the green and NIR  
18 portions of the spectrum later in the growing season. Similar wavebands were selected for yield  
19 estimation in both maturity groups, with 715 (11-MGIII; 12-MGIV) and 915 (5-MGIII; 5-  
20 MGIV) utilized the most and 1300 (1) and 1245 (1) the least.

21 MGIII regression models for yield estimation based on growth stage explained from 47 to  
22 85% of the variability in seed yield using 1–4 wavebands, with the exception of three  
23 environments with no significant regression models identified (Table 3.5). Root means square

1 error values ranged from 0.32 to 0.56 t ha<sup>-1</sup>. The R<sup>2</sup> for each water regime explained a similar  
2 amount of yield variability in irrigated environments (R<sup>2</sup> = 0.47 - 0.85) and water-stressed  
3 environments (R<sup>2</sup> = 0.51 to 0.79) when comparing growth stages. Environments in 2012 (R<sup>2</sup> 0.47  
4 to 0.85) tended to explain more of the variation in yield than 2011 (R<sup>2</sup> = 0.51 to 0.73)  
5 environments; however, environment A-I had all observation days contributing to the final  
6 training model, whereas no other environment besides B-D had more than two observations  
7 contributing to the final training model dataset. For Field A, the R3-R4 growth stage in the AWI  
8 environment exhibited the highest R<sup>2</sup> for seed yield. The highest yield variability explained was  
9 in environment C-I 1 at the R6 (late seed fill) growth stage (R<sup>2</sup> = 0.85). The R3 and R3-4 growth  
10 stage observation on B-I and R3 growth stage observation on C-I 1 were not significant.

11 MGIV regression models for yield estimation based on growth stage explained from 30 to 89%  
12 of the variability in seed yield using 1–5 wavebands, with the exception of three environments  
13 with significant regression models identified (Table 3.6). Root mean square values ranged from  
14 0.31 to 0.66 t ha<sup>-1</sup>, with the R5 growth stage in the A-D environment exhibiting the lowest and  
15 the R4 growth stage in B-I exhibiting the highest values. Unlike the MGIII experiment, 2011  
16 environments (R<sup>2</sup> = 0.54 to 0.89) tended to account for a larger amount of yield variability than  
17 2012 data (R<sup>2</sup> = 0.30 to 0.86), and environment A-I was also the most consistent, with all  
18 observation days selected for final training model creation. The regression model created using  
19 the R3-R4 growth stage on A-I exhibited the highest coefficient of determination value, but also  
20 used the most wavebands (5), suggesting the model is most likely over-fit and the R<sup>2</sup> value was  
21 inflated. The same conclusion could be made about the R5 observation on B-I, but these growth  
22 stages were kept due to similar wavebands used in other models. The lack of fit observed for the  
23 A-I 2 environment can be explained by the previously explained irrigation malfunction. Also, as

1 in the MGIII experiment, the R2-R3 observation for B-I was discarded due to inconsistent  
2 spectra, which may have been related to high humidity and temperature conditions during  
3 spectral measurements.

#### 4 *Yield Estimation Model Development*

5 Selected observation days from the individual environment analysis were combined into  
6 a single dataset for each maturity group and used to build the final training models for yield  
7 estimation in both maturity groups. Datasets were means calculated from singular observation  
8 day data. The summary statistics and equation for the selected growth stage observations based  
9 on two-year spectra and yield means for MGIII and MGIV genotypes are presented in Table 3.7  
10 and Figure 3.2. For the MGIII genotypes, through multiple linear regression, the estimation  
11 model explained 83% of the variability within yield between genotypes. Red-edge region 715  
12 explained the most yield variability in models (73%), and the 1100 waveband region explained  
13 10% of the yield variability. In the training model, the  $\beta$  parameter estimate for the 715  
14 waveband was negative, suggesting varieties with high values for the 715 will have decreased  
15 yields (Figure 3.2). This result is consistent with previous research findings that lower reflection  
16 values in the red region of the spectra correlates with higher grain yields (Weber et al., 2012).  
17 The 1100 waveband was positive, which is consistent with previous research suggesting  
18 increased reflectance in the NIR area can correlate with higher yields (Weber et al., 2012).

19 For the MGIV experiment, the training model accounted for 81% of the yield variability  
20 between genotypes. The 715 (700–730 nm) and 915 (910–920 nm) wavebands were selected in  
21 the training model, which is consistent with the red edge and NIR measurements seen in the  
22 MGIII training model. 715 explained the most yield variability at 70%, and 915 wavebands  
23 explained 11% of the variability in yield. The  $\beta$  parameter estimate for the 715 waveband was

1 negative, suggesting genotypes with high values for the 715 will have decreased yields, as in the  
2 MGIII models. The 915 waveband was also positive, which was consistent with MGIII  
3 genotypes and previous research (Reynolds et al., 1999; Lin et al., 2012; Weber et al., 2012).

4 Results suggest that selecting significant growth stage observations improved yield  
5 estimation models. Results also indicate that the 715 waveband explains a large portion of the  
6 variability within seed yield, and previous research concluded that soybean yield can be directly  
7 related to chlorophyll content (Morrison et al., 1999). Although not as important as chlorophyll,  
8 this study found wavebands in the NIR to be highly effective in estimating yield when combined  
9 with the red edge. Observations by Morrison et al. (1999) and Voldeng et al. (1997) that  
10 increases observed in soybean seed yield can be attributed to increased chlorophyll content and  
11 photosynthetic capacity. Reynolds et al. (1999) also concluded that increases observed in wheat  
12 yield were due to a better partitioning of photosynthetic components; however, Lin et al. (2012)  
13 concluded that the NIR regions from 760–1030 nm contributed the most to rice cultivar  
14 discernment.

### 15 *Yield Estimation Model Validation*

16 Validation of training models on individual environments delivered mixed results for  
17 both maturity groups, with coefficient of determination values ranging from 29 to 79% for the  
18 MGIII genotypes and 1 to 83% for the MGIV genotypes (Table 3.8). As in the observation-day  
19 selection analysis, the training model accounted for a large portion of the variability in yield,  
20 whereas in other environments and observation days, the training models did not account for a  
21 significant portion of the variability in yield. For the MGIII genotypes, the mean  $R^2$  for the  
22 irrigated water regime was 56%, whereas in the water-stressed regime, the mean was 63%.  
23 Similar results were observed in the MGIV genotypes, with the irrigated regime accounting for



1 49% of the variability in with the C-I 2 environments and 59% without. The water-stressed  
2 environment mean accounted for 62% of variability, and when comparing water regimes within  
3 the same field, the water-stressed environment mean accounted for a larger portion in three of the  
4 four instances, with A-I for the MGIV genotypes as the lone exception. These results are similar  
5 to observations by Ma et al. (2001) that stressed environments accounted for more variability  
6 than optimal environments. The authors concluded that results were due to greater differences in  
7 genotypes between higher and lower yielding spectra in the non-optimal compared with the  
8 optimal environments. In three of six environments for MGIII and four of six environments for  
9 MGIV genotypes, the season totals (ST) accounted for as much or more of the variation in yield  
10 than individual growth stages. These results are somewhat surprising because season total means  
11 would be expected to be more robust and have less error associated with the values than single  
12 observations, resulting in higher  $R^2$  values.

13 For the MGIII genotypes, the highest  $R^2$  value was observed in the C-I 1 environment ( $R^2$   
14 = 0.79) season total dataset. The growth stage observation with the highest validation  $R^2$  was  
15 observed in the C-I 1 environments as well, with an  $R^2$  value of 0.75. The year averages were  
16 consistent for the MGII genotypes, with each year spectra mean dataset accounting for 68% of  
17 the variability within yield between genotypes. For the MGIV genotypes, the highest  $R^2$   
18 observed was the season total validation dataset for the B-D environment ( $R^2 = 0.83$ ). The  
19 highest single growth stage was observed for the R1–R2 growth stage for environment B-I ( $R^2 =$   
20 0.79). Contrary to the MGIII training model, the MGIV training model did not have consistent  
21 performance for year means, with the 2011 mean dataset accounting for 65% and the 2012 mean  
22 dataset accounting for 79% of the variability within yield. This is surprising given that single  
23 growth stage validations on Field A in 2011 were more consistent than 2012 validations;



1 key biophysical/biochemical components that have been proven to contribute to yield in many  
2 crops. Regression models built based on two-year means explained a large portion of the  
3 variability within soybean yield in both maturity groups. The red-edge area and portions of the  
4 NIR were the most important portions of the electromagnetic spectra, and creation of yield  
5 prediction models based on these waveband regions can account for a significant amount of  
6 variability within soybean seed yield. Variability was high within and between growth stages,  
7 water regimes, environments, and years for validation of training models. Environmental factors  
8 such as weather, time of day, and other factors appear to affect spectral reflectance  
9 tremendously, leading the training models performing better or worse on different validation  
10 datasets. The performance was not as consistent as hoped, but still accounted for a significant  
11 portion of variability in seed yield in most environments. The training models also had the ability  
12 to distinguish the top three highest yielding genotypes within the top 50% of the genotypes in  
13 most validation datasets.

14 This experiment demonstrated that canopy reflectance can be used to characterize  
15 soybean seed yield using a diverse set of genotypes. These genotypes allowed for significant  
16 variation in model training datasets; however, experiments need to be conducted with genotypes  
17 that have less diversity to validate the models. Integrating spectral reflectance measurements into  
18 a high-throughput platform also is necessary before this technology can be adopted in breeding  
19 programs.

## 20 **References**

21 Adams, M.L., W.D. Philpot, and W.A. Norvell. 1999. Yellowness index: an application of  
22 spectral 2nd derivatives to estimate chlorosis of leaves in stressed vegetation. *Int. J. of*  
23 *Remote Sensing*. 20:3663–3675.

- 1 Aparicio, N., D. Villegas, J. Araus, J. Casadesus, and C. Royo. 2002. Relationship between  
2 growth traits and spectral vegetation indices in durum wheat. *Crop Sci.* 42(5):1547–1555.
- 3 Babar, M., M. Reynolds, M. van Ginkel, A. Klatt, W. Raun, and M. Stone. 2006a. Spectral  
4 reflectance indices as a potential indirect selection criteria for wheat yield under  
5 irrigation. *Crop Sci.* 46(2):578–588.
- 6 Babar, M., M. Reynolds, M. Van Ginkel, A. Klatt, W. Raun, and M. Stone. 2006b. Spectral  
7 reflectance to estimate genetic variation for in-season biomass, leaf chlorophyll, and  
8 canopy temperature in wheat. *Crop Sci.* 46(3):1046–1057.
- 9 Ball, S., and C. Kozak. 1993. Relationship between grain-yield and remotely-sensed data in  
10 wheat breeding experiments. *Plant Breeding.* 110(4):277–282.
- 11 Baret, F., and G. Guyot. 1991. Potentials and limits of vegetation indices for LAI and APAR  
12 assessment, *Remote Sens. Environ.* 35:161–174.
- 13 Blackmer, T.M., J.S. Schepers, and G.E. Varvel. 1994. Light reflectance compared with other  
14 nitrogen stress measurements in corn leaves. *Agron. J.* 86:934–938.
- 15 Chang, J., D.E. Clay, K. Dalsted, S. Clay, M. O'Neill. 2003. Corn (*Zea Mays* L.) yield prediction  
16 using multispectral and multirate reflectance. *Agron. J.* 95:1447–1453.
- 17 Chappelle, E.W., M.S. Kim, and J.E. McMurtrey, III. 1992. Ratio analysis of reflectance spectra  
18 (RARS): An algorithm for the remote estimation of the concentrations of chlorophyll a,  
19 chlorophyll b, and carotenoids in soybean leaves. *Remote Sens. Environ.* 39:239–247.
- 20 Clevers, J.G.P.W. 1997. A simplified approach for yield prediction of sugar beet based on optical  
21 remote sensing data. *Remote Sens. Environ.* 61:221–228.
- 22 Datt, B. 1999. Remote sensing of water content in Eucalyptus leaves. *Australian Journal of*  
23 *Botany.* 47:909–923.

- 1 Datt, B., T.R. McVicar, T.G. Van Niel, D.L.B. Jupp, and J.S. Pearlman. 2003. Pre-processing  
2 EO-1 Hyperion hyperspectral data to support the application of agricultural indexes.  
3 IEEE Transactions on Geoscience and Remote Sensing. 41:1246–1259.
- 4 Daughtry, C.S.T., C.L. Walthall, M.S. Kim, E. Brown de Colstoun, and J.E. McMurtrey, III.  
5 2000. Estimating corn leaf chlorophyll content from leaf and canopy reflectance. Remote  
6 Sens. Environ. 74:229–239.
- 7 De Jong, S. 1993. SIMPLS: an alternative approach to partial least squares regression.  
8 Chemometrics and Intelligent Laboratory Systems. 18(3):251–263.
- 9 Deering, D.W. 1978. Rangeland reflectance characteristics measured by aircraft and spacecraft  
10 sensors. Ph.D. diss. Texas A&M Univ., College Station.
- 11 Dusek, D.A., R.D. Jackson, and J.t. Musick. 1985. Winter wheat vegetation indices calculated  
12 from combinations of seven spectral bands. Remote Sensing of Environment, 18:255–  
13 267.
- 14 Fehr, W.R., and C.E. Caviness. 1977. Stages of Soybean Development, Cooperative Extension  
15 Service, Agriculture and Home Economics Experiment Station Iowa State University,  
16 Ames, Iowa
- 17 Gamon, J.A., J. Peñuelas, and C.B. Field. 1992. A narrow-waveband spectral index that tracks  
18 diurnal changes in photosynthetic efficiency. Remote Sens. Environ. 41:35–44.
- 19 Gao, B.C. 1996. NDWI—a normalized difference water index for remote sensing of vegetation  
20 liquid water from space. Sens. Environ. 58:257–266.
- 21 Garbulsky, M. 2011. The photochemical reflectance index (PRI) and the remote sensing of leaf,  
22 canopy and ecosystem radiation use efficiencies. Remote Sensing of Environment.  
23 115:281–297.

- 1 Gitelson, A., Y. Gritz, and M. Merzlyak. 2003. Relationships between leaf chlorophyll content  
2 and spectral reflectance and algorithms for non-destructive chlorophyll assessment in  
3 higher plant leaves. *Journal of Plant Physiology*. 160:271–282.
- 4 Gitelson, A.A., A. Vi.a, D.C. Rundquist, V. Ciganda, and T.J. Arkebauer. 2005. Remote  
5 estimation of canopy chlorophyll content in crops. *Geophys. Res. Lett.* 32:108403  
6 doi:10.1029/2005GI022688.
- 7 Gitelson, A.A., P.S. Thenkabail, J.G. Lyon, A. Huete. 2011. Remote Sensing estimation of crop  
8 biophysical characteristics at various scales. Chapter 15 in *Hyperspectral Remote Sensing*  
9 *of Vegetation*. 329–358, Taylor and Francis.
- 10 Gutierrez, M., M. Reynolds, W. Raun, M. Stone, and A. Klatt. 2010. Spectral water indices for  
11 assessing yield in elite bread wheat genotypes under well-irrigated, water-stressed, and  
12 high-temperature conditions. *Crop Sci.* 50:197–214.
- 13 Gutierrez-Rodriguez, M., M.P. Reynolds, J.A. Escalante-Estrada, M.T. Rodriguez-Gonzalez.  
14 2004. Association between canopy reflectance indices and yield and physiological traits  
15 in bread wheat under drought and well-irrigated conditions. *Australian J. of Ag.*  
16 *Research.* 55: 1139–1147.
- 17 Hansen, P.M., J.R. Jorgensen, A. Thomsen. 2002. Predicting grain yield and protein content in  
18 winter wheat and spring barley using repeated canopy reflectance measurements and  
19 partial least squares regression. *J. of Ag. Sci.* 139:307–318.
- 20 Harshman, R., and M. Lundy. 1994. PARAFAC: Parallel factor analysis. *Computational*  
21 *Statistics and Data Analysis*, 18:39–72.
- 22 Hatfield, J., and J. Prueger. 2010. Value of using different vegetative indices to quantify  
23 agricultural crop characteristics at different growth stages under varying management

- 1 practices. *Remote Sensing*. 2:562–578.
- 2 Hatfield, J.L. 1983. Remote sensing estimators of potential and actual crop yield. *Remote Sens.*  
3 *Environ.* 13:301–311.
- 4 Hong, S.Y., K.A. Sudduth, N.R. Kitchen, H.L. Palm, and W.J. Weibold. 2001. Using  
5 hyperspectral remote sensing data to quantify within-field spatial variability [CD  
6 ROM]. *Proc. Int. Conf. on Geospatial Inf. in Agric. and Forestry*, 3rd, Denver, CO. 5–7  
7 Nov. 2001. Altatum, Ann Arbor, MI.
- 8 Jordan, C.F. 1969. Derivation of leaf area index from quality of light on the forest floor. *Ecology*  
9 50:663–666.
- 10 Kaul, M., R.L. Hill, and C. Walthall. 2005. Artificial neural networks for corn and soybean yield  
11 prediction. *Agricultural Systems* 85:1–18.
- 12 Lin, W.S., C.M. Yang, and B.J. Kuo. 2012. Classifying cultivars of rice (*Oryza sativa* L.) based  
13 on corrected canopy reflectance spectra data using the orthogonal projections of latent  
14 structures (O-PLS) method. *Chemometrics and Intelligent Laboratory Systems*. 115:25–  
15 36.
- 16
- 17 Loss, S.P., and K.H.M. Siddique. 1994. Morphological and physiological traits associated with  
18 wheat yield increases in Mediterranean environments. *Advances in Agronomy*. 52: 229–  
19 276.
- 20 Ma, B.L., L.M. Dwyer, C. Costa, E.R. Cober, M.J. Morrison. 2001. Early Prediction of Soybean  
21 yield from canopy reflectance measurements. *Agron. J.* 93:1227–1234.
- 22 Marti, J., J. Bort, G. Slafer, and J. Araus. 2007. Can wheat yield be assessed by early  
23 measurements of normalized difference vegetation index? *Annals of Applied Biology*,

- 1           150:253–257.
- 2 Morrison, M.J., H.D. Voldeng, and E.R. Cober. 1999. Physiological changes from 58 years of  
3           genetic improvement of short-season soybean cultivars in Canada. *Agron. J.* 91:685–689.
- 4 Naes, T., T. Isaksson, T. Faern, T. Davis. 2004. A User-friendly Guide to Multivariate  
5           Calibration and Classification. NIR Publications, Chichester, West Sussex, p. 344.
- 6 Peñuelas, J., F. Baret, and I. Filella. 1995. Semi-empirical indices to assess  
7           carotenoids/chlorophyll a ratio from leaf spectral reflectance. *Photosynthetica* 31:221–  
8           230.
- 9 Peñuelas, J., I. Filella, C. Biel, L. Serrano, and R. Save. 1993. The reflectance at the 950–970  
10          mm region as an indicator of plant water status. *International Journal of Remote Sensing.*  
11          14:1887–1905.
- 12 Pimstein, A., A. Karnieli, and D. Bonfil. 2007. Wheat and maize monitoring based on ground  
13          spectral measurements and multivariate data analysis. *Journal of Applied Remote*  
14          *Sensing.* 1:013530.
- 15 Pimstein, A., A. Karnieli, S. Bansal, and D. Bonfil. 2011. Exploring remotely sensed  
16          technologies for monitoring wheat potassium and phosphorus using field spectroscopy.  
17          *Field Crops Research.* 121:125–135.
- 18 Prasad, B., B. Carver, M. Stone, M. Babar, W. Raun, and A. Klatt. 2007a. Genetic analysis of  
19          indirect selection for winter wheat grain yield using spectral reflectance indices. *Crop*  
20          *Sci.* 47:1416–1425.
- 21 Prasad, B., B. Carver, M. Stone, M. Babar, W. Raun, and A. Klatt. 2007b. Potential use of  
22          spectral reflectance indices as a selection tool for grain yield in winter wheat under Great  
23          Plains conditions. *Crop Sci.* 47:1426–1440.



- 1 Price, J.C., and W.C. Bausch. 1995. Leaf area index estimation from visible and near-infrared  
2 reflectance data. *Remote Sens of Environ.* 52:55–65.
- 3 Reynolds, M., Y. Manes.A. IZANLOO,P. LANGRIDGE. 2009. Phenotyping approaches for  
4 physiological breeding and gene discovery in wheat. *Annals of Appl. Bio.* 155(3):309–  
5 320.
- 6 Reynolds, M.P., S. Rajaram, and K.D. Sayre. 1999. Physiological and genetic changes of  
7 irrigated wheat in the post-green revolution period and approaches for meeting projected  
8 global demand. *Crop Sci.* 39:1611–1621.
- 9 Rouse, J.W., Jr., R.H. Haas, J.A. Schell, and D.W. Deering. 1973. Monitoring vegetation  
10 systems in the Great Plains with ERTS. p. 309–317. In *Proc. Earth Res. Tech. Satellite-1*  
11 *Symp.*, Goddard Space Flight Cent., Washington, DC. 10–14 Dec. 1973.
- 12 Royo, C., N. Aparicio, D. Villegas, J. Casadesus,P. Monneveux,and J. Araus. 2003. Usefulness  
13 of spectral reflectance indices as durum wheat yield predictors under contrasting  
14 Mediterranean conditions. *International Journal of Remote Sensing.* 24:4403–4419.
- 15 SAS Institute Inc., SAS 9.2. Cary, NC: SAS Institute Inc., 2008.
- 16 Shanahan, J.F., J.S. Schepers, D.D. Francis, G.E. Varvel, W.W. Wilhelm, J.S. Tringe, M.R.  
17 Schlemmer, and D.J. Major. 2001. Use of remote sensing imagery to estimate corn grain  
18 yield. *Agron. J.* 93:583–589.
- 19 Sims, D.A., AND J.A. Gamon.2003. Estimation of vegetation water content and photosynthetic  
20 tissue area from spectral reflectance: a comparison of indices based on liquid water and  
21 chlorophyll absorption features. *Remote Sens. Environ.* 84:526–537.

- 1 Stark, P.J., D. Zhao, W.A. Phillips, S.W. Coleman. 2006. Development of canopy reflectance  
2 algorithms for real-time prediction of Bermudagrass pasture biomass and nutritive values.  
3 Crop Sci. 46: 927–934.
- 4 Trotter, G. M., D. Whitehead, and E. J. Pinkney. 2002. The photochemical reflectance index as a  
5 measure of photosynthetic light use efficiency for plants with varying foliar nitrogen  
6 contents. International J. of Remote Sens. 23:1207–1212.
- 7 Tucker, C. J. and P.J. Sellers. 1986. Satellite remote sensing of primary production. International  
8 Journal of Remote Sensing. 7:395–1416.
- 9 Tucker, C.J. 1979. Red and photographic infrared linear combinations for monitoring vegetation.  
10 Remote Sens. Environ. 8:127–150.
- 11 Voldeng, H.D., E.R. Cober, D.J. Hume, C. Gillard, and M.J. Morrison. 1997. Fifty-eight years of  
12 genetic improvement of short-season soybean cultivars in Canada. Crop Sci. 37:428–431.
- 13 Vollmann, J., H. Walter, T. Sato, and P. Schweiger. 2011. Digital image analysis and chlorophyll  
14 metering for phenotyping the effects of nodulation in soybean. Computers and  
15 Electronics in Agriculture. 75:190–195.
- 16 Walter, A., B. Studer, R. Kolliker. 2012. Advanced phenotyping offers opportunities for  
17 improved breeding of forage and turf species. Annals of Botany. 1–9.
- 18 Weber, V.S., J.L. Araus, J.E. Cairns. C. Sanchez, A.E. Melchinger, E. Orsini. 2012. Prediction of  
19 grain yield using reflectance spectra of canopy and leaves in maize plants grown under  
20 different water regimes. Field Crops Research. 128:82–90.
- 21 Wenjiang, H., W. Jihua, W. Zhijie, Z. Jiang, L. Liangyun, and W. Jindi. 2004. Inversion of foliar  
22 biochemical parameters at various physiological stages and grain quality indicators of  
23 winter wheat with canopy reflectance. Int. J. Remote Sensing. 25 (12):2409–2419.

- 1 White, J.W., P. Andrade-Sanchez, M.A. Gore, K.F. Bronson, T.A. Coffelt, M.M. Conley, K.A.  
2 Feldmann, A.N. French, J.T. Heun, D.J. Hunsake, M.A. Jenks, B.A. Kimball, R.L. Roth,  
3 R.J. Strand, K.R. Thorp, G.W. Wall, and G. Wang. 2012. Field-Based phenomics for  
4 plant genetics research. *Field Crops Research*, 133:101–112.
- 5 Wiegand, C., A. Richardson, D Escobar, and A Gerbermann.. 1991. Vegetation indexes in crop  
6 assessment. *Remote Sensing of Environment*. 35:105–119.
- 7 Wold, H. 1966. Estimation of principal components and related models by iterative least squares.  
8 In Krishnaiaah, P.R.. *Multivariate Analysis*. New York: Academic Press. 391–420.
- 9 Zhao, D., K.R. Reddy, V.G. Kakani, J.J. Read, and S. Koti. 2006. Canopy reflectance in cotton  
10 for growth assessment and lint yield prediction. *Europ. J. Agronomy*. 26:335–344.

11  
12  
13  
14  
15  
16  
17  
18  
19  
20  
21  
22  
23  
24  
25  
26  
27  
28  
29  
30  
31  
32  
33

1 **Table 3.1. Mean seed yield by environments and range in yield across genotypes within**  
 2 **environments.**

Year	Field	Water regime	Mean	LSD	Range
Maturity group III					
t ha <sup>-1</sup>					
2011	A	IRR	2.98	0.43	2.52
2011	A	DRY	1.75	0.60	2.01
2012	B	IRR	3.63	0.58	2.67
2012	B	DRY	2.78	0.92	2.31
2012	C	IRR1	3.99	0.60	2.86
2012	C	IRR2	3.94	0.59	3.33
Maturity group IV					
2011	A	IRR	3.20	0.52	3.27
2011	A	DRY	1.76	0.55	1.81
2012	B	IRR	3.59	0.38	3.63
2012	B	DRY	3.23	0.41	2.49
2012	C	IRR1	3.77	0.74	2.14
2012	C	IRR2	3.99	0.51	2.68

3  
4  
5  
6  
7  
8  
9  
10  
11  
12  
13  
14  
15  
16  
17  
18  
19  
20  
21  
22  
23  
24  
25  
26

1  
2 **Table 3.2. Maturity group III (MGIII) and maturity group IV (MGIV) analysis of variance**  
3 **F-values for seed yield, maturity (Mat), and spectral wavelengths used for yield estimation**  
4 **models.**

Source	DF	Yield	Mat	415	550	680	715	915	940	990	1100	1140	1245	1300
MGIII														
Gen (G)	19	111.6**	75.0**	10.2**	17.3**	12.6**	14.7**	5.1**	4.5**	4.6**	3.5**	3.9**	4.7**	4.7**
Env (E)	5	109.1**	94.3**	18.3**	11.0**	8.7*	8.3*	45.1**	38.9**	40.8**	36.4**	14.9**	28.3**	23.6**
G × E	95	3.1**	4.5**	3.3**	3.5**	3.2**	3.5**	2.1*	2.0*	1.9*	1.7*	1.5*	1.7*	1.7*
MGIV														
Gen (G)	19	99.9**	40.4**	90.9**	16.3**	8.5**	14.9**	3.0*	2.5*	2.8*	2.9*	2.2*	2.1*	2.1*
Env (E)	5	84.5**	567.4**	112.3**	137.6**	139.7**	139.6**	50.7**	59.3**	55.5**	49.5**	64.9**	61.1**	58.8**
G × E	95	3.9**	2.6**	1.0	1.4*	1.1	1.5*	0.8	0.6	0.6	0.6	0.5	0.5	0.5

\* = Pr < 0.05 \*\* = Pr < 0.01

5  
6  
7  
8  
9  
10  
11  
12  
13

**Table 3.3. Maturity group III (MGIII) and maturity group IV (MGIV) analysis of variance F-values for 2011 and 2012 experiments, and wavelengths used for yield estimation models.**

MGIII														
Year	Field-Env	Growth Stage	DF	Wavelength (nm)										
				415	550	680	715	915	940	990	1100	1140	1245	1300
2011	A-I	R3-R4	19	2.77**	3.41**	2.20**	2.94**	1.57	1.58	1.43	0.96	1.29	0.74	0.79
2011	A-I	R4	19	6.27**	9.82**	4.36**	9.98**	3.29**	2.86**	2.46**	2.32**	2.08**	2.25**	2.27**
2011	A-I	R5	19	3.77**	8.22**	1.86*	5.55**	3.71**	3.10**	2.41**	1.96*	1.80*	1.84*	1.86*
2011	A-I	R6	19	3.15**	8.31**	8.19**	5.73**	3.86**	3.48**	2.94**	2.24**	2.02**	1.93*	1.87*
2011	A-D	R3-R4	19	4.31**	6.89**	3.35**	6.79**	1.84*	1.75*	1.83*	1.35	1.44	1.52	1.52
2011	A-D	R5	19	7.16**	19.44**	5.92**	17.97**	4.26**	3.75**	3.97**	3.58**	3.13**	3.93**	3.93**
2011	A-D	R6	19	16.12**	17.37**	18.58**	10.90**	8.31**	7.06**	5.61**	4.12**	2.79**	2.12**	1.95*
2012	B-I	R2	19	5.35**	8.81**	3.93**	9.17**	1.31	3.49**	2.47**	3.18**	2.33**	3.33**	3.30**
2012	B-I	R3	19	2.73**	4.32**	2.38**	4.57**	1.44	1.43	1.45	NS	1.42	1.50	1.51
2012	B-I	R3-R4	19	2.03**	3.84**	2.15**	4.12**	1.71*	1.70*	1.78*	1.59	1.69*	1.82*	1.83*
2012	B-I	R5-R6	19	6.16**	8.86**	7.00**	9.53**	1.82*	1.98*	2.24**	2.07**	2.49**	2.77**	2.84**
2012	B-D	R3	19	3.35**	2.95**	1.97*	4.14**	1.67*	1.66*	1.65	1.30	1.40	1.64	1.67*
2012	B-D	R4	19	6.64**	7.85**	5.47**	11.26**	1.91*	1.72*	1.85*	1.64	1.72*	2.22**	2.31**
2012	C-I1	R2	19	9.38**	18.06**	9.25**	13.45**	1.45	1.60	1.67*	1.39	1.77*	1.92*	2.01**
2012	C-I1	R3	19	1.71*	3.34**	1.94*	3.01**	0.73	0.71	0.71	NS	0.72	0.74	0.75
2012	C-I1	R4-R5	19	3.38**	4.50**	2.49**	5.21**	1.61	1.76*	1.77*	1.46	1.80*	1.85*	1.92*
2012	C-I1	R6	19	5.58**	6.01**	4.44**	7.63**	2.75**	2.65**	3.34**	2.72**	2.80**	3.65**	3.69**
2012	C-I2	R2	19	1.83*	2.73**	1.61*	3.93**	1.45	1.46	1.54	1.70*	1.38	1.56	1.59
2012	C-I2	R4-R5	19	4.17**	6.29**	3.69**	9.74**	4.01**	4.29**	4.54**	3.00**	3.74**	4.09**	4.14**

MGIV														
Year	Field-Env	Growth Stage	DF	Wavelength (nm)										
				415	550	680	715	915	940	990	1100	1140	1245	1300
2011	A-I	R3	19	2.87**	3.91**	2.35**	4.57**	2.20**	2.09**	1.59	1.57	1.52	1.43	1.45
2011	A-I	R3-R4	19	3.92**	6.46**	4.38**	4.81**	4.93**	4.09**	3.50**	3.10**	2.11**	2.11**	2.00*
2011	A-I	R5	19	4.75**	6.59**	3.87**	4.94**	9.78**	8.28**	6.27**	5.03**	3.70**	2.84**	2.68**
2011	A-I	R5-R6	19	2.81**	3.01**	2.81**	2.65**	5.57**	5.00**	3.51**	2.64**	2.14**	1.69*	1.64
2011	A-D	R2-R3	19	7.05**	6.57**	4.98**	5.11**	2.13**	2.01**	2.00**	1.98*	1.77*	1.83*	1.80*
2011	A-D	R3-R4	19	7.87**	7.36**	4.25**	6.19**	4.05**	4.03**	3.73**	3.50**	3.43**	3.36**	3.34**
2011	A-D	R5	19	6.17**	5.69**	6.41**	6.69**	7.84**	7.22**	5.42**	4.28**	3.23**	2.45**	2.36**
2012	B-I	R1-R2	19	5.01**	8.20**	3.02**	9.89**	4.52**	4.93**	3.94**	3.39**	3.54**	2.95**	2.97**
2012	B-I	R2-R3	19	3.91**	4.77**	2.37**	4.23**	0.76	1.03	1.23	1.43	1.95*	1.75*	1.48
2012	B-I	R4	19	1.82*	2.30**	1.84*	2.32**	1.68	1.78*	1.66	2.00*	1.68*	1.29	1.32
2012	B-I	R5	19	4.58**	6.97**	4.08**	6.77**	3.05**	2.77**	2.77**	2.16**	1.84*	2.02**	1.98*
2012	B-I	R5-R6	19	3.09**	4.74**	2.96**	4.32**	2.81**	2.62**	2.47**	2.45**	2.31**	2.34**	2.34**
2012	B-D	R3	19	4.63**	3.43**	2.33**	3.49**	1.72*	1.88*	1.76*	1.36	1.48	1.51	1.75*
2012	B-D	R4	19	5.58**	4.97**	3.34**	4.57**	3.96**	3.45**	3.22**	3.26**	2.58**	2.61**	2.54**
2012	B-D	R6	19	3.81**	6.89**	3.47**	6.85**	6.35**	5.74**	4.89**	4.69**	3.90**	3.48**	3.37**

2012	C-1	R1-R2	19	7.04**	11.90**	6.55**	8.27**	1.10	1.05	1.33	1.24	1.28	1.58	1.58
2012	C-11	R2-R3	19	1.67*	2.17**	1.05	1.69*	0.77	0.71	0.72	0.65	0.78	0.60	0.50
2012	C-11	R4	19	4.99**	6.19**	3.57**	5.98**	2.57**	2.41**	2.35**	1.91*	1.77*	1.82	1.78*
2012	C-11	R5-R6	19	8.10*	7.30**	6.39**	7.71**	3.27**	3.40**	3.26**	2.82**	2.91**	2.78**	2.77**
2012	C-12	R3	19	1.53	1.33	1.44	1.67*	1.21	1.29	2.07**	1.08	1.78*	2.02**	2.05**
2012	C-12	R4	19	1.37	1.31	1.26	1.29	1.89*	1.83*	1.82*	1.58	1.49	1.51	1.47

\* = Pr>0.05, \*\* = Pr>0.01

**Table 3.4. Maturity group III (MGIII) Pearson's correlation coefficients and p-values for two-year averages of seed yield, maturity, and wavebands used for yield estimation models. MGIII on upper right; maturity group IV (MGIV) on lower left.**

	Yield	mat	415	550	680	715	915	940	990	1100	1140	1245	1300
yield	----	0.35	-0.58**	-0.80**	-0.64**	-0.83**	0.39	0.30	0.18	0.27	0.06	-0.12	-0.17
mat	0.68**	----	0.19	-0.12	0.01	-0.18	0.72**	0.73**	0.70**	0.69**	0.66**	0.53*	0.51*
415	-0.60**	-0.48*	----	0.84**	0.93**	0.77**	0.04	0.16	0.26	0.20	0.37	0.47*	0.50*
550	-0.75**	-0.52*	0.85**	----	0.93**	0.98**	-0.08	0.02	0.14	0.07	0.27	0.43	0.48*
680	-0.78**	-0.59**	0.91**	0.94**	----	0.87**	-0.01	0.10	0.20	0.15	0.31	0.44*	0.48*
715	-0.75**	-0.53*	0.78**	0.99**	0.91**	----	-0.07	0.03	0.16	0.07	0.28	0.46*	0.51*
915	0.46*	0.57**	-0.17	0.03	-0.17	0.08	----	0.99**	0.96**	0.98**	0.92**	0.82**	0.80**
940	0.39	0.53*	-0.12	0.10	-0.09	0.16	0.99**	----	0.99**	0.99**	0.96**	0.88**	0.86**
990	0.19	0.36	0.07	0.31	0.13	0.38	0.94**	0.97**	----	0.99**	0.99**	0.94**	0.92**
1100	0.32	0.46*	0.01	0.21	0.05	0.26	0.96**	0.97**	0.97**	----	0.96**	0.90**	0.88**
1140	0.03	0.21	0.19	0.46*	0.30	0.53*	0.85**	0.90**	0.97**	0.93**	----	0.97**	0.96**
1245	-0.12	0.05	0.34	0.60**	0.47*	0.66**	0.73**	0.79**	0.91**	0.85**	0.98**	----	1.00**
1300	-0.18	0.01	0.37	0.64**	0.51*	0.70**	0.69**	0.76**	0.89**	0.82**	0.96**	1.00**	----

\* Pr > 0.05 \*\* Pr > 0.01



**Table 3.5. Results of the maturity group III (MGIII) stepwise regression models by growth stage within environments, coefficient of determination (R<sup>2</sup>), root means square error (rMSE), percentage rMSE of dependent means (% rMSE of mean), and waveband(s) in final model.**

Environment	Growth stage	R <sup>2</sup>	rMSE t ha <sup>-1</sup>	% rMSE of mean	Waveband(s)
<b>A-I</b>	<b>R3-R4</b>	<b>0.73</b>	<b>0.47</b>	<b>15.66</b>	<b>415 680</b>
<b>A-I</b>	<b>R4</b>	<b>0.66</b>	<b>0.53</b>	<b>17.64</b>	<b>715 940</b>
<b>A-I</b>	<b>R5</b>	<b>0.62</b>	<b>0.56</b>	<b>18.80</b>	<b>550 915</b>
<b>A-I</b>	<b>R6</b>	<b>0.69</b>	<b>0.51</b>	<b>17.02</b>	<b>415 715</b>
A-D	R3-R4	0.51	0.49	26.99	680 940
A-D	R5	0.57	0.46	25.35	715 940
A-D	R6	0.55	0.45	25.08	680
<b>B-D</b>	<b>R3</b>	<b>0.66</b>	<b>0.42</b>	<b>14.49</b>	<b>715 915</b>
<b>B-D</b>	<b>R4</b>	<b>0.70</b>	<b>0.38</b>	<b>13.32</b>	<b>715</b>
B-I	R2	0.47	0.66	17.18	550
B-I	R3	NS	NS	NS	
B-I	R3-R4	NS	NS	NS	
<b>B-I</b>	<b>R5-R6</b>	<b>0.80</b>	<b>0.44</b>	<b>11.86</b>	<b>550 715 915</b>
<b>C-I 2</b>	<b>R2</b>	<b>0.66</b>	<b>0.51</b>	<b>12.47</b>	<b>550 715 915</b>
<b>C-I 2</b>	<b>R4-5</b>	<b>0.79</b>	<b>0.40</b>	<b>10.02</b>	<b>415 550 915 940</b>
<b>C-I 1</b>	<b>R2</b>	<b>0.78</b>	<b>0.37</b>	<b>9.10</b>	<b>680 715</b>
C-I 1	R3	NS	NS	NS	
<b>C-I 1</b>	<b>R4-5</b>	<b>0.78</b>	<b>0.38</b>	<b>9.30</b>	<b>550 715 990</b>
<b>C-I 1</b>	<b>R6</b>	<b>0.85</b>	<b>0.32</b>	<b>7.79</b>	<b>550 715 990</b>

**BOLD** = Selected observations used for training model creation.

**Table 3.6. Results of the maturity group IV (MGIV) stepwise regression models by growth stage with experiment, coefficient of determination (R<sup>2</sup>), root means square error (rMSE), percentage rMSE of dependent mean (% rMSE of mean), and wavebands in final model (wavebands).**

Experiment	Growth stage	R <sup>2</sup>	rMSE t ha <sup>-1</sup>	% rMSE of mean	Wavebands
<b>A-I</b>	<b>R3</b>	<b>0.73</b>	<b>0.56</b>	<b>17.10</b>	<b>715 1100</b>
<b>A-I</b>	<b>R3-R4</b>	<b>0.89</b>	<b>0.39</b>	<b>11.86</b>	<b>415 680 715 915 1300</b>
<b>A-I</b>	<b>R5</b>	<b>0.75</b>	<b>0.53</b>	<b>16.45</b>	<b>715 915</b>
<b>A-I</b>	<b>R5-R6</b>	<b>0.73</b>	<b>0.56</b>	<b>17.27</b>	<b>715 915</b>
<b>A-D</b>	<b>R2-R3</b>	<b>0.69</b>	<b>0.31</b>	<b>17.48</b>	<b>940 1100 1245</b>
A-D	R3-R4	0.54	<b>0.38</b>	21.25	680 715 940
<b>A-D</b>	<b>R5</b>	<b>0.66</b>	<b>0.31</b>	<b>17.14</b>	<b>550</b>
<b>B-D</b>	<b>R3</b>	<b>0.79</b>	<b>0.37</b>	<b>11.32</b>	<b>715 940</b>
<b>B-D</b>	<b>R4</b>	<b>0.77</b>	<b>0.39</b>	<b>11.78</b>	<b>715 1100</b>
<b>B-D</b>	<b>R6</b>	<b>0.67</b>	<b>0.45</b>	<b>13.69</b>	<b>550</b>
<b>B-I</b>	<b>R1-R2</b>	<b>0.79</b>	<b>0.47</b>	<b>12.94</b>	<b>715 940</b>
B-I	R2-R3	NS	NS	NS	
B-I	R4	0.57	0.66	18.38	715 915
<b>B-I</b>	<b>R5</b>	<b>0.86</b>	<b>0.40</b>	<b>11.07</b>	<b>550 715 915 990</b>
<b>B-I</b>	<b>R5-R6</b>	<b>0.71</b>	<b>0.53</b>	<b>14.62</b>	<b>550</b>
C-I 2	R3	NS	NS	NS	
C-I 2	R4	NS	NS	NS	
<b>C-I 1</b>	<b>R1-R2</b>	<b>0.52</b>	<b>0.43</b>	<b>11.15</b>	<b>715</b>
C-I 1	R2-R3	0.47	0.45	11.74	715
C-I 1	R4	0.30	0.52	13.49	415
C-I 1	R5-R6	0.37	0.49	12.80	415

**BOLD** = Selected observations used for training model creation.

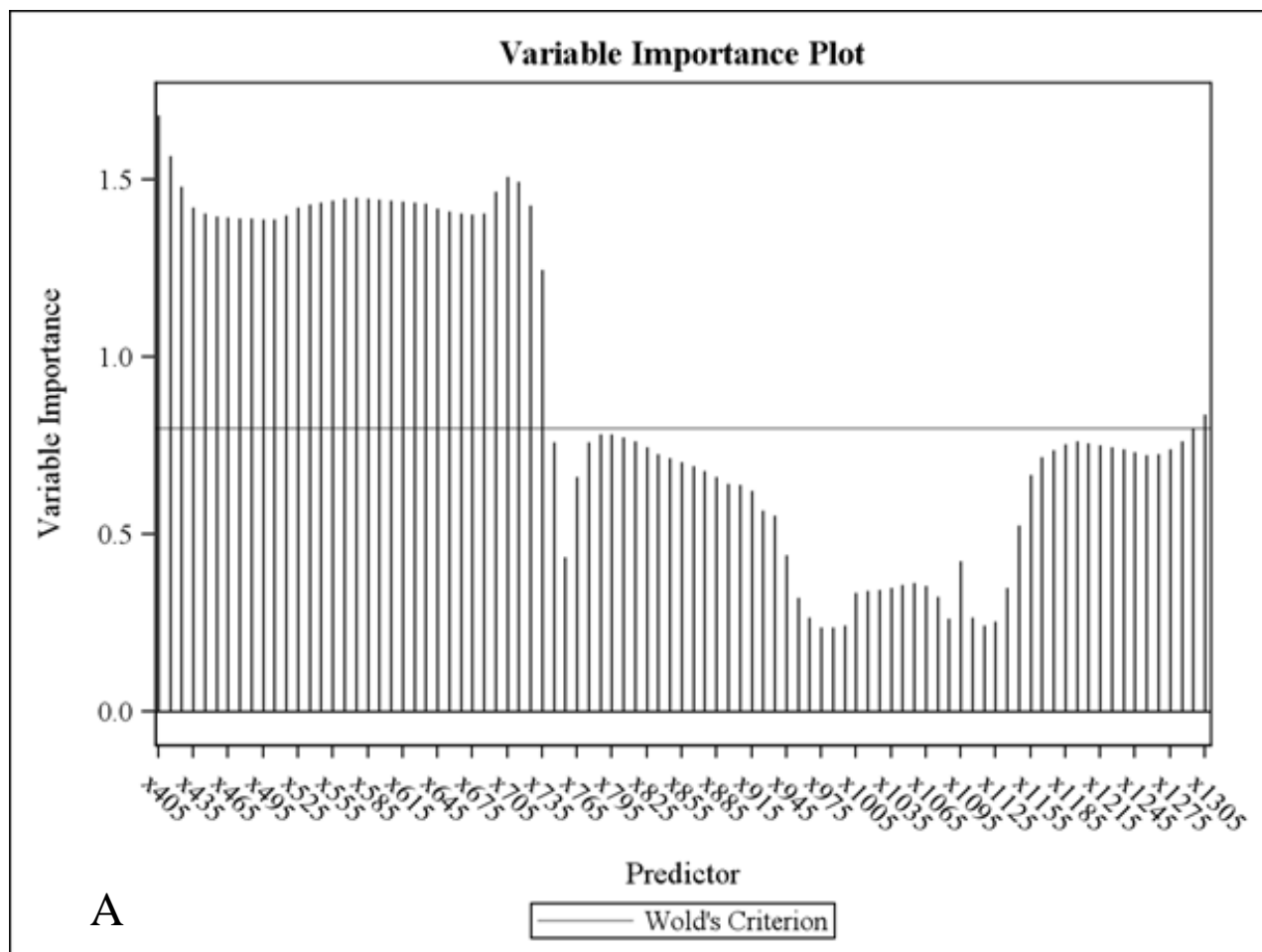
**Table 3.7. Results of stepwise regression yield estimation models for maturity group III (MGIII) and maturity group IV (MGIV) selected datasets.**

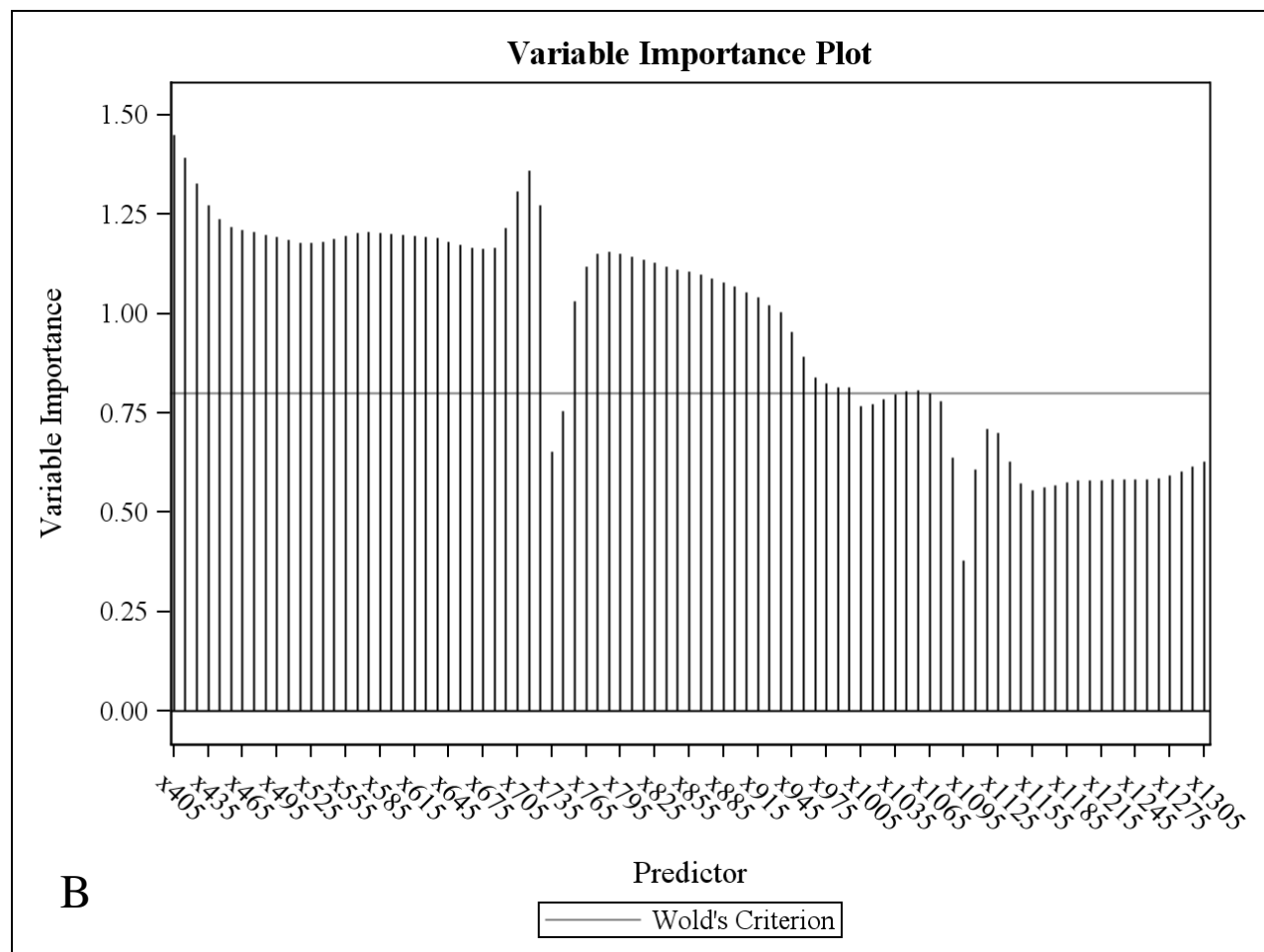
Model	Variable (nm)	Variable R <sup>2</sup>	Model R <sup>2</sup>	Equation
MGIII	715	0.73	0.83	Yield = -52.35 - 556.42 (715 nm) + 275.28 (1100 nm)
	1100	0.10		
MGIV	715	0.70	0.81	Yield = -45.13 - 619.09 (715 nm) + 172.24 (915 nm)
	915	0.11		

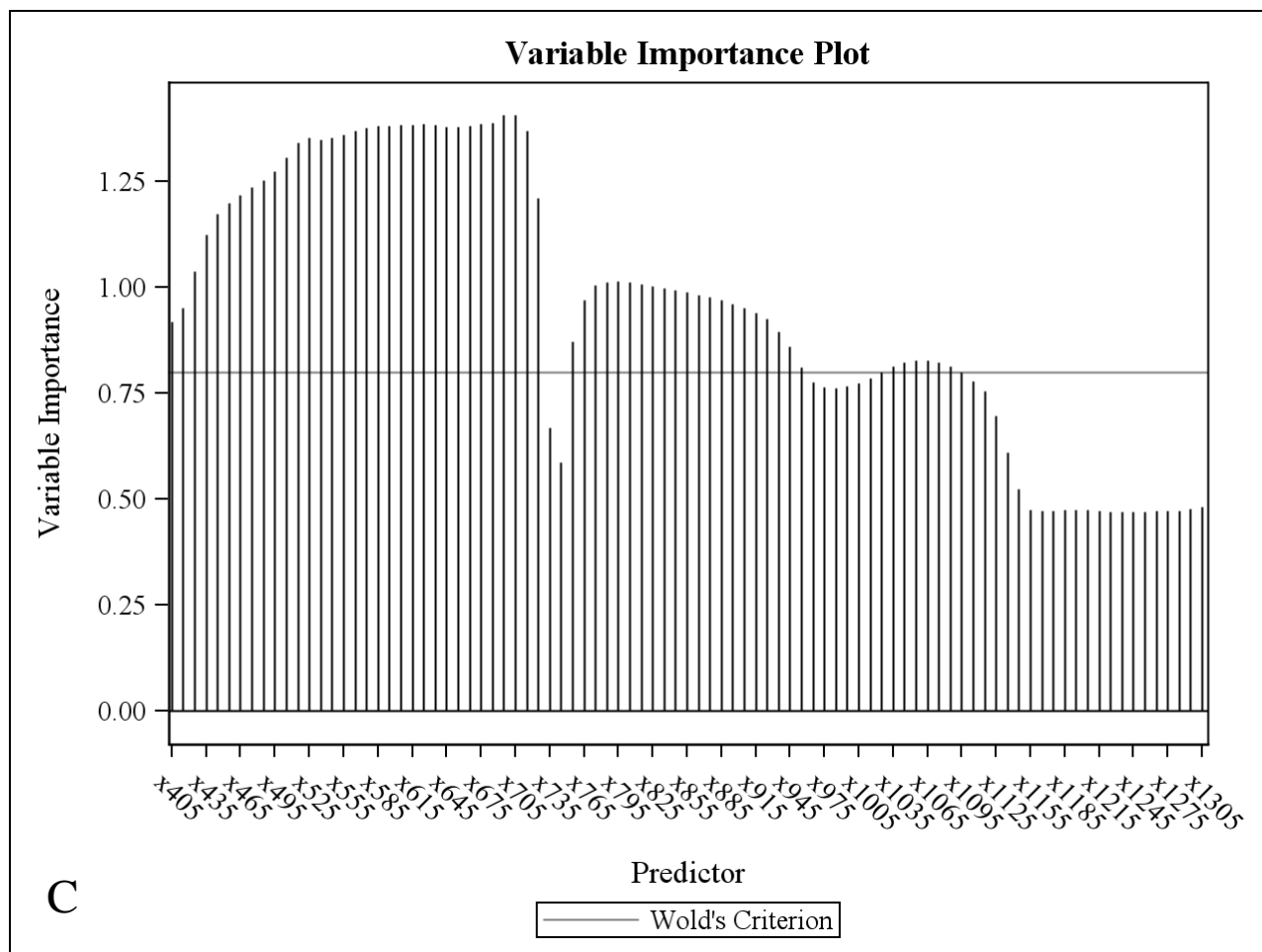
**Table 3.8. Yield estimation model validation results for maturity group III (MGIII) and maturity group IV (MGIV) growth stages and season totals (ST) for optimized yield**

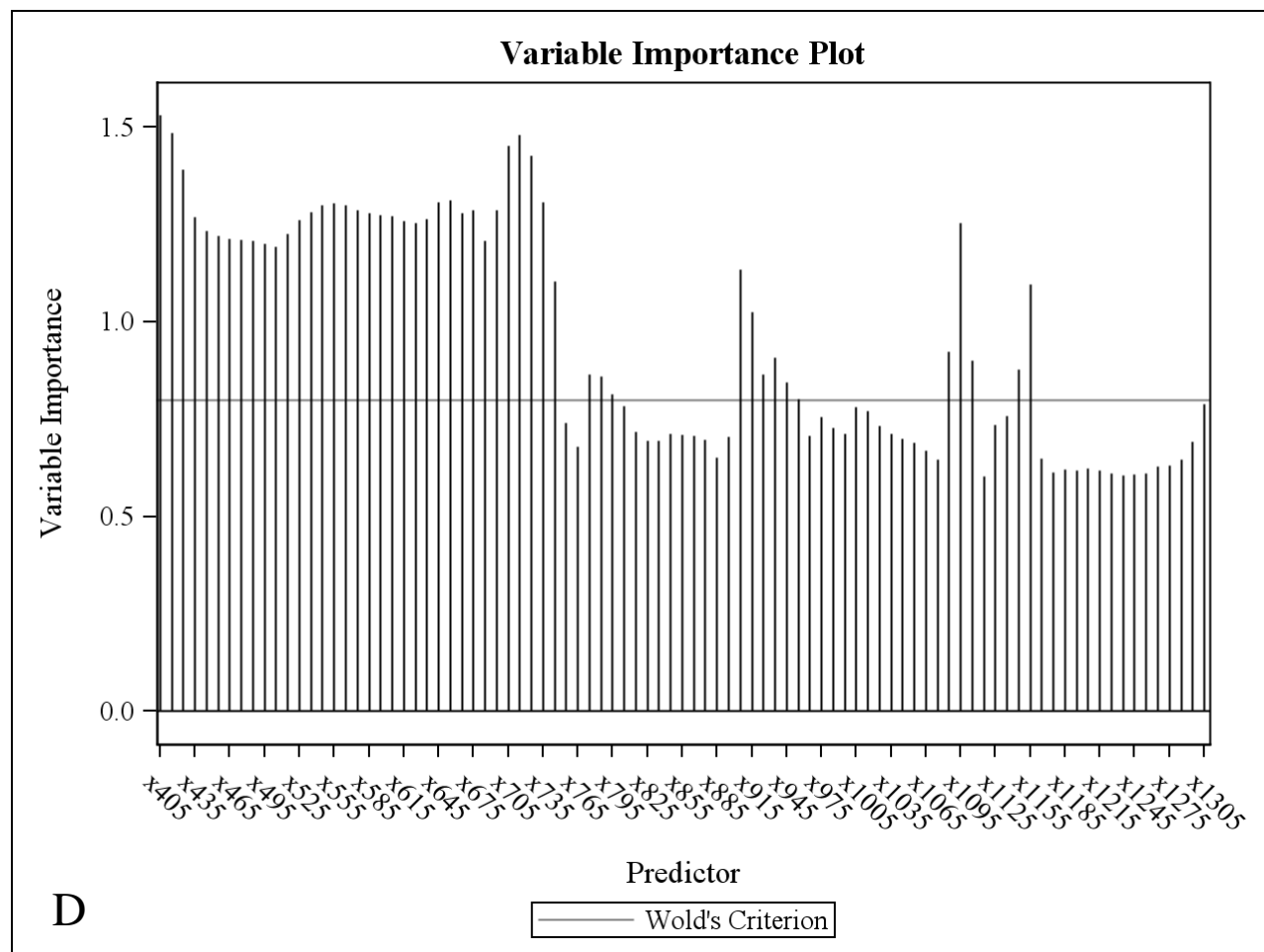
estimation models. **I** indicates an irrigated environment; **D** indicates a water-stressed environment.

Environment	Growth stage	R <sup>2</sup>	Environment	Growth stage	R <sup>2</sup>
MGIII			MGIV		
A-I	R3-R4	0.49	A-I	R3	0.72
A-I	R4	0.51	A-I	R3-R4	0.75
A-I	R5	0.66	A-I	R5	0.75
A-I	R6	0.62	A-I	R5-R6	0.72
A-I	ST	0.53	A-I	ST	0.78
A-D	R3-R4	0.62	A-D	R2-R3	0.43
A-D	R5	0.55	A-D	R3-R4	0.44
A-D	R6	0.64	A-D	R5	0.60
A-D	ST	0.67	A-D	ST	0.51
B-D	R3	0.64	B-D	R3	0.77
B-D	R4	0.61	B-D	R4	0.72
B-D	ST	0.66	B-D	R6	0.64
B-I	R2	0.54	B-D	ST	0.83
B-I	R3-R4	0.29	B-I	R1-R2	0.79
B-I	R5-R6	0.64	B-I	R4	0.38
B-I	ST	0.59	B-I	R5	0.56
C-I 2	R2	0.46	B-I	R5-R6	0.61
C-I 2	R4-5	0.42	B-I	ST	0.68
C-I 2	ST	0.45	C-I 2	R3	0.01
C-I 1	R2	0.75	C-I 2	R4	0.01
C-I 1	R4-5	0.53	C-I 2	ST	0.02
C-I 1	R6	0.64	C-I 1	R1-R2	0.54
C-I 1	ST	0.79	C-I 1	R2-R3	0.41
2011 avg.	ST	0.68	C-I 1	R4	0.28
2012 avg.	ST	0.68	C-I 1	R5-R6	0.40
			C-I 1	ST	0.49
			2011 avg.	ST	0.65
			2012 avg.	ST	0.79

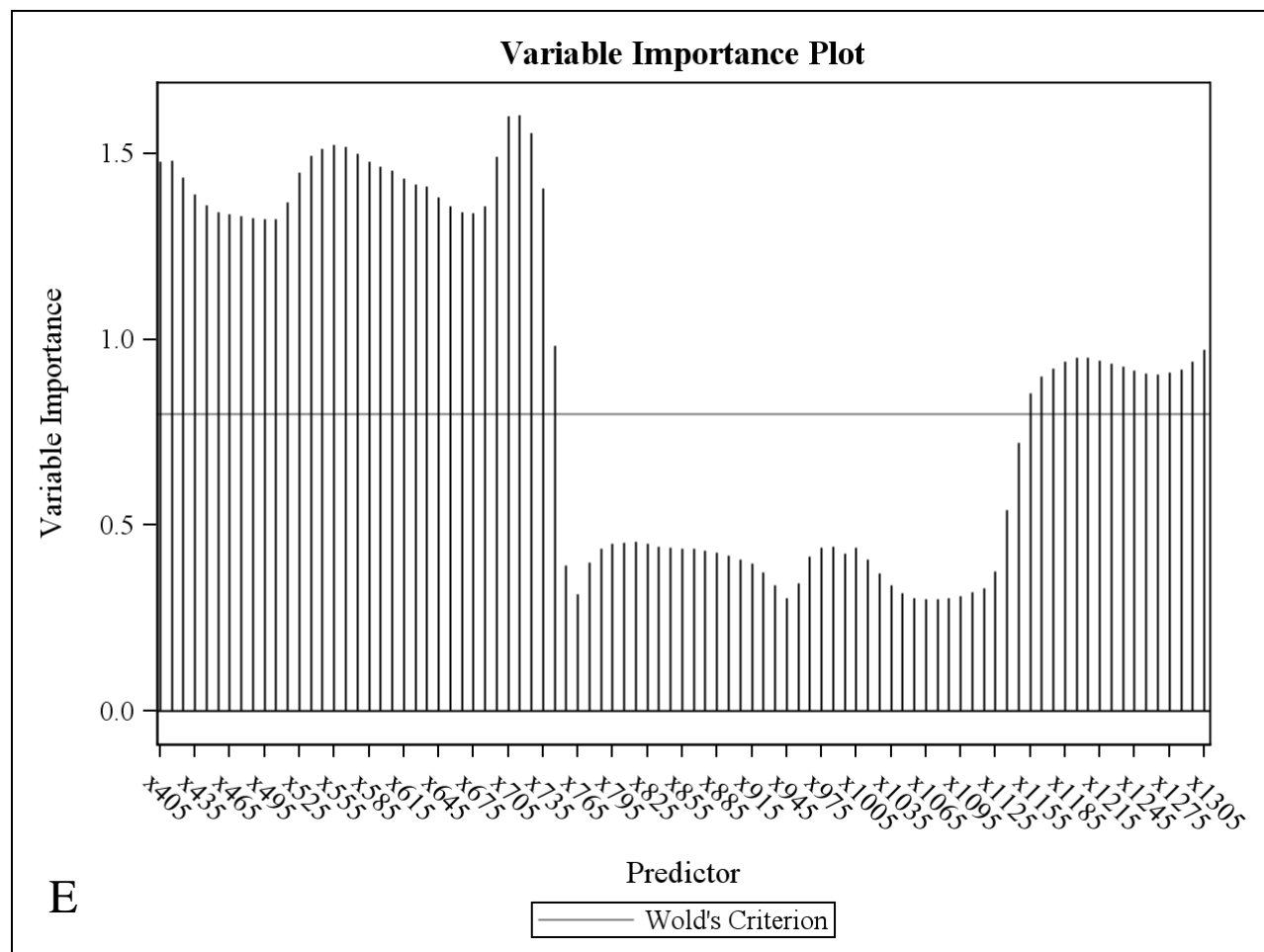


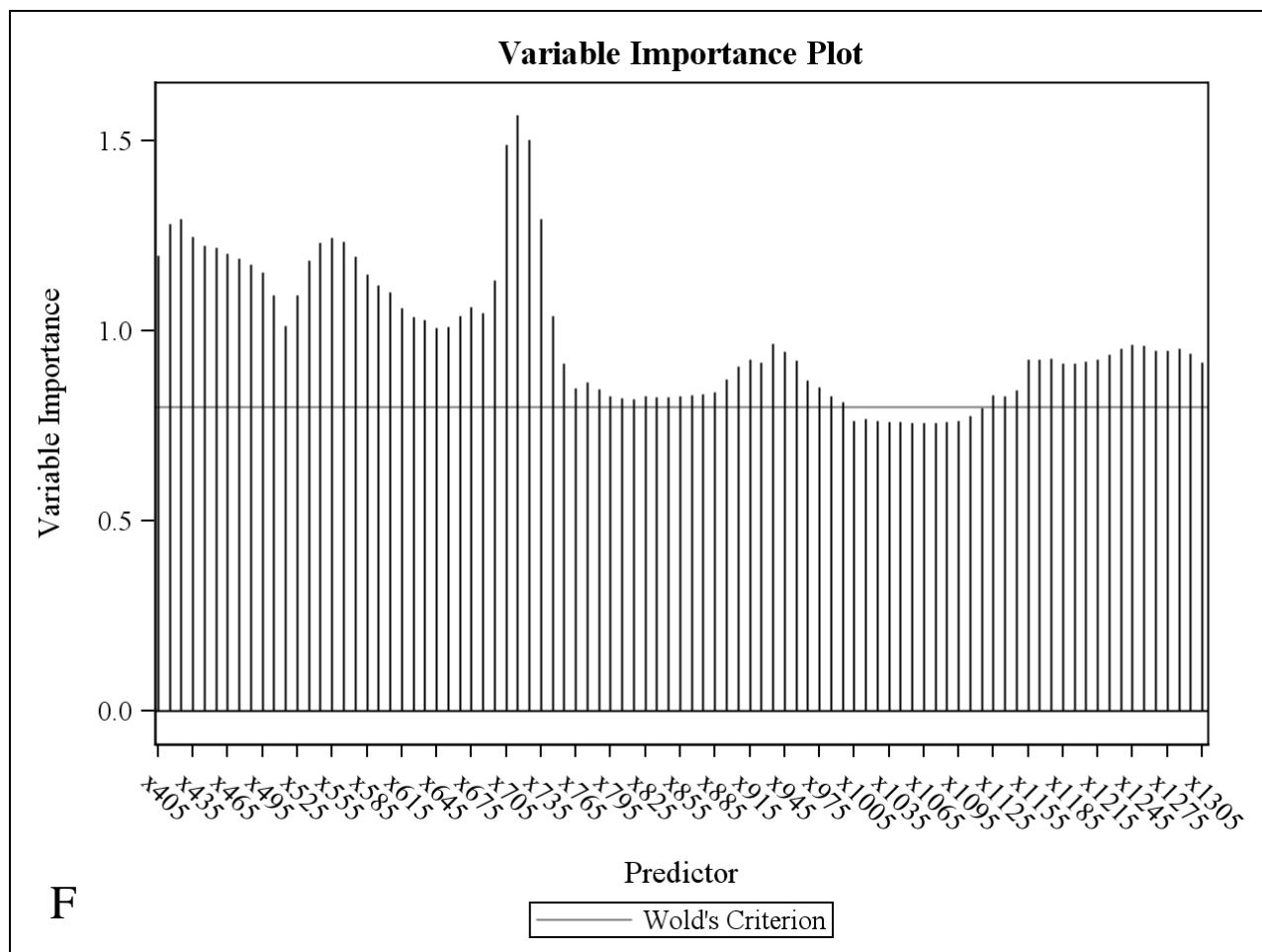


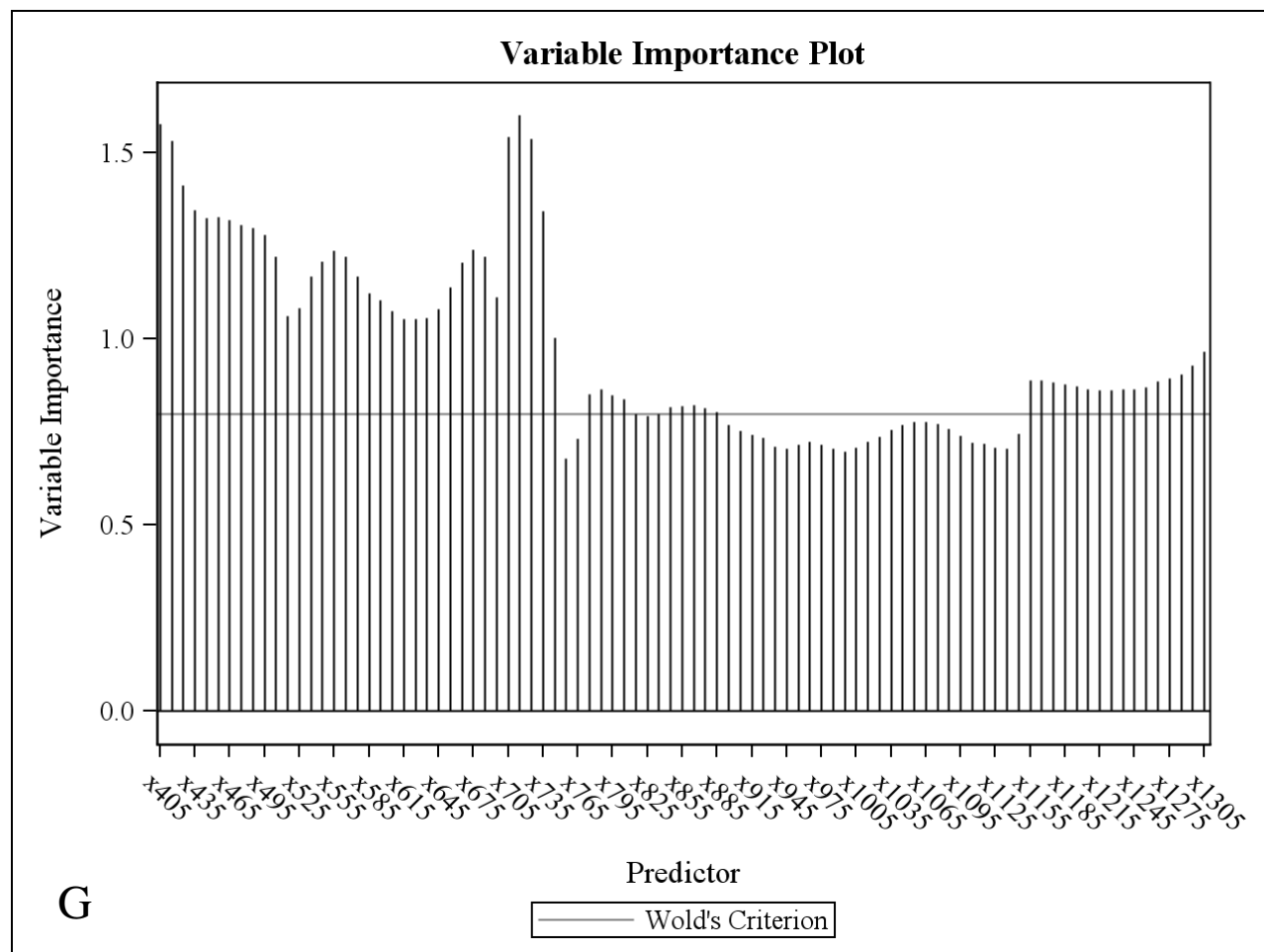


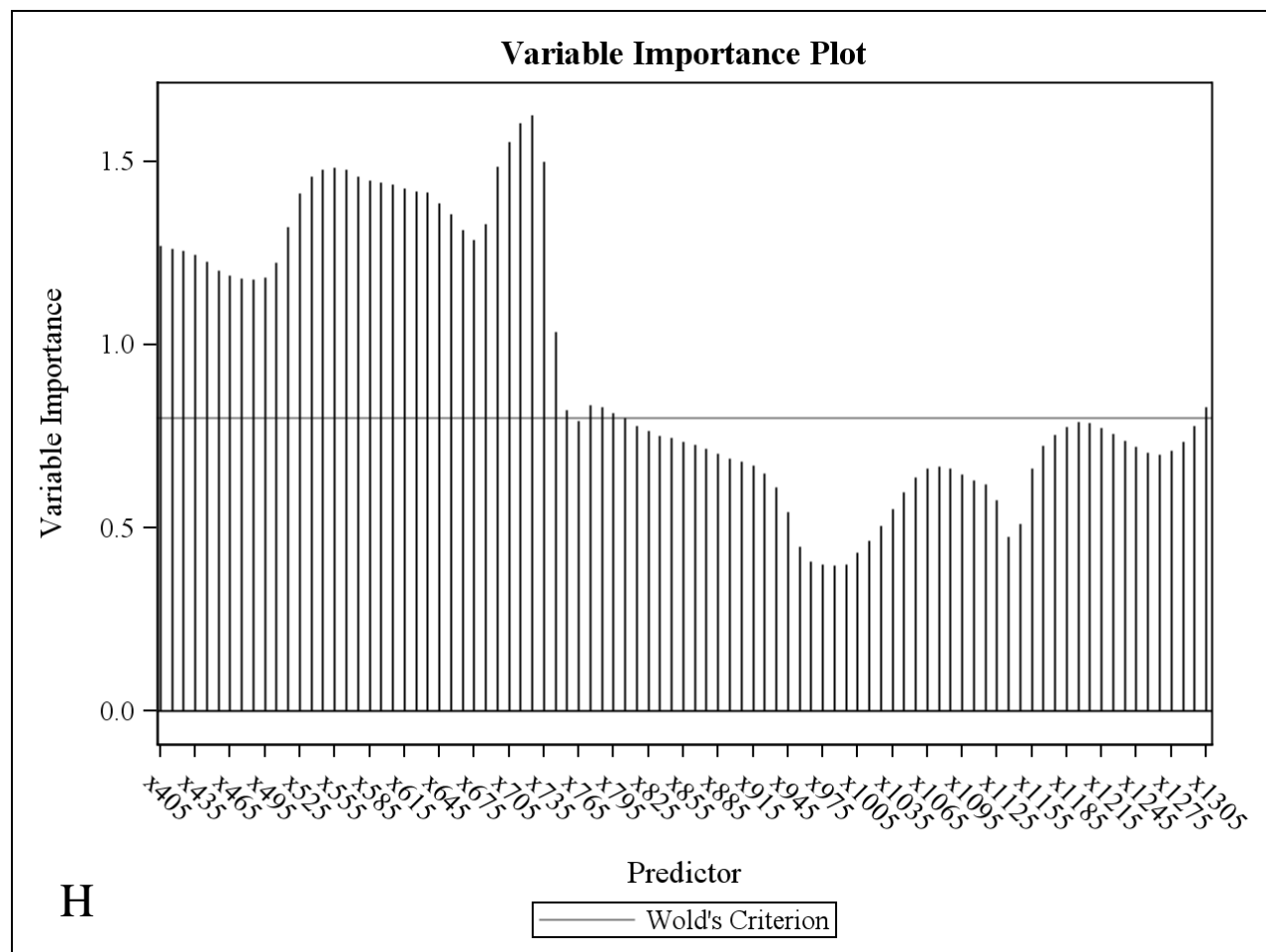


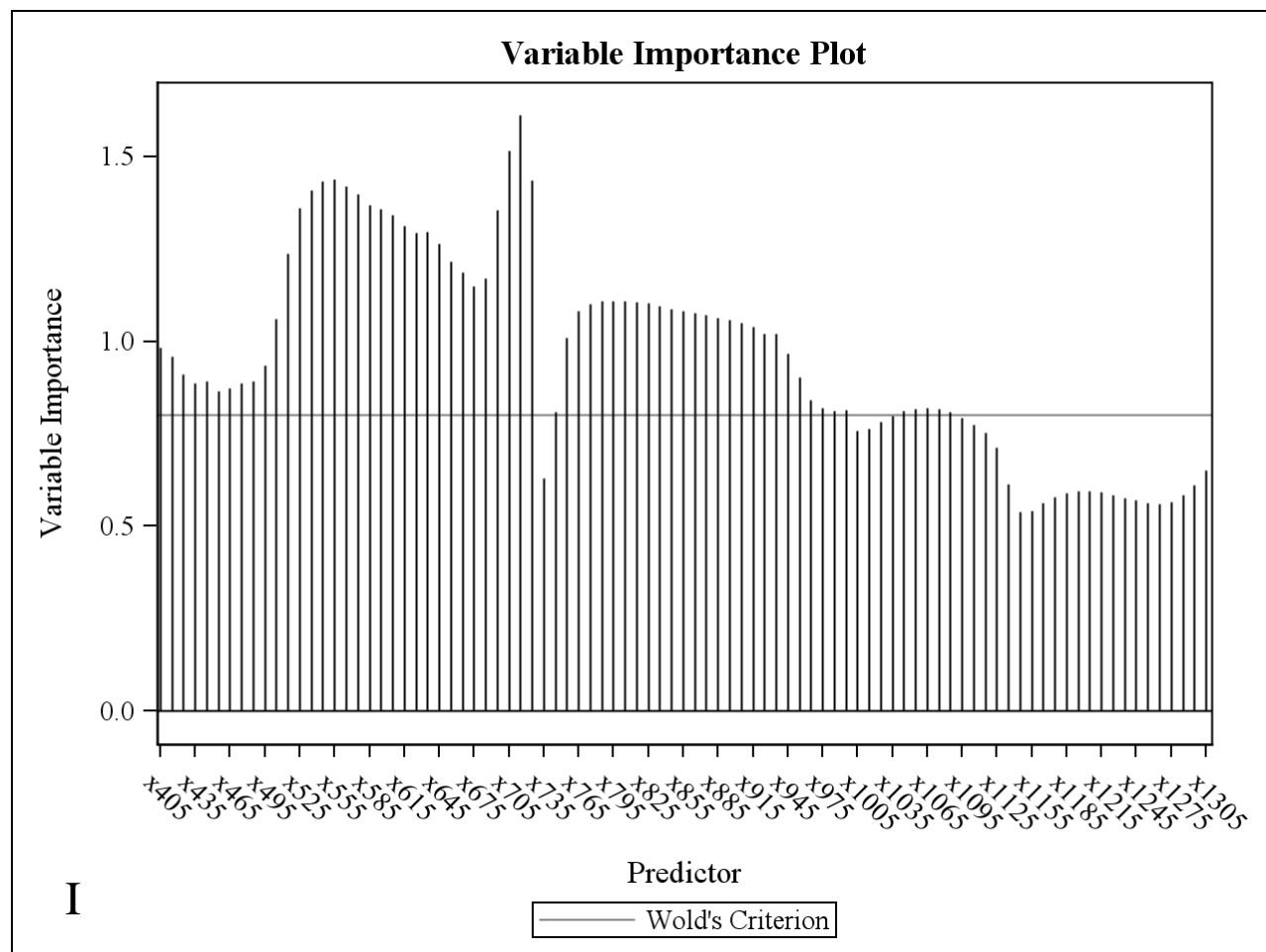


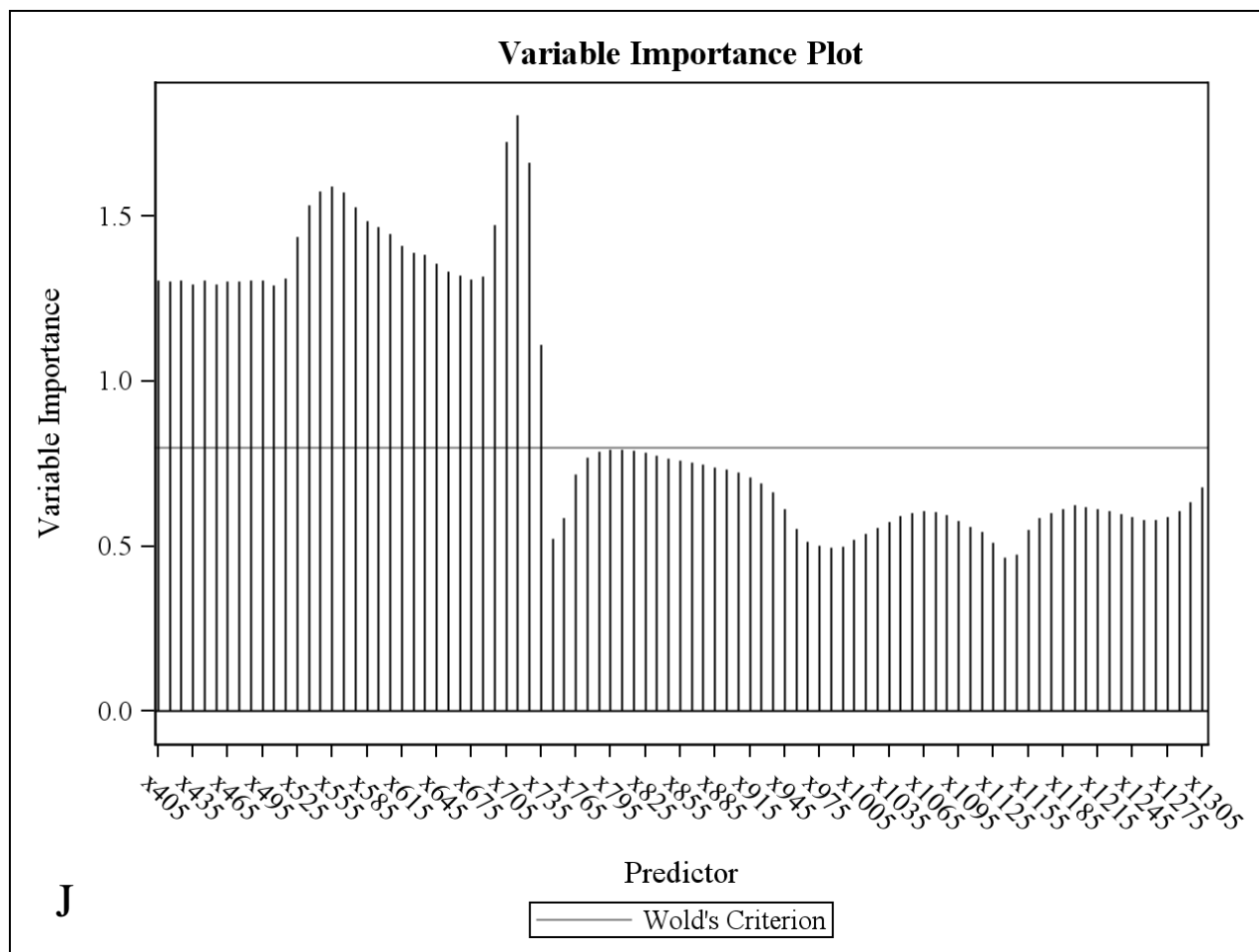


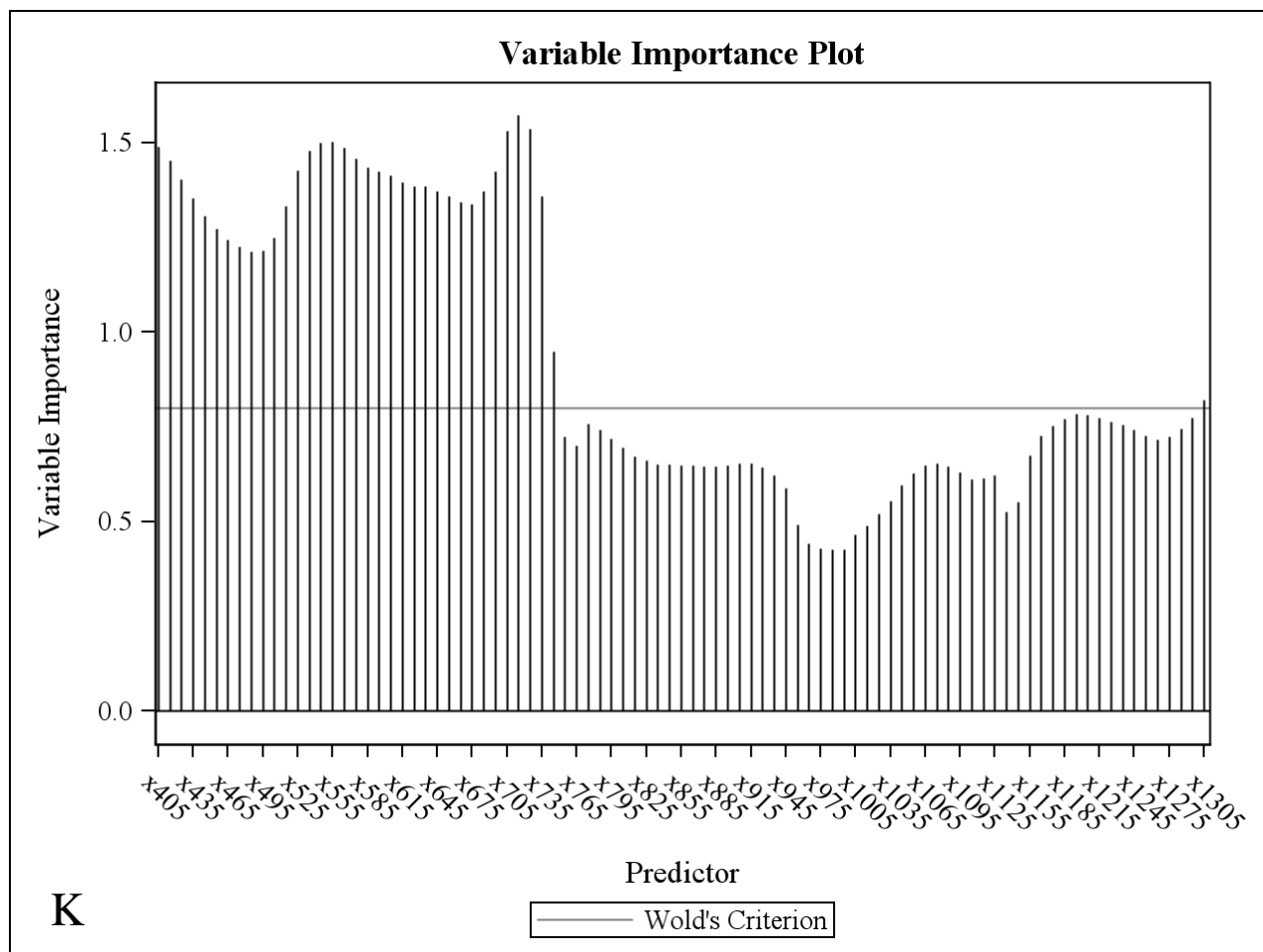


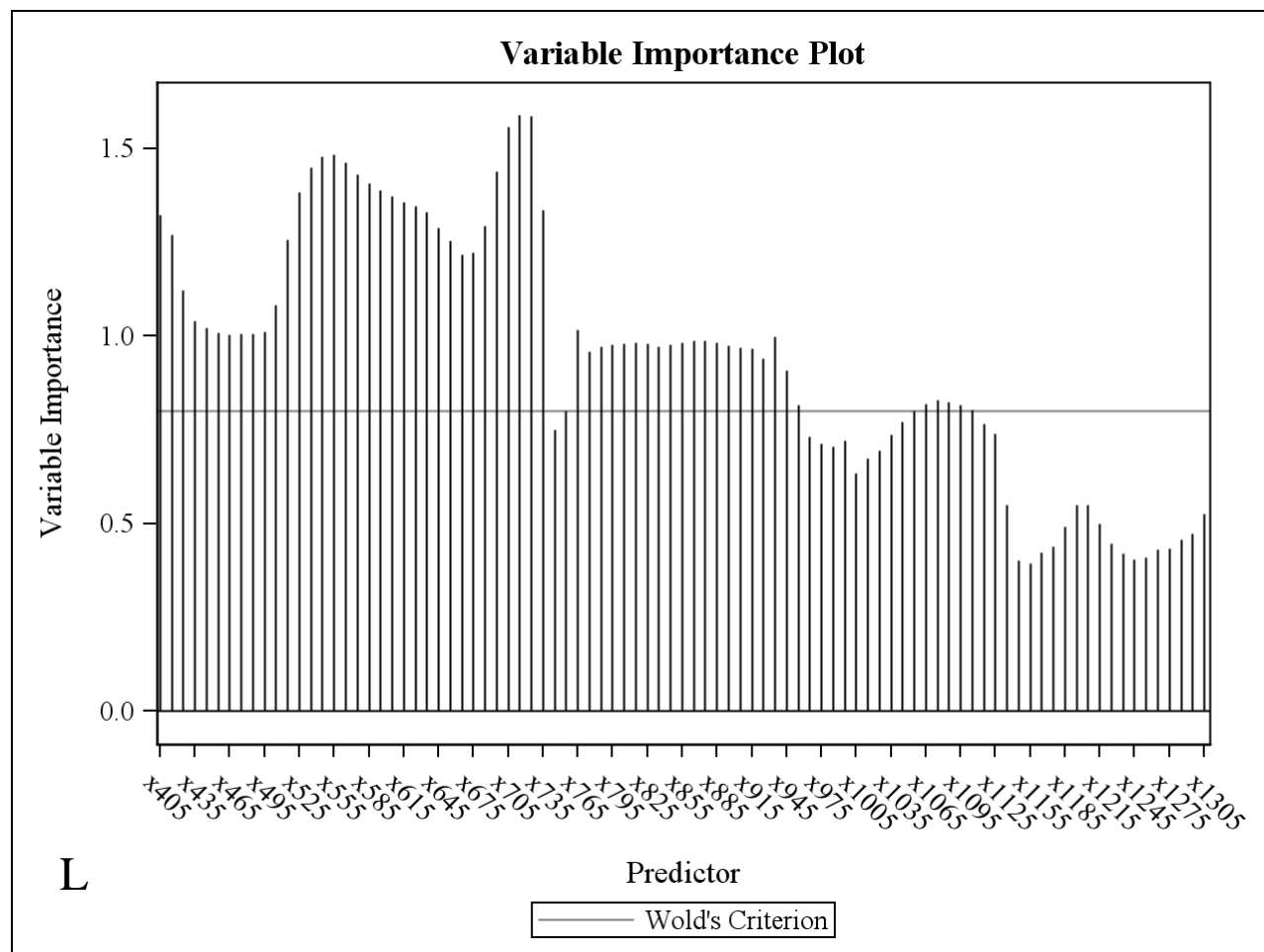














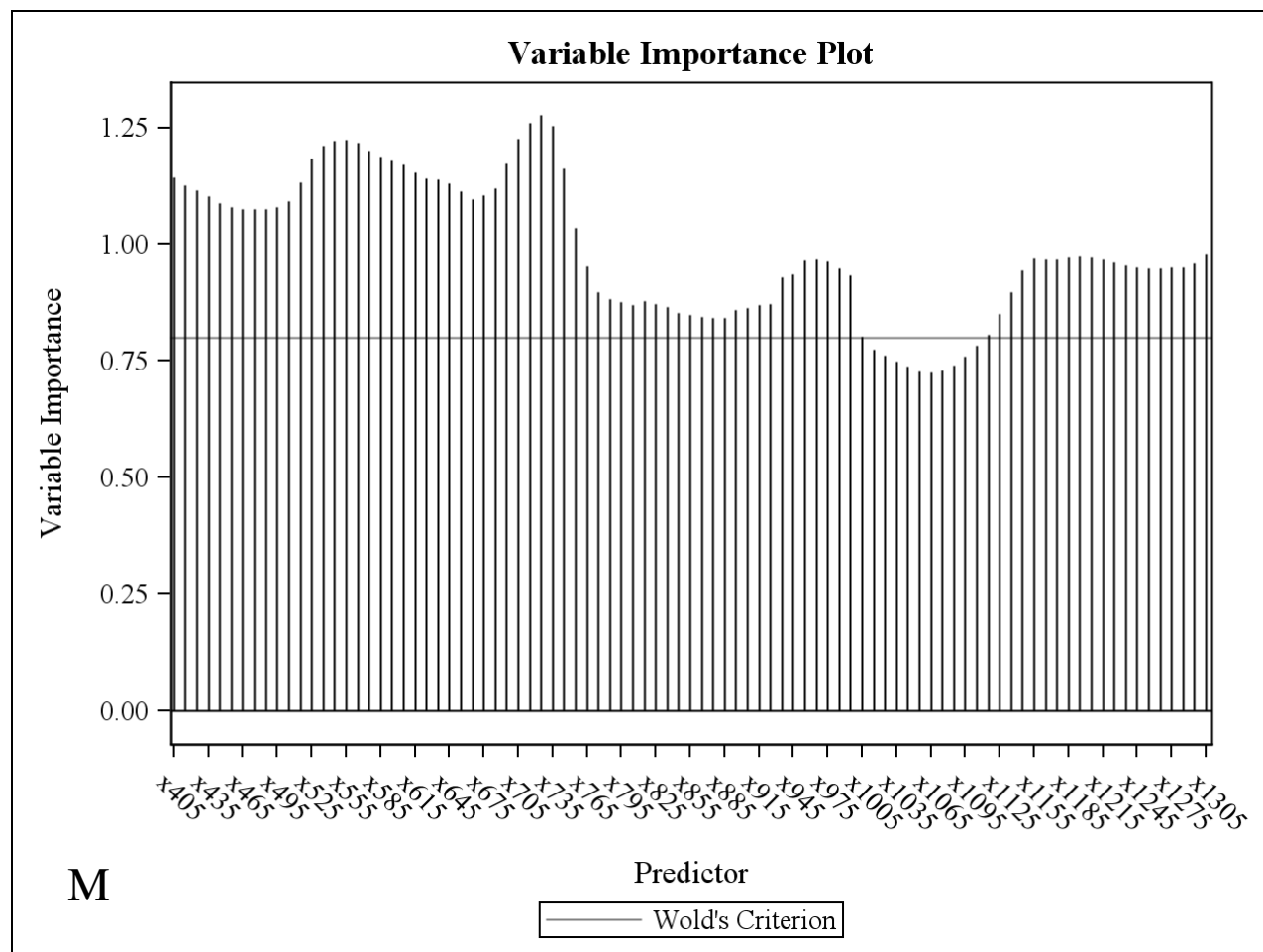


**Figure 3.A. Variable importance in projection plots displaying results from partial least squares regression (PLS) analyses. (A) Maturity group III (MGIII) 2011–2012 two-year means, (B) MGIII 2011 A-I means, (C) MGIII 2011 A-D means, (D) MGIII 2012 B-I means, (E) MGIII 2012 B-D means, (F) MGIII 2012 C-I 1 means, (G) MGIII 2012 C-I 2 means, (H) maturity group IV (MGIV) 2011–2012 two-year means, (I) MGIV 2011 A-I means, (J) MGIV 2011 A-D means, (K) MGIV 2012 B-I means, (L) MGIV 2012 B-D means, (M) MGIV 2012 C-I 1 means.**

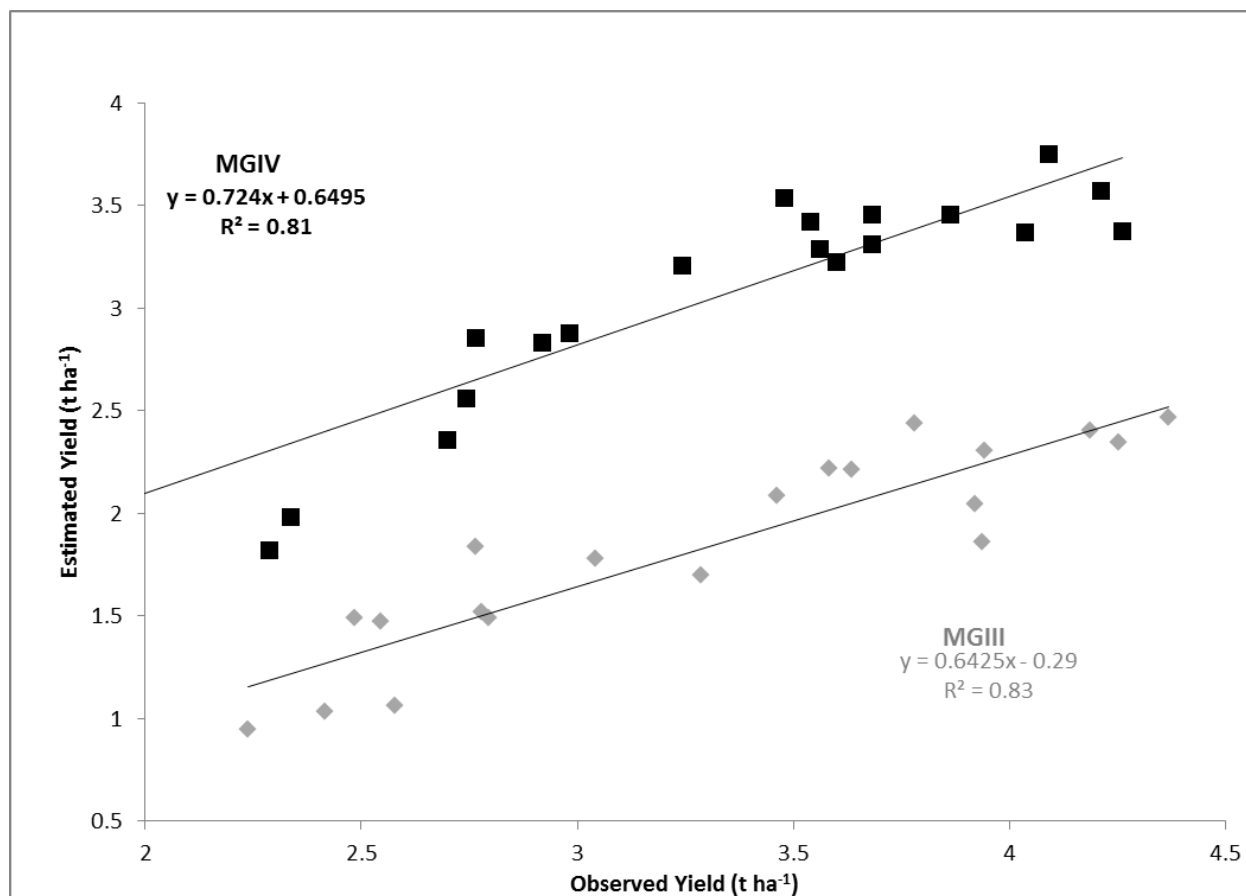


**Figure 3.B. Relationships between observed and predicted seed yield for maturity group III (MGIII) and maturity group IV (MGIV) two-year waveband means with selected growth stage**